T.R.
GEBZE TECHNICAL UNIVERSITY
GRADUATE SCHOOL

PRODUCTION OF AMMONIUM SULFATE FROM HUMAN URINE WITH AN ENZYMATIC POLYHIPE REACTOR AND ITS USE AS FERTILIZER ON WHEAT GROWTH

Büşra ŞAHİN

A THESIS OF DOCTORATE
DEPARTMENT OF BIOTECHNOLOGY

ADVISOR: ASSOC.PROF.DR.ÇİĞDEM BALÇIK

OCTOBER 2025

T.R.
GEBZE TECHNICAL UNIVERSITY
GRADUATE SCHOOL

PRODUCTION OF AMMONIUM SULFATE FROM HUMAN URINE WITH AN ENZYMATIC POLYHIPE REACTOR AND ITS USE AS FERTILIZER ON WHEAT GROWTH

BÜŞRA ŞAHİN

A THESIS OF DOCTORATE
DEPARTMENT OF BIOTECHNOLOGY

ADVISOR: ASSOC.PROF.DR. ÇİĞDEM BALÇIK

OCTOBER 2025

T.C.
GEBZE TEKNİK ÜNİVERSİTESİ
LİSANSÜSTÜ EĞİTİM ENSTİTÜSÜ

ENZİMATİK POLİHİPE REAKTÖRÜ İLE İNSAN İDRARINDAN AMONYUM SÜLFAT ÜRETİMİ VE BUĞDAY YETİŞTİRİCİLİĞİNDE GÜBRE OLARAK KULLANIMI

BÜŞRA ŞAHİN

DOKTORA TEZİ
BİYOTEKNOLOJİ ANABİLİM DALI

DANIŞMAN: DOÇ.DR. ÇİĞDEM BALÇIK

EKİM 2025

DOCTORATE JURY APPROVAL FORM

A thesis submitted by Büşra ŞAHİN, defended on 16/10/2025 before the jury formed with the 14/10/2025 date and 2025/60 numbered decision of the GTU Graduate Administration Board, has been accepted as a DOCTOR of PHILOSOPHY thesis in the Department of Biotechnology.

JURY

MEMBER (THESIS ADVISOR)	: ASSOC.PROF.DR.ÇİĞDEM BALÇIK
MEMBER	:PROF.DR.NADİR DİZGE
MEMBER	:ASSOC.PROF.DR.MÜGE İŞLETEN HOŞOĞLU
MEMBER	:ASSOC.PROF.DR.BAHAR ÖZBEY ÜNAL
MEMBER	:ASSOC.PROF.DR.AYŞE YÜKSEKDAĞ

APPROVAL

Gebze Technical University Graduate Administration Board

……/……./……..date and ……../……../……numbered decision.

SIGNATURE/SEAL

To my
Family

ABSTRACT

This study investigates the immobilization of the urease enzyme on various High Internal Phase Emulsion (polyHIPE) materials, evaluating their properties, efficiency, and performance, while examining the effects of polyHIPE type, amount, incubation time, and other parameters on the process and enzyme activity. The surface morphology and functional groups of the polyHIPE materials were analyzed using scanning electron microscopy (SEM) and Fourier transform infrared spectroscopy (FT-IR), revealing significant changes after modification with polyglutaraldehyde (PGA). Maximum immobilization efficiency of 95% was achieved by incorporating PGA into the polyHIPE materials with a 15-hour incubation period. Optimal conditions for the immobilized enzyme were determined using response surface methodology (RSM) with a Box-Behnken design (BBD). Furthermore, the immobilized enzyme demonstrated promising reusability, retaining 75% of its initial activity after six cycles, and maintained shelf-life stability, retaining over 40% of its activity after 10 days at room temperature. Kinetic analyses showed that immobilized urease exhibited higher affinity for the substrate compared to the free enzyme, although it had a lower substrate conversion rate. These results provide valuable insights into optimizing urease immobilization processes and improving urease stability and activity, with potential applications in biotechnology and biocatalysis.

Furthermore, the study investigated the recovery of ammonium sulfate from human urine using urease immobilized on a polyHIPE support material and its potential as fertilizer for durum wheat. Optimal conditions for urease activity in human urine were found to be pH 7 and 45°C; the immobilized enzyme retained 53% of its activity over 10 cycles and 50% after 10 days at room temperature. In enzyme immobilized polyHIPE reactor studies, when the reactor was operated at linear feed rates of 0.5 and 1 m^3/m^2.hour, urea hydrolysis yields of over 95% were obtained even at a linear rate of 1 m^3/m^2.hour. In ammonia stripping studies, ammonia stripping efficiencies above 80% were achieved, particularly at operating temperatures of 40°C and 65°C and pH values of 10 and 11. When the operating temperature was increased to 65°C, an ammonia stripping yield of around 80% was achieved even at a pH of 9, while at a pH of 10, almost all of the ammonia could be stripped. X-ray diffraction confirmed the similarity of the recovered ammonium sulfate to commercial versions. As a fertilizer, the recovered ammonium sulfate showed comparable results to commercial products in terms of plant growth, with no significant differences observed in height, ear length, or spikelets. Producing ammonium sulfate from abundant and cost-effective human urine offers a sustainable and economical alternative to synthetic fertilizers, supporting environmental and agricultural goals.

Keywords: urease immobilization, polymeric high internal phase emulsion,urea removal, human urine, ammonium sulfate recovery

ÖZET

Bu çalışma, çeşitli Yüksek İç Faz Emülsiyon (polyHIPE) malzemeleri üzerinde üreaz enziminin immobilizasyonunu araştırarak, bunların özelliklerini, verimliliğini ve performansını değerlendirirken, polyHIPE tipi, miktarı, inkübasyon süresi ve diğer parametrelerin süreç ve enzim aktivitesi üzerindeki etkilerini incelemektedir. PolyHIPE malzemelerinin yüzey morfolojisi ve fonksiyonel grupları, taramalı elektron mikroskobu (SEM) ve Fourier dönüşümü kızılötesi spektroskopisi (FT-IR) kullanılarak analiz edilmiş ve poliglutaraldehit (PGA) ile modifikasyondan sonra önemli değişiklikler ortaya çıkmıştır. 15 saatlik inkübasyon süresi ile PGA'nın polyHIPE malzemelerine dahil edilmesi ile %95'lik maksimum immobilizasyon verimliliği elde edilmiştir. İmmobilize enzim için optimal koşullar, Box-Behnken tasarımı (BBD) ile yanıt yüzeyi metodolojisi (RSM) kullanılarak belirlendi. Ayrıca, immobilize enzim, altı döngüden sonra başlangıçtaki aktivitesinin %75'ini koruyarak umut verici bir yeniden kullanılabilirlik gösterdi ve oda sıcaklığında 10 gün sonra aktivitesinin %40'ından fazlasını koruyarak raf ömrü stabilitesini sürdürdü. Kinetik analizler, immobilize üreazın, serbest enzime kıyasla substrat dönüşüm oranı daha düşük olmasına rağmen, substrat için daha yüksek afinite sergilediğini gösterdi. Bu sonuçlar, biyoteknoloji ve biyokataliz alanlarında potansiyel uygulamalarla birlikte, üreaz immobilizasyon süreçlerinin optimize edilmesi ve üreaz stabilitesi ve aktivitesinin iyileştirilmesi konusunda değerli bilgiler sağlamaktadır.

Bununla birlikte, yapılan çalışmada polyHIPE destek malzemesi üzerinde immobilize edilmiş üreaz kullanarak insan idrarından amonyum sülfatın geri kazanılmasını ve bunun makarnalık buğdayı için gübre olarak kullanım potansiyelini de araştırılmaktadır. İnsan idrarında üreaz aktivitesi için optimal koşullar pH 7 ve 45°C'de bulunmuştur; immobilize enzim, 10 döngü boyunca aktivitesinin %53'ünü ve oda sıcaklığında 10 gün sonra %50'sini korumuştur. Enzim immobilize edilmiş poliHIPE reaktör çalışmalarında ise reaktör 0,5, ve 1 m^3/m^2.saat lineer besleme hızlarında çalıştırıldığında 1 m^3/m^2.saat lineer hız da dahi %95'in üzerinde üre hidroliz verimleri elde edilmiştir.Amonyak sıyırma çalışmalarında ise özellikle 40°C ve 65 °C çalışma sıcaklıklarında pH 10 ve 11 değerlerinde %80'nin üzerinde amonyak sıyırma verimlerine ulaşılmıştır. 65 °C çalışma sıcaklığına geçildiğinde ise pH 9 değerinde dahi %80 civarı amonyak sıyırma verimi elde edilirken, pH 10 değerine çıkıldığında amonyağın neredeyse tamamı sıyrılabilmiştir. X-ışını difraksiyonu, geri kazanılan amonyum sülfatın ticari versiyonlarla benzerliğini doğrulamıştır. Gübre olarak, geri kazanılan amonyum sülfat, bitki büyümesi açısından ticari ürünlerle karşılaştırılabilir sonuçlar gösterdi ve yükseklik, başak uzunluğu veya başakçıklar açısından önemli bir fark görülmedi. Bol miktarda bulunan ve maliyet etkin insan idrarından amonyum sülfat üretmek, sentetik gübrelere sürdürülebilir ve ekonomik bir alternatif sunarak çevresel ve tarımsal hedefleri desteklemektedir.

Anahtar Kelimeler: üreaz immobilizasyonu, polimerik yüksek iç faz emülsiyonu, üre giderimi, insan idrarı, amonyum sülfat geri kazanımı

ACKNOWLEDGEMENTS

First and foremost, I would like to thank my thesis advisor, Assoc. Prof. Dr. Çiğdem Balçık, for giving me the opportunity to work on her project, which enabled me to develop myself in both environmental engineering and biotechnology, fostered a multidisciplinary work culture, and provided all kinds of support.

I would also like to thank my esteemed professor, Assoc. Prof. Dr. Bahar Özbey Ünal, who has been a great source of motivation and support not only for this project but also for other studies conducted in the Environmental Engineering Laboratory throughout my doctoral education.

I am grateful to TÜBİTAK (Scientific and Technological Research Council of Turkey) for the financial support provided under project number 121Y525 within the scope of the 1001 project.

Gratitude is extended to Dr. Aliye Pehlivan of the Ankara Field Crops Research Institute for her invaluable assistance in measuring grain colour, size, moisture content, and hardness.

Sincere thanks are also due to Prof. Dr.Yelda Özden Çiftçi and Dr. Nida Arslan of the Department of Molecular Biology and Genetics at Gebze Technical University for their invaluable support in research investigating the impact of ammonium sulfate, derived from human urine, as a fertilizer on the yield and quality parameters of durum wheat.

I would like to thank my colleagues and close friends, Rabia Aslan, Habibe Kurt, and Naciye Yağız, who have always stood by me since I began my master's degree at Gebze Technical University through my doctoral studies, for their valuable friendship and help.

I would also like to thank my childhood friends, Merve Demirkapı Kara and Şeyma Karabicak, who have accompanied me throughout this long academic journey, offering understanding and moral support, and sharing both my joys and sorrows.

I would like to express my deepest gratitude to my mother, Süreyya Şahin, and my father, Nizamettin Şahin, for their lifelong support, tolerance, respect, and all the values they have instilled in me.

Finally, I am deeply grateful to my dear sister, Suzan Şahin Doğan, for the emotional support, positive energy, and guidance she has given me, acting as both a mother and a sister.

TABLE OF CONTENTS

LIST OF SYMBOLS AND ABBREVIATIONS

g	: gram
L	: liter
µL	: microliter
h	: hour(s)
m^2	: square meters per gram
kg/ha	: kilograms per hectare
MPa	: megapascal
mM	: millimolar
°C	: Celsius degree
v/v	: volume per volume
polyHIPE	: High Internal Phase Emulsion
NH_4^+	: Ammonium
Al_2O_3	: Aluminum oxide
CO_2	: carbon dioxide
N_2	: Nitrogen gas
St/DVB	: Styrene/Divinylbenzene
SiO_2	: Silicon dioxide
NaCl	: Sodium chloride
$CaCl_2$	: Calcium chloride
BA	: Butyl acrylate
EHA	: 2-ethylhexyl acrylate
PCL-M	: polycaprolactone methacrylate
EHMA	: 2-ethylhexyl methacrylate
DDBSS	: Sodium dodecylbenzenesulfonate
EO	: Electrochemical oxidation
OH	: Hydroxyl radicals
NO_3^-	: Nitrate ions
$(NH_4)_2SO_4$	: Ammonium sulfate
GA	: Glutaraldehyde
$K_2S_2O_8$	: Potassium peroxydisulfate
NaOAc	: Sodium acetate
PGA	: Polyglutaraldehyde
CH_3COOH	: Acetic acid
BBD	: Box-Behnken design
CALB	: Candida antarctica lipase B
COD	: Chemical Oxygen Demand
FAO	: Food and Agriculture Organization
FRP	: Free radical polymerization
FT-IR	: Fourier transform infrared spectroscopy
RO	: Reverse osmosis
RSM	: Response surface methodology
SEM	: Scanning electron microscopy
TDS	: Total dissolved solids
TKN	: Total Kjeldahl Nitrogen
UPW	: Ultra-pure water
w/o	: water-in-oil

LIST OF FIGURES

LIST OF TABLES

1. INTRODUCTION

Urea, a major end product of protein metabolism in living organisms, is a nitrogen-rich compound that is widely distributed in the environment. In addition to being a metabolic byproduct, it is present in various bodily fluids, including sweat, urine, blood, and saliva. Owing to its high nitrogen content and low production cost, urea is extensively utilized across multiple industries. In agriculture, it is primarily applied as a nitrogen fertilizer to enhance plant growth, development, and nutrient composition. Furthermore, urea serves as an important raw material in the production of plastics and pharmaceuticals **[Weerakoon et al., 2023]**. The widespread industrial utilization of urea, along with its presence in domestic waste, results in the generation of substantial amounts of urea-containing wastewater. Moreover, urea-rich wastewater may leach into the environment and agricultural soils, resulting in harmful impacts on both public health and ecological stability. One of the main environmental concerns associated with urea is its toxicity and its conversion, through hydrolysis, into another harmful compound—ammonia. The ammonia generated from urea hydrolysis contributes significantly to eutrophication in aquatic ecosystems. Therefore, the development and implementation of environmentally friendly and sustainable urea removal methods are both important and necessary **[Weerakoon et al., 2023; Zaher and Shehata, 2021; Li et al., 2023]**.

In healthy individuals, urea produced as a byproduct of metabolic activity is excreted by the kidneys. However, in cases of kidney failure, urea and other waste compounds that accumulate in the bloodstream are removed through treatments such as dialysis. A typical dialysis session, lasting approximately four hours, requires around 120 liters of purified water. Implementing Technologies such as reverse osmosis (RO) aimed at removing urea and other solutes from dialysis effluent may help reduce operational costs and water consumption by potentially shortening duration and enhancing process efficiency **[Weerakoon et al., 2023; Ben Hmida et al., 2023; Abraham and Goldfarb, 2025].**

Urea can enter wastewater systems through multiple sources, including human urine, agricultural runoff, and industrial effluents. Human urine, for example, contains approximately 22–23 g/L of urea. In agricultural settings, urea-based fertilizers may

infiltrate water bodies through surface runoff or leaching. Additionally, urea-rich wastewater generated from industrial processes—such as in the production of formaldehyde resins—must be treated to remove toxic components before environmental discharge. If untreated, the release of urea into natural ecosystems contributes to eutrophication, a process that promotes the excessive growth of algae which disturbs the ecological balance and releases ammonia that is toxic to fish. This uncontrolled proliferation poses significant risks to aquatic ecosystems, environmental quality, and animal health. In this context, an effective urea removal method can not only eliminate urea from wastewater but also enable the recovery of valuable components, contributing to resource efficiency and environmental sustainability **[Weerakoon et al., 2023; Li et al., 2023; Habib and Weinman, 2022].**

In recent years, the demand for ultra-pure water (UPW) has risen sharply across the biotechnology, pharmaceutical, and electronics industries. Recovering high-purity water from urea-containing wastewater is essential not only for meeting stringent industrial requirements but also for supporting sustainable resource management. In the semiconductor sector in particular, trace amounts of urea in UPW can significantly reduce product yield and introduce process uncertainties. However, conventional organic matter treatment systems struggle to effectively remove low molecular weight, electrically neutral, and highly hydrophilic compounds such as urea. Current UPW production involves multiple stages—including activated carbon filtration, mixed-bed ion exchange, RO, and ultraviolet treatment—but these methods have demonstrated limited efficiency in eliminating trace urea **[Wang et al., 2023; J. Choi and Chung, 2019].** Therefore, the development of advanced and selective urea removal technologies is critical to ensure both the production of high-quality UPW and the sustainability of water resources.

Similarly, the dairy industry is among the sectors with the highest water consumption. According to a report by the Food and Agriculture Organization of the United Nations, global demand for dairy products is projected to increase by 82% by 2050. Meeting this growing demand with limited water resources necessitates the adoption of sustainable production practices. One current challenge is the presence of urea in the permeate obtained from RO processing of milk and whey. Urea in the RO permeate poses a risk by promoting microbial growth. Therefore, developing effective technologies for urea removal from RO permeate is essential to ensure both product

quality and process sustainability **[Choi et al., 2024;Al-Tayawi et al., 2023; Weerakoon et al., 2023].**

In response to growing demands in industrial production, pharmaceuticals, and other sectors, Table 1.1. below summarizes the key areas where urea removal is applied and the methods developed in recent years.

Table 1.1: An overview of the key application areas for urea removal and the corresponding methods employed.

Urea removal area	Applied methods
Small molecules and organic compounds removel in UPW production	Urease-coated reverse osmosis membrane **[Choi et al., 2024],** Adsorption, photocatalytic treatment, photolysis, and electrochemical oxidation **[Zhang et al., 2021].**
Urea removal in synthetic and domestic wastewater	Electrochemical oxidation, Adsorption, Hydrolysis, Biological treatment, Membrane separation, Photocatalysis [**Zaher and Shehata, 2021; Zhang et al., 2021**].
Urea removal in artificial kidney systems	Enzymatic hydrolysis of urea, Electro chemical decomposition of urea, Urea sorbents **[van Gelder et al., 2020].**

1.1. Current Technologies for Urea Removal and Management

Currently, various technologies are being investigated for the treatment of urea-rich wastewater and the concurrent recovery of valuable resources. While several of these methods have already been implemented at practical scales, others remain under development. These technologies differ significantly in terms of their physicochemical principles, operational domains, and process configurations. Regardless of these differences, the overarching goals are consistent: to reclaim clean water and high-value compounds from wastewater streams while mitigating environmental contamination. Most existing approaches involve the oxidation of urea into benign end-products such as carbon dioxide (CO_2), water (H_2O), and nitrogen gas (N_2), or its transformation into inorganic ions like ammonium (NH_4^+). The products are then typically subjected to downstream ion-removal or purification techniques in order to complete the treatment process **[Weerakoon et al., 2023; Shaban et al., 2024]**. The majority of these methods require substantial energy input and involve multiple biological stages.

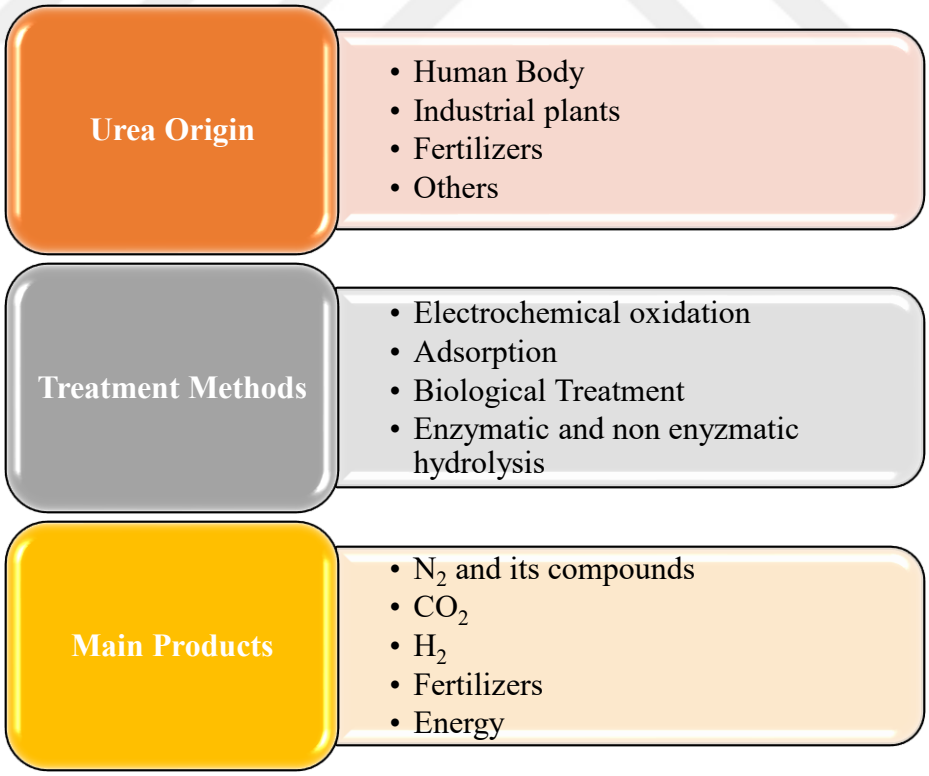

Figure 1.1: Major urea removal methods and their resulting products **[Zaher and Shehata, 2021]**.

To minimize the environmental and health risks associated with urea-rich wastewater and ensure effective urea removal, several highly efficient methods have been developed (Figure 1.1.). These include electrochemical oxidation (EO) **[Ge et al., 2023],** catalytic decomposition **[Gao et al., 2024]**, strong oxidants **[K. Zhang et al., 2023]**, biofilm-based treatments **[Murshid et al., 2023]** , adsorption **[Asiain-Mira et al., 2024]**, and hydrolysis (with or without enzymatic assistance). While each method offers distinct advantages, they also face limitations in terms of practical application, cost, and scalability.

1.1.1. Electrochemical Treatment of Urea

Electrochemical systems have been applied in various configurations and scenarios, resulting in different urea degradation pathways. Electrochemical oxidation involves the decomposition of urea through the loss of electrons, converting it into compounds such as nitrogen gas, hydrogen gas, and carbon dioxide through reactions with the solution. The general equation for this reaction is shown below (1.1) **[H. Wang et al., 2023].**

$$\begin{aligned} &\text{Anode (water) :} 4OH^- \rightarrow H_2O + O_2 + 4e^- \\ &\text{Anode (urea):}\ \ Ure + OH^- \rightarrow N_2 + CO_2 + H_2O \\ &\text{Cathode: } 6H_2O + 6e^- \rightarrow 3H_2 + 6OH^- \end{aligned} \qquad (1.1)$$

The anodic oxidation of urea typically depends on factors such as the anode potential, environmental pH and temperature, urea concentration, and the type of electrolyte used. When different electrolytes are employed, varying by-products may form during the oxidation of urea. For instance, hydroxyl radicals (OH) are produced by the oxidation of water at an active anode. These radicals facilitate the breakdown of urea. Initially, the radicals interact with the electrode surface, triggering its oxidation. The resulting reactive species then further react with urea, oxidizing it. In alkaline conditions, the typical end-products are nitrogen gas, carbon dioxide, and water. At an inactive anode, the generated hydroxyl radicals remain free in the solution and directly react with urea, leading to the formation of ammonium ions (NH_4^+), nitrate ions (NO_3^-), and CO_2. (Figure 1.2.) **[Weerakoon et al., 2023; Zaher and Shehata, 2021; H. Wang et al., 2023].**

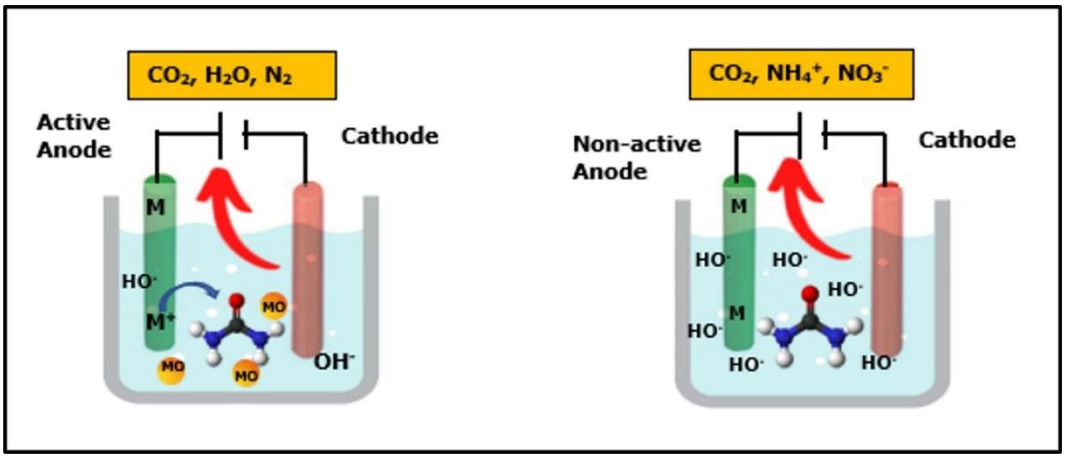

Figure 1.2: Conversion of Urea-Containing Wastewater by Electrochemical Oxidation **[Weerakoon et al., 2023].**

Although electrochemical oxidation has shown promising results in urea removal, several critical factors must be considered, including the choice of electrode material, the applied current, and the oxidation potential of urea **[Mukimin et al., 2025].** For instance, degradation or corrosion of the electrode material may lead to the release of toxic metals and harmful chemicals into the environment. Additionally, the process often requires the use of large quantities of salts as electrolytes, which can significantly increase the total dissolved solids (TDS) content of the treated water. This, in turn, raises both the environmental impact and the cost of subsequent treatment steps needed for electrolyte recovery or purification **[Weerakoon et al., 2023]**.

1.1.2. Elimination of Urea by Absorption Processes

Among current urea removal methods, absorption—used both for urea recovery from urine and in kidney treatment—is one of the primary approaches. This method involves passing urea-containing wastewater through an absorbent bed to capture and remove urea. Sorption in these systems can occur via two mechanisms: physical and chemical. Physical sorption relies on low energy van der Waals interactions, while chemical sorption involves stronger interactions such as covalent or metallic bonding. Commonly used absorbent materials include zeolites, polymeric compounds, and silica-based fillers **[Huang et al., 2024]** . However, several challenges hinder the large-scale application of this method. These include the high cost of absorbent materials, and difficulties in optimizing critical parameters such as surface area, surface morphology, functional groups and pore size distribution. Additionally, the efficiency of urea absorption is highly sensitive to environmental conditions such as pH and

temperature. Once the absorbent reaches saturation, its effectiveness diminishes, requiring regeneration or replacement. Regeneration processes, however, typically involve extra material, time, energy, and cost—making continuous operation less sustainable **[Satyam and Patra, 2024 ; Weerakoon et al., 2023; Zaher and Shehata, 2021].**

1.1.3. Biological Treatment of Urea-rich wastewater

The biological urea treatment method involves exposing urea-containing wastewater to biofilters containing microorganisms capable of breaking down urea. These biofilters house various bacterial strains, such as nitrifying bacteria (*Nitrosomonas* and *Nitrobacter*) and denitrifying bacteria, which transform organic nitrogen into molecular nitrogen. In the biological treatment process, nitrogen bacteria first convert organic nitrogen into ammonium ions. Then, *Nitrosomonas* bacteria oxidize ammonium ions into nitrite ions, followed by *Nitrobacter* bacteria converting nitrite ions into nitrate ions. In the final stage, denitrifying bacteria reduce nitrate ions to molecular nitrogen. However, several challenges hinder the efficiency of this method. These include the sensitivity of microorganisms to environmental conditions, the complexity of the multi-step reaction, and difficulties in maintaining control over the process. Additionally, the method is relatively costly due to the need to regulate parameters such as temperature, pH, inhibitors, initial concentration, and urea flow rate **[Zaher and Shehata, 2021; Urbańczyk et al., 2016].**

1.1.4. Urea Hydrolysis: Enzymatic and Non-Enzymatic Approaches

The hydrolysis of urea leads to the formation of ammonia and carbon dioxide under elevated temperature and pressure conditions. For instance, urea-rich wastewater is typically heated to 200–220 °C under a pressure of 2–3 MPa for approximately 30 minutes. Following heating, the wastewater is cooled to facilitate hydrolysis, resulting in a nitrogen removal efficiency of up to 94% before discharge **[Urbańczyk et al., 2016].** Mahalik and coworkers have reported that higher urea concentrations and elevated temperatures enhance both the urea conversion rate and the overall reaction rate, whereas the mixing rate has a relatively minor effect **[Mahalik et al., 2010]**. According to the literature, thermal hydrolysis exhibits high efficiency in urea removal. When implemented at large scale, it has proven effective in treating urea-

containing wastewater. However, this method presents several limitations, including the requirement for high temperature and pressure conditions, elevated energy consumption, increased operational costs, and the necessity for additional advanced treatment processes to remove ammonia generated during hydrolysis **[Urbańczyk et al., 2016; Zaher and Shehata, 2021; Weerakoon et al., 2023].**

On the other hand, enzymatic decomposition of urea is a highly effective method. In particular, urease enzyme (EC number: 3.5.1.5) catalyze the hydrolytic decomposition of urea and can be utilized in either free or immobilized forms. The catalytic activity of ureases is primarily governed by the nickel atoms located at their active sites and the structural configuration of these sites (Figure 1.3.). Studies have shown that one of the two nickel atoms binds to the carbon atom of urea, while the other interacts with a nitrogen atom, facilitating the cleavage of the molecule **[Saito and Takano, 2022]** .

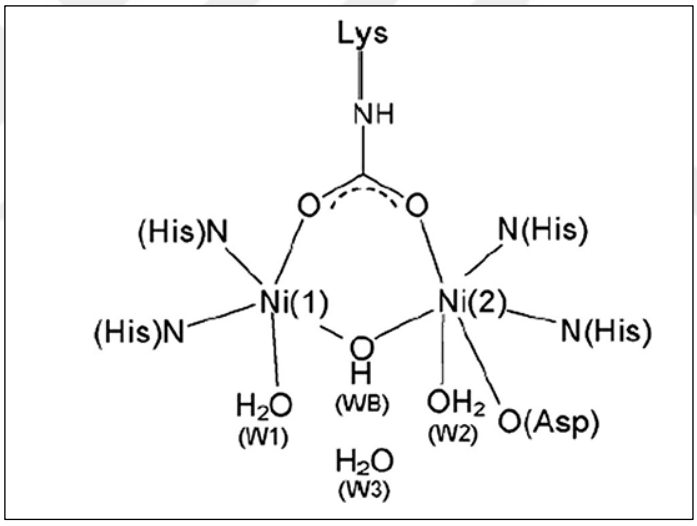

Figure 1.3: Structural representation of the active site of urease enzyme **[Urbańczyk et al., 2016].**

This enzymatic reaction results in the formation of ammonia and carbonic acid. Although enzymatic hydrolysis is considered a promising and environmentally friendly method for treating urea-rich wastewater, it is hindered by several challenges, including enzyme stability, sensitivity to temperature and pH, limited storage time, and lack of reusability. To address these limitations, enzyme immobilization techniques have been developed, offering improved stability, reusability, and resistance to harsh environmental conditions **[Urbańczyk et al., 2016; Yavaşer Boncooğlu, 2024].**

1.2. Immobilization Techniques and Supporting Materials for Urease Enzyme Immobilization

Enzymes are extensively utilized in numerous industrial sectors due to their ability to facilitate environmentally sustainable bioprocessing technologies, enhance production efficiency, and optimize substrate specificity and yield. However, for these biocatalysts to be cost-effective and sustainable, it is essential to improve characteristics that limit their use, such as reusability and shelf life, in industrial applications. Maintaining enzyme activity under industrial conditions is challenging due to their sensitivity to environmental factors. Despite the relatively high cost of immobilized enzymes, they represent a valuable alternative owing to their ability to enhance reusability, prolong shelf life, and ensure stability within the bioprocess **[Califano and Costantini, 2021; Maghraby et al., 2023; Wahab, 2025]**.

The primary objective of enzyme immobilization is to stabilize the enzyme by isolating it from its reaction environment and confining it within a solid support material. This approach mitigates the effects of environmental changes, such as variations in temperature, ionic strength, and humidity, on enzymatic activity. In this context, a wide range of immobilization techniques and solid support materials have been investigated to optimize enzyme performance. Beyond cost-effectiveness, solid support materials are also evaluated based on properties such as inertness, physical strength, stability, renewability, the ability to enhance enzyme specificity and activity, and their capacity to reduce product inhibition, non-specific adsorption, and microbial contamination **[Hormozi Jangi et al., 2020; Wahab, 2025].**

In this context, biopolymer support materials such as alginate, cellulose, and chitosan provide functional groups that can be readily modified for urease enzyme binding **[J. Zhang et al., 2019; Alatawi et al., 2018]** .As seen in Figure 1.4. the effectiveness of immobilization depends not only on the type and properties of the support material but also on the selected immobilization technique, such as covalent binding, encapsulation, or adsorption **[Hormozi Jangi et al., 2020; Kutcherlapati et al., 2016]**.

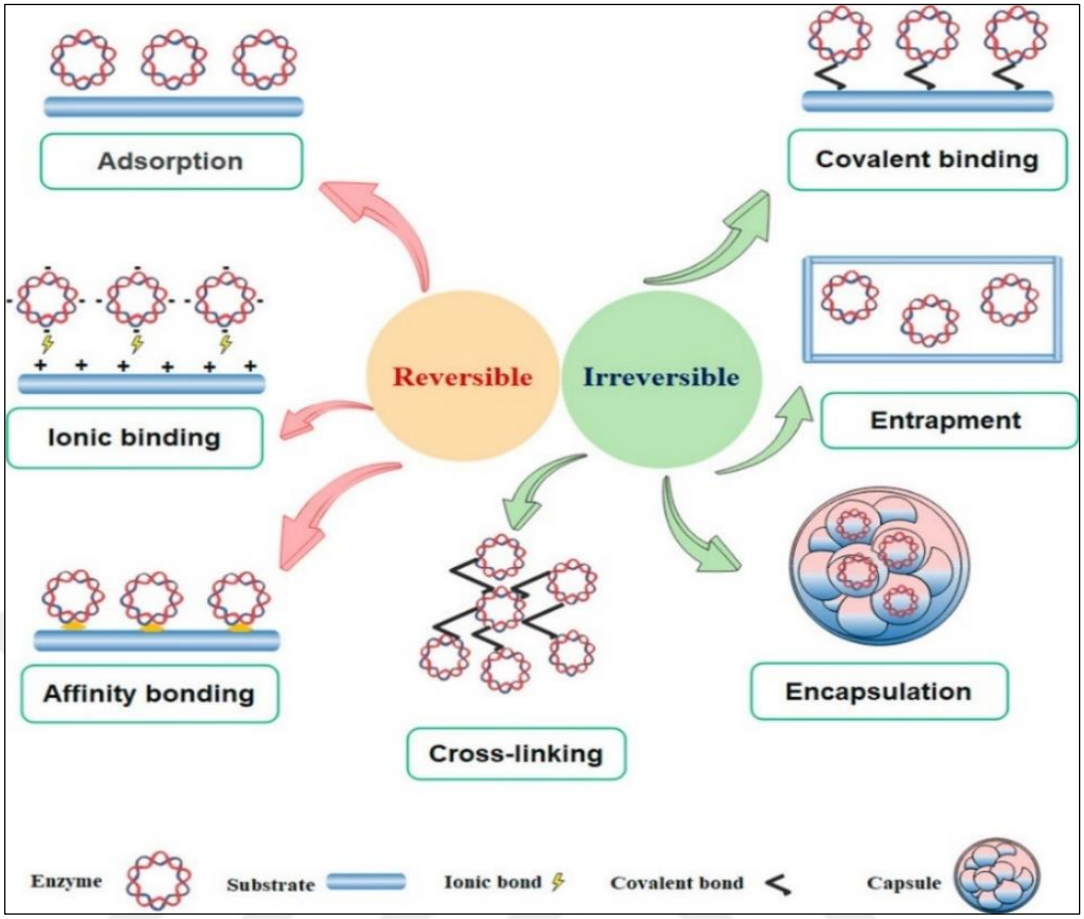

Figure 1.4: The figure provides an overview of the major techniques of enzyme immobilization **[Maghraby et al., 2023].**

Polymers such as collagen, cellulose, and κ-carrageenan are commonly used in the trapping method, whereas membrane entrapment involves liposome and microcapsule formulations. In the process of encapsulation, the enzyme is entrapped within a cell, thereby immobilizing it in the desired configuration for the intended application. However, if the products inside the cell accumulate rapidly, issues such as membrane rupture and leakage may occur. In the trapping technique, enzymes are confined within a membrane formed by polymeric networks, while still allowing permeability and diffusion. The disadvantages of this method include enzyme leakage from the carrier and diffusion limitations **[Wahab, 2025; Maghraby et al., 2023].**

The adsorption/carrier binding method employs insoluble carriers, including polysaccharide derivatives, synthetic polymers, and glass. Enzyme adsorption is defined as the physical and reversible binding of an enzyme to a support material. This process is mediated by weak interactions in a liquid medium, where the enzyme associates with the support based on its affinity. Alternatively, adsorption can be

achieved by applying an electric current in a liquid electrolyte to direct the enzyme toward the support. During adsorption, the enzyme undergoes minimal conformational changes, thereby preserving its functional integrity. Moreover, adsorption has been reported to protect enzymes from aggregation, proteolysis, and unfavorable interactions with hydrophobic interfaces. Despite its simplicity and cost-effectiveness, the method has several limitations, including sensitivity to pH, temperature, and ionic strength, as well as enzyme leakage and weak binding **[Wahab, 2025; Maghraby et al., 2023].**

Among these techniques, covalent binding is often considered the preferred method due to the stronger interactions formed between the enzyme and the support material. The cross-linking/covalent method relies on bi- or multifunctional reagents, such as glutaraldehyde, bisdiazobenzidine, and hexamethylene diisocyanate. In the context of covalent binding, the carrier surface is typically activated using binding agents such as glutaraldehyde. Following this activation step, the enzyme binds to the activated surface, thereby facilitating covalent immobilization. The strength and stability of the covalent bond prevent enzyme leakage, while the enzyme's localization within the carrier material ensures efficient contact with the substrate **[Wahab, 2025; Maghraby et al., 2023].** Extensive research has focused on improving the thermal stability, reusability, and shelf life of the urease enzyme through covalent immobilization on different support materials.

For example, a study was conducted to remove urea from human serum by covalently immobilizing the urease enzyme onto poly(AAm-AGE) cryogel material. This material exhibits desirable properties, including a macroporous structure that facilitates diffusion, a spongy and elastic morphology, and high mechanical strength. The researchers reported that the immobilized urease retained approximately 45.4% of its initial activity after incubation at 65 °C for 300 minutes, compared to 33.8% for the free enzyme. Furthermore, the immobilized urease maintained 62.2% of its activity after storage at 4 °C for 40 days **[Yavaşer Boncooğlu, 2024].** In another study, the urease enzyme was covalently immobilized on an amino-functionalized Al_2O_3/SiO_2 nanocomposite, where the immobilized enzyme retained more than 50% of its initial activity after the ninth reuse cycle. Moreover, following a 45-day storage period at 4 °C, the enzyme preserved 50% of its activity **[Aggarwal and Ikram, 2025].**

Regarding urease enzyme immobilization, parameters such as the homogeneous distribution of the support material, its diffusion properties, and the ability to modify its pore size and structure are of particular importance for both immobilization efficiency and enzyme stability. Extensive research on support materials and immobilization techniques is currently being conducted.

Recent developments highlight the use of porous carriers with high specific surface areas, such as monoliths and beads, as promising alternatives for enzyme immobilization. In particular, High Internal Phase Emulsions (HIPEs) offer several advantages, including facile separation from the enzyme without material loss, recyclability, and potential application as enzyme reactors **[M. Wang et al., 2019] .**

1.3. General Review of High Internal Phase Emulsions (HIPEs) as Promising Carriers for Urease Enzyme Immobilization

Polymeric support materials, such as polyHIPEs formed by the polymerization of HIPEs, possess a highly porous structure with a well-defined open cellular framework, which distinguishes them from other porous polymers **[Wu et al., 2025].** This property makes them suitable for a wide range of applications, including solid-phase peptide synthesis, catalysis, and ion exchange resins **[Dai et al., 2024].** The hydrophilic or hydrophobic nature, porosity, and mechanical properties (softness or hardness) of polyHIPEs can be tailored by optimizing the volume ratio of the aqueous and organic phases during polymerization. Furthermore, the pore size, interconnectivity of cellular windows, and permeability of the support material can be adjusted by varying the type and amount of crosslinking agents, such as glutaraldehyde. These tunable features enable the production of polyHIPE supports with desired properties, making them more versatile than other support materials **[Pashneh-Tala et al., 2023].**

The preparation of polyHIPEs in a laboratory setting involves the careful addition of the internal phase, drop by drop, into the continuous phase under constant stirring with an overhead stirrer. polyHIPEs are typically synthesized via conventional free radical polymerization (FRP), similar to the first St/DVB polyHIPEs, using surfactant-stabilized w/o HIPEs (Figure 3). In this process, the dispersed (internal) phase, located inside the container, generally comprises water, a stabilizer (salts such as sodium chloride (NaCl), calcium chloride ($CaCl_2$)), and an initiator. In contrast, the continuous

(external) phase, surrounding the dispersed phase, consists of a solution of monomer, co-monomer, surfactant, crosslinker, and initiator. The morphology and size of the interconnected pores are influenced by both the type and concentration of the surfactant. The surfactant promotes the thinning of the monomer film that separates each droplet within the emulsion. Continuous stirring has been shown to yield a homogeneous emulsion, as the persistent mixing of the two phases breaks large droplets into smaller ones and suppresses droplet coalescence. Once formed, the HIPE is poured into a mold of the desired size and shape, after which polymerization occurs. During this process, the continuous phase solidifies around the internal phase droplets. This unique feature allows HIPEs to be manipulated through molding, dispersion in immiscible solvents, or casting, enabling the formation of monoliths, beads, and films **[Dhavalikar et al., 2021]**.

The polymerization of HIPEs can be initiated through thermal, ultraviolet, redox, or catalytic methods, each converting the liquid monomer into a solid polymer network. Following polymerization, residual components are removed via washing procedure using water and a low-alcohol solution, typically performed by Soxhlet extraction. This step effectively eliminates the internal droplet phase as well as unreacted monomers. The resulting polymer is subsequently dried under vacuum, yielding a highly porous material with a well-defined internal architecture, commonly referred to as polyHIPE **[T. Zhang et al., 2019].**

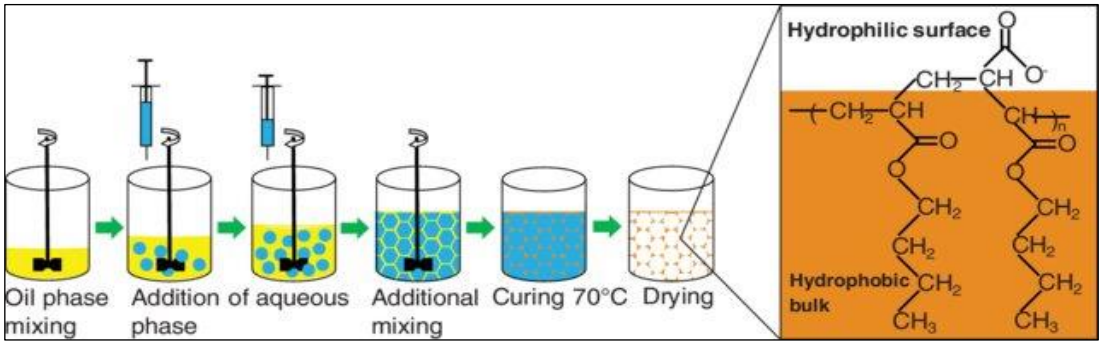

Figure 1.5: Illustration of the conversion of high internal phase emulsions (HIPEs) into porous polyHIPE material via phase mixing, curing, and drying **[Malakian et al., 2019].**

The final polymer has a special structure with pores of different sizes. This structure is mainly affected by the type of HIPE, the polymerization time, and the temperature. When the thin layer between the droplets breaks, the droplets merge **[T. Zhang et al., 2019].** After the droplet phase is removed, empty spaces called pores or cavities appear

as seen in Figure 1.6. These pores are connected to each other, open, and allow fluids to pass through.

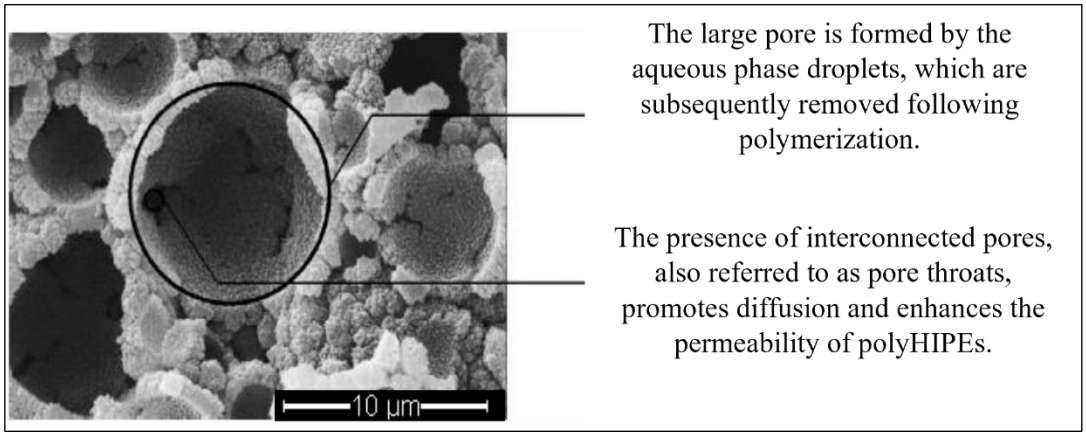

Figure 1.6: SEM (scanning electron microscope) image illustrating the highly porous, interconnected morphology of polyHIPEs, characterized by large voids and pore throats generated through the polymerization of HIPE **[Thumbarathy D., 2018].**

As demonstrated by the SEM image of the polyHIPE material (Figure 1.6), structures with large pores are referred to as lattices, voids, cells, or pores, while smaller pores are described in the literature as interconnections, windows, or pore throats. PolyHIPE synthesis is typically based on styrene and divinylbenzene (Sty-DVB) monomers due to their emulsion stability and ease of polymerization, as demonstrated by extensive research. However, polyHIPEs developed from Sty-DVB exhibit hydrophobic and brittle properties, which may be undesirable for many applications **[McKenzie and Ayres, 2023].** In addition to styrene, other hydrophobic monomers, including butyl acrylate (BA), 2-ethylhexyl acrylate (EHA), and 2-ethylhexyl methacrylate (EHMA), have been employed for the synthesis of polyHIPEs from w/o emulsions. PolyHIPEs also exhibit porosities that frequently exceed 90%, and unmodified polyHIPEs typically possess a surface area of 3–20 m^2/g. Consequently, numerous studies have aimed to enhance the properties of polyHIPEs and expand their applications across diverse domains. For instance, Wu et al., (2025) used butyl acrylate monomer at elevated concentrations from 41.7 mol% to 75 mol% , together with styrene and divinylbenzene (DVB), and employed sorbitan monooleate (Span 80) and sodium dodecylbenzenesulfonate (DDBSS) as surfactants, to produce BA/St/DVB polyHIPE membranes with a substantial open-cell structure and improved durability and porosity compared to St/DVB polyHIPE **[Wu et al., 2025].** Additionally, monomers such as

(meth)acrylics, (meth)acrylamides, silicones, polyesters, and polyurethanes are employed to tailor the physical, mechanical, and chemical properties of polyHIPEs, thereby producing membranes with enhanced elasticity and hydrophilicity for applications including flexible separation membranes, energy storage in soft robotics, and 3D-printed soft tissue engineering scaffolds **[McKenzie and Ayres, 2023].** Similarly,polyHIPE studies incorporating organic soluble monomers, such as gellan gum, into styrene and divinylbenzene have also resulted in materials with more elastic, hydrophilic and porous structures **[Akbari et al., 2024].**

In addition to monomers, surfactants used in polyHIPE synthesis are known as surface-active agents. These agents stabilize emulsions by reducing the surface tension between the inner and outer phases and by forming a rigid film at the interface. Surfactants consist of both hydrophilic head groups and hydrophobic tail sections. They are classified according to the electric charge carried by their head groups: if the head group carries a negative charge, the surfactant is termed anionic; if it carries a positive charge, it is termed cationic; and if it carries no apparent charge, it is termed nonionic. Zwitterionic surfactants, by contrast, have head groups that carry both positive and negative charges. The most commonly used surfactants in polyHIPE synthesis are Span 80, Hypermer 2296, and Hypermer B246SF. Surfactants play two essential roles: they reduce interfacial tension and prevent droplet re-coalescence by promoting breakup. The extent of re-coalescence depends largely on surfactant concentration in the emulsion. When the concentration is insufficient, the protective layer around droplets weakens, causing them to merge upon collision. Because a large portion of the major phase must be dispersed within the minor phase, the surfactant required for stabilization can reach as high as 30% of the external phase by weight **[T. Zhang et al., 2019; Thumbarathy D., 2018].** A study conducted by Dhavalikar reported that an increase in surfactant concentration (5, 10, or 20 wt%) leads to a decrease in pore size and a narrower pore distribution. The researcher also highlighted the effect of surfactant concentration on the production of support materials with the desired pore sizes and distributions **[Dhavalikar et al., 2021].**

A variety of strategies and approaches exist for the functionalization of polyHIPEs, which can be utilized for industrial applications. The recent surge of interest in their chemical functionalization has led to the development of novel porous polymers with a broad spectrum of applications, ranging from tissue engineering to enzyme

immobilization. The capacity to engineer and tailor polyHIPE materials with a wide range of mechanical, chemical, and degradation properties—through the incorporation of monomers, co-monomers, surfactants, and various chemicals and salts—renders them a highly promising alternative material compared to existing support materials.

1.3.1. Potential Application of polyHIPEs for Tissue Engineering

The modification of polyHIPE materials to enhance elasticity, hydrophilicity, porosity, and surface area—thereby overcoming their inherently rigid and brittle morphology—makes them particularly well-suited for tissue engineering applications. For example, it has been reported that polyHIPE scaffolds which were modified by gellan gum, an organic monomer, have high porosity (91–95%) and mechanical stability, and that the monomer contribution increases hydrophilicity and improves surface properties. Furthermore, the usability of the produced material in 3D printing has been demonstrated through in vitro live/dead experiments. Analyses confirmed the cytotoxicity compatibility of the produced polyHIPE scaffolds with human fibroblast cells, revealing their potential to mimic tissue structures such as bone and cartilage, support cell activity, enabling nutrient diffusion, and facilitate vascularization **[Akbari et al., 2024].**

Moreover, it is important to develop a fast, low-cost, and simple method for producing multi-scale porous scaffolds for tissue engineering. The parameters used during the polyHIPE production process directly influence the structure of the final material. Physical factors such as mixing speed, water addition rate, and emulsion temperature affect the internal phase distribution, geometry, and overall porosity, as they act as templates around which droplets polymerize in the continuous phase. Additionally, the type and amount of emulsion components also determine the final architecture, including the internal phase volume, monomer type, solvent addition, surfactant concentration, initiator solubility, and electrolyte concentration in the aqueous phase. These limitations can be addressed by modifying polysaccharides, which are widely used in tissue engineering due to their biocompatibility, biodegradability, and abundance, thereby enabling the formation of additional pores **[Owen et al., 2020].** In a study conducted by Owen and colleagues, alginate beads at ratios of 0%, 50%, and 100% were incorporated into polyHIPEs to rapidly, easily, and cost-effectively introduce larger-scale porosity into polyHIPE-based scaffolds. The cellular activities

of MLO-A5 post-osteoblast cells on alginate-modified polyHIPE scaffolds were then evaluated. Results showed that seeding efficiency was significantly higher compared to unmodified polyHIPEs, while mineralized matrix accumulation was more homogeneous in porous leached scaffolds, accompanied by enhanced cell infiltration **[Owen et al., 2020].**

Furthermore, substrates for in vitro tissue cultures are generally produced using natural or synthetic polymers. For tissue scaffolds designed to support cancer cell growth and vascularization, it is crucial to develop support materials with a suitable pore size and morphological structure that allow oxygen and nutrient transport, as well as waste removal. For example, in one study, researchers modified polyHIPEs based on polycaprolactone methacrylate (PCL-M) as support materials for 3D breast cancer cell (MDA-MB-231) culture. To achieve this, they incorporated gelatin—a low-toxicity, biodegradable, and biocompatible polymer—as a surfactant in the tissue scaffolds to both adjust the pore size and stabilize the emulsions. In vitro evaluation revealed that PCL-M-based polyHIPEs containing gelatin supported 3D breast cancer cell growth with vascular infiltration and tissue integration **[Jackson et al., 2023].**

1.3.2. The Utilization of polyHIPEs in Agricultural Applications

PolyHIPE support materials have the potential to function as soil additives, thereby creating microenvironments within agricultural processes. Specifically, hydrophilic polyHIPE materials have been demonstrated to retain water in soil, thereby ensuring the long-term water requirements of plants. They have also been shown to promote interactions between nutrients and microorganisms, supporting the growth of beneficial microbial communities. In soils supplemented with polyHIPE materials containing fertilizers such as ammonium sulfate, fertilizers are more readily absorbed by plant roots, and fertilizer loss due to leaching is reduced **[Akay, 2023; Kovačič et al., 2022; Vedovello et al., 2024; Zowada and Foudazi, 2023].**

Water loss in arid agricultural lands negatively affects plant growth, the development of beneficial microorganisms, and overall soil fertility. PolyHIPE materials with hydrogel structures and hydrophilic properties can not only reduce water loss due to their water retention capacity but also enable controlled release. In one study, acrylate-based polyHIPE materials were produced, and their effect on soil water kinetics was investigated. The produced materials were ground into powder and added to soil.

Macroporous polyHIPEs exhibited an approximate 700% increase in weight through water absorption in less than one minute **[Zowada and Foudazi, 2023].**

In addition to their water retention capacity, polyHIPE materials can help improve soil quality by removing contaminants from soil and water. For example, atrazine, a widely used herbicide for weed control, can cause toxic effects in soil and drinking water. One study reported that piperazine-derived polyHIPEs were effective in removing atrazine from aqueous solutions. 4-nitrophenylacrylate- and piperazine-modified polyHIPEs facilitated atrazine removal by forming covalent bonds with the contaminant **[Pulko et al., 2007].**

1.3.3. The Use of PolyHIPE as a Solid Support Material for Enzyme Immobilization

Enzymes have numerous applications across various industries, including food, agriculture, and pharmaceuticals. Despite their widespread use, free enzymes generally lack long-term stability and are difficult to recover from the reaction system for reuse. This challenge complicates their repeated application and increases overall enzyme usage costs. Therefore, the immobilization of enzymes has been extensively studied, as it has proven to be an effective strategy for maintaining structural stability, extending shelf life, ensuring reusability, and preventing enzyme inactivation.

PolyHIPE materials support enzyme stability by enabling covalent binding, owing to their porous structure, diffusion properties, durability, and tunable hydrophobic or hydrophilic characteristics. Importantly, compared to other solid support materials, the porosity, chemical functionality, and morphological properties of polyHIPEs can be easily modified. This versatility contributes to sustainability by saving energy, time, and cost in enzyme immobilization processes **[Zverina et al., 2021].**

In one study, the enzyme Candida antarctica lipase B (CALB) was covalently immobilized onto polyHIPE beads. The immobilized enzyme exhibited improved thermal stability, retaining approximately 85% of its initial activity after five reaction cycles and 60% after 30 days of storage **[M. Wang et al., 2019].** Similarly, in another study, *Candida antarctica* lipase B was covalently immobilized on polyHIPE support material, and it was found that the enzyme retained approximately 50% of its initial activity after 10 reuse cycles. In comparison, the lipase retained 42.8 ± 21% of its relative activity after exposure to 60 °C and 49.4 ± 16% after exposure to pH 3.

Notably, the lipase stabilized on the polyHIPE support material maintained its activity at high temperatures and low pH values compared to the free enzyme, thereby increasing its potential for utilization under harsh industrial conditions **[Andler and Goddard, 2018].** Dizge et al. reported that *Thermomyces lanuginosus* lipase immobilized on polyHIPE material demonstrated prolonged activity, maintaining its functionality for 30 days in storage and 15 repeated uses when compared to the free enzyme. The researchers emphasized that the polyHIPE support material preserved enzyme activity with high immobilization efficiency and also enabled the immobilization of large amounts of protein (11.4 mg/g support) **[Dizge et al., 2008].** Andler and Goddard (2018) investigated the immobilization of lipase onto polyHIPE for biodiesel production from industrial oil wastes. The polyHIPE support material, with its internal pores, provides a suitable surface area for the lipase enzyme. The researchers reported that immobilized lipase exhibited a 139% increase in enzyme activity compared to free lipase. Additionally, during the operational cycle, the immobilized enzyme retained 50% of its initial activity, while at high temperatures and low pH values, it maintained 42.8% and 49.4% of its activity, respectively. According to the researchers, these findings demonstrate the potential of polyHIPE materials as solid supports for enzyme stabilization in industrial waste reutilization processes **[Andler and Goddard, 2018].**

Ruan et al., (2016) studied the bioactivity, regeneration capacity, and long-term stability of trypsin immobilized on polyHIPE. They found that the immobilized trypsin could digest bovine serum albumin and cytochrome proteins within 10 minutes, and protein residues were easily removed from the immobilized enzymatic reactor. The researchers highlighted the potential of polyHIPE as a support material for immobilized enzymatic bioreactors, enabling efficient protein hydrolysis, enzyme reusability, and favorable permeability properties **[Ruan et al., 2016].**

As seen in the literature, there are limited studies on the use of polyHIPE as a promising alternative support material in enzyme immobilization. In this thesis study, it was hypothesized that polyHIPE support material would serve as a promising carrier for the covalently immobilization of urease, an enzyme with important and widespread industrial applications, by extending its shelf life and reusability potential while maintaining stability under conditions such as temperature and pH fluctuations.

Apart from this study, no other research has reported the covalent immobilization of urease on polyHIPE support material or tested its pH, temperature, storage stability, and reusability properties in both synthetic and real urea-containing wastewater.

1.4. Resource Recovery from Urea-Rich Human Urine for Agricultural Applications

Ammonia (NH_3) is widely produced and utilized, primarily because of its dual importance as a sustainable resource for clean energy production and as a fertilizer in agriculture. Approximately 80% of global ammonia output is dedicated to the manufacture of nitrogen fertilizers for agricultural use, while the remaining 20% serves as a raw material in the production of other nitrogen-based compounds, such as ammonium nitrate and urea. According to the Food and Agriculture Organization (FAO), global agricultural production demand is projected to increase by 1.1% annually between 2007 and 2050, which will, in turn, drive a parallel rise in the demand for nitrogen fertilizers **[Demirhan et al., 2019].**

Nitrogen is essential for plant growth and development, as it plays a central role in the synthesis of proteins, nucleic acids, phytohormones, chlorophyll, and various other biomolecules. Moreover, nitrogen fertilization has been shown to enhance root nutrient and water uptake, stimulate root growth, boost protein production and nutrient-use efficiency, and promote biomass accumulation. Beyond these benefits, nitrogen application improves both crop yield and quality while also strengthening plants against abiotic and biotic stresses **[Anas et al., 2020].**

Currently, nitrogen fertilizer production relies heavily on non-renewable natural gas. Although plants can acquire nitrogen through biological nitrogen fixation in soils, this method would require approximately 50% more agricultural land—an expansion that is neither feasible nor sustainable, as it threatens biodiversity and natural ecosystems. At present, nitrogen fertilizers are primarily produced in large-scale industrial facilities using natural gas, a byproduct of oil and gas extraction. In recent years, however, the Haber–Bosch (HB) process utilizing renewable feedstocks instead of natural gas has been explored as a promising alternative **[Bertilsson and Kirchmann, 2021].**

HB technology is capable of synthesizing over 90% of ammonia by combining nitrogen and hydrogen gases under extreme conditions (100–200 bar, 400–500 °C). Currently, about 96% of the hydrogen used originates from fossil fuels, mainly natural

gas. During production, ammonia is collected by cooling the reaction mixture from 400–500 °C down to –18 to –24 °C, which condenses ammonia and unreacted gases. Despite its industrial success, the HB process faces significant drawbacks, including high energy demand, operation under extreme pressure, and substantial greenhouse gas emissions. Even with the integration of carbon capture and storage technologies, production costs remain highly sensitive to fluctuations in natural gas prices **[Osorio-Tejada et al., 2022].**

Meeting the growing demand for nitrogen fertilizers in a sustainable manner requires the exploration of cost-effective and environmentally friendly bio-based alternatives. Recent studies have investigated resource recovery methods such as chemical precipitation, ammonia stripping, and electrochemically driven extraction to reclaim value-added compounds—including ammonium sulfate, urea, and struvite—from urea-rich waste streams, particularly human urine **[Luther et al., 2015].**

In urea-rich wastewater, such as human urine, ammonium and phosphate can be removed through chemical precipitation. However, this method is not effective for nitrogen removal. Alternative techniques, including adsorption, membrane separation, and ion exchange, are more complex and time-intensive, as they generate brine streams with high nitrogen and phosphate concentrations. Electrochemical processes—such as electroreduction and electrooxidation—have recently attracted attention as promising approaches for nitrogen and phosphate removal. Nonetheless, these methods face challenges, including increased mass transfer resistance and low transfer efficiency **[Lu et al., 2024].**

By contrast, ammonia stripping enables efficient mass transfer through gas–liquid contact within a packed column, allowing high ammonia recovery from wastewater when temperature, pH, and column material are optimized. The main limitations of this technique are the need for elevated operating temperatures and substantial chemical input. These drawbacks, however, can be mitigated by utilizing waste heat to raise the process temperature, which reduces both energy demand and the quantity of chemicals required for pH adjustment **[Wang et al., 2023].**

1.4.1. Human Urine as a Potential Sustainable Source of Nitrogen Fertilizers

Human urine has emerged as a promising renewable biological resource for the bio-based economy, sustainability, and the development of value-added products in agriculture due to its valuable chemical composition. The complex chemical composition of human urine, comprising urea, ammonia, nitrogen, phosphate, potassium, calcium, magnesium, and sulfur, has been identified as a promising resource for the production of diverse nitrogen fertilizer forms **[Simha et al., 2018; Zuo et al., 2023].**

When urine fertilizer is utilized in agricultural contexts, encouraging outcomes have been documented in relation to crop yield and quality metrics when contrasted with synthetic fertilizer application. The utilization of urine in fertilizer application has been demonstrated to enhance efficiency in both biomass production and phytoremediation. For example, one study examined fresh bean and turnip cultivation in terms of key parameters such as yield, plant tissue chemical composition, nutrient uptake efficiency, and soil nutrient content, comparing human urine fertilizer with synthetic fertilizer. Four different treatments were applied: (1) synthetic fertilizer, (2) urine supplemented with synthetic fertilizer, (3) urine only, and (4) a control group without fertilizer. The highest yields for fall turnips and spring green beans were obtained in treatments 1 and 2, while the turnip yield in the urine-only treatment was significantly higher than in the fertilizer-free control. The study emphasized that human urine, with its nutrients readily available for plant uptake, could serve as an alternative to synthetic fertilizers, showing positive effects on crop yield, root nutrient absorption, and soil nutrient content **[Pandorf et al., 2019].** In another study, the application of human urine as a fertilizer in cabbage cultivation was shown to enhance growth, biomass, and chloride content compared to synthetic fertilizer. Furthermore, the study highlighted that urine fertilization did not pose any hygienic risks to cabbage pickles nor impart a noticeable taste to food products **[Pradhan et al., 2007]**.

Moreover, the upstream separation of urea from urine has the potential to reduce downstream wastewater treatment costs, as human urine comprises 80% of the ammonia nitrogen in domestic wastewater and constitutes 1% of domestic waste. This separation can also reduce the amount of other pharmaceutical compounds entering the sewage system **[Courtney and Randall, 2023; Volpin et al., 2020]**.

1.4.2. Utilization of Urine derived Ammonium Sulfate in Wheat Cultivation

The recovery of ammonium sulfate $(NH_4)_2SO_4$ from human urine has gained increasing attention as a sustainable strategy to address the growing demand for nitrogen fertilizers. Ammonium sulfate is a widely used fertilizer, providing both sulfur (S) and nitrogen (N), and accounts for approximately half of global sulfur consumption. Containing 21% nitrogen (w/w) and 24% sulfur (w/w), ammonium sulfate is considered a highly effective fertilizer for agricultural applications **[Powlson and Dawson, 2022].**

In wheat cultivation, nitrogen fertilization represents a key input that growers can actively manage to enhance both yield and grain quality. The concept of quality extends beyond merely meeting predefined standards to encompass suitability for a range of applications. Wheat protein content and quality are critical determinants of overall grain quality, typically ranging from 7–14%, depending on species, variety, environmental conditions (including climate, soil, and pest or disease pressure), the availability of nitrogen in the soil, and cultural practices such as fertilization, irrigation, and mechanized farming. Grain yield is influenced by the genetic yield potential of the variety, nitrogen availability, climate factors, and agricultural management practices. Thousand-grain weight, a key agronomic trait, is both genetically determined and shaped by factors such as variety, climate, soil conditions, and soil nitrogen levels **[Çakır Öngören S, 2013; Liu et al., 2025]**.

Studies have demonstrated that the application of ammonium sulfate can enhance both the yield and quality of wheat, particularly in bread and durum wheat varieties, with notable effects on traits such as ear height, the number of spikelets per ear, flag leaf area, and water use efficiency **[Hafez et al., 2014]**. For instance,in experiments involving the cultivation of *Triticum aestivum* L. cv. Rezgary and *Triticum durum* desf. cv. Cymito, the application of three different nitrogen fertilizers—ammonium sulfate (AS), diammonium phosphate (DAP), and urea—was reported to significantly improve both yield and quality parameters. Additionally, Çakır Öngören (2013) investigated the effects of different nitrogen fertilizer forms on the yield and quality of various wheat (*Triticum aestivum L.*) varieties, including Victoria, Anapo, Ziyabey, Cumhuriyet-75, and Sagittario. In this study, ammonium nitrate and ammonium sulfate were applied as fertilizers. Key yield parameters, such as spike length, number

of spikes per square meter, grain yield, thousand-grain weight, number of grains per spike, as well as quality indicators including protein and starch content, were evaluated. The results indicated that ammonium sulfate had a positive effect on both yield and quality compared to other fertilizer forms, with particularly positive impacts on thousand-grain weight and starch content **[Çakır Öngören S, 2013].**

The present study was developed in response to promising findings reported in the existing literature. The central hypothesis is that both the yield and quality of wheat cultivation can be improved through the recovery of ammonium sulfate from human urine using an immobilized polyHIPE reactor system. The use of urease enzyme covalently bound to polyHIPE support material to treat human urine and produce ammonium, which is then collected as ammonium sulfate for use as fertilizer, represents a new approach that has not yet been explored in the literature. The overall research design is illustrated in the accompanying **Figure 2.1.**

2. PURPOSE OF THE STUDY

The objective of this study is to apply immobilized enzymatic hydrolysis—recognized as one of the most effective strategies for treating urea-rich wastewater. This was achieved by immobilizing urease within a polyHIPE support material, enabling the conversion of urea into valuable end products such as ammonium sulfate. This approach is particularly promising for industries facing challenges in managing urea-containing effluents.

The central hypothesis of the study is that urea in wastewater can be transformed into useful products, specifically ammonium sulfate, with potential applications in agriculture. To test this, the study explores the use of an enzymatic polyHIPE reactor as an efficient system for urea hydrolysis. The initial focus is placed on evaluating the effects of this reactor on enzyme performance, storage stability, and reusability. Subsequently, the agricultural potential of ammonium sulfate recovered from human urine is assessed.

The specific objectives of the project are as follows:

1. To provide practical solutions for industries dealing with urea-based wastewater through innovative treatment strategies.
2. To recover ammonium sulfate from urea, addressing a critical challenge by converting waste into an agriculturally useful product.
3. To design and develop an enzymatic polyHIPE reactor capable of efficient urea degradation.
4. To contribute to the literature by immobilizing urease on polyHIPE, a versatile material, and operating a reactor that converts urea into ammonia.
5. To evaluate the agricultural impact of applying ammonium sulfate, derived from human urine, as a fertilizer in durum wheat cultivation—a crop of high importance in Türkiye.
6. To develop a domestically produced fertilizer enriched with sulfur and nitrogen, advancing sustainable fertilizer production by utilizing locally available resources.

Additionally, this study investigates the effects of covalent urease immobilization on polyHIPE with respect to pH tolerance, thermal stability, storage duration, and reusability. The goal is to enhance the enzyme's applicability in urea removal and to improve hydrolysis efficiency. The lack of studies on the effectiveness of polyHIPE-immobilized urease reactors for urea hydrolysis, as well as on the agricultural reuse of urea-derived ammonium sulfate from human urine, highlights the unique aspect of this thesis study.

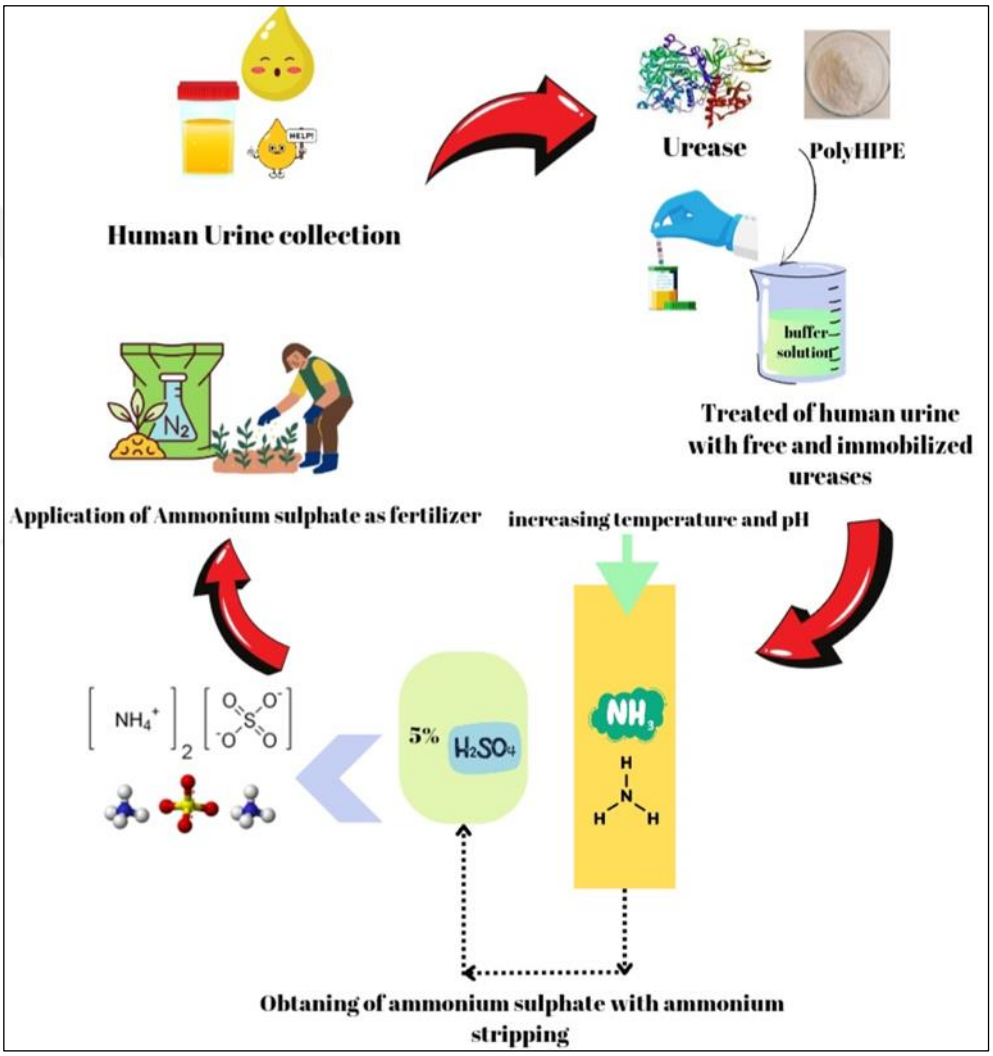

Figure 2.1: Schematic flow of fertilizer potential of human urine using urease-immobilized polymeric high internal phase emulsion.

3. MATERIAL AND METHODS

3.1. Materials

The following chemicals were used in this study: Canavalia ensiformis (jack bean, U4002), glutaraldehyde (GA) solution, sodium hydroxide (NaOH), hydrochloric acid (HCl), and potassium peroxydisulfate ($K_2S_2O_8$). Additional reagents included tris(hydroxymethyl)aminomethane (Tris), sodium acetate (NaOAc), acetic acid (CH_3COOH), sodium chloride (NaCl, ≥99%), ethylene glycol dimethacrylate, Span 80, and urea (99%). A solution with the following composition was prepared: 5% crystal, 85% Tris, and 5% ortho-phosphoric acid. All chemicals were purchased from Sigma-Aldrich (Germany).

From Merck (Germany), styrene (STR), divinylbenzene (DVB), sulfuric acid (95–97%, analytical grade), tert-butanol (for synthesis), and fumed hydrochloric acid (37%, analytical grade) were obtained. Teksoll (96% pure) and Nessler reagent were supplied by Tekkim (Türkiye). Potassium persulfate was purchased from Bio Basic (Canada). Potassium dihydrogen phosphate (ACS reagent) and extra pure sodium hydroxide pellets were obtained from AFG.

3.1.1. Laboratory devices

All laboratory devices used throughout the experiments were shown in Table 3.1.

Table 3.1: Laboratory devices used in thesis study.

Type and Model of Infrastructure/Equipment in the Department (Laboratory, Vehicle, Machinery-Equipment, etc.)	**Purpose of Use in the Project**
Scanning Electron Microscope	Examination of the surface areas of the produced polyHIPE material and measurement of pore sizes.
BET surface area measurement	Measurement of the surface area of the produced polyHIPE material.

Table 3.1: Continued

FTIR	Characterization of the produced polyHIPE materials.
XRD	Characterization of the produced ammonium sulphate.
Drying Machine	Drying the chemicals and glass materials in the study.
Laminar flow cabinet (GTU, MBG Department)	Seed sterilization, Bacteria studies
Sterilizer (GTU, MBG Department)	Sterilization of metal forceps were used for seed sterilization
Plant growth room (GTU, MBG Department)	Seed germination
Greenhouse (GTU, MBG Department)	Pot trials of the product prototype

3.2. Methods

3.2.1. Production Studies of polyHIPE Material

3.2.1.1. Synthesis of polyHIPE Support Material

The production and characterization of the polyHIPE material, as well as the immobilization of urease on the polyHIPE matrix, were carried out using a method previously developed and patented by Prof. Dr. Bülent Keskinler and Prof. Dr. Nadir Dizge **[Dizge et al., 2009]**. In their study, Dizge et al., (2009) immobilized lipase on a polyHIPE material composed of styrene, divinylbenzene, and polyglutaraldehyde , and successfully produced biodiesel from canola oil. Their results demonstrated that STR–DVB–PGA-based polyHIPE is an excellent support medium for enzyme immobilization. This conclusion was attributed to several factors: its potential for economical large-scale preparation within a short time, its high protein immobilization capacity (14 g protein per 1 g polymer), and the presence of dual immobilization mechanisms—covalent bonding and adsorption—enabled by the functional groups of polyglutaraldehyde **[Dizge et al., 2009].**

The synthesis of STR–DVB and STR–DVB–PGA polyHIPE materials with varying GA ratios was performed using the high internal phase emulsion (HIPE) technique. The composition of the synthesized polyHIPE materials is presented in Table 3.2.

Table 3.2: The composition of synthesized polyHIPE materials.

	Organic Phase				Aqueous Phase	
	STR (%)	**DVB (%)**	**Span 80 (%)**	**PGA solution (%)**	**GA (%) in PGA solution**	**$K_2S_2O_8$ (%)**
PolyHIPE0	50	20	30	0	0	1.5
PolyHIPE10	50	20	30	98.5	10	1.5
PolyHIPE15	50	20	30	98.5	15	1.5
PolyHIPE20	50	20	30	98.5	20	1.5
PolyHIPE25	50	20	30	98.5	25	1.5

3.2.1.2. Synthesis of STR-DVB polyHIPE Support Material

PolyHIPE was synthesized by polymerizing the continuous phase of a high-internal-phase emulsion (HIPE) consisting of 13% (v/v) organic phase and 87% (v/v) aqueous phase (Figure 3.1.). The organic phase contained styrene, divinylbenzene, and Span 80, while the aqueous phase contained potassium persulfate. Polymerization was initiated by gradually adding the aqueous phase to the organic phase over 10 minutes under stirring at 450 rpm. Emulsification was continued for a total of 40 minutes using a top-mounted stirrer. The emulsion was then transferred into a cylindrical mold (2.7 cm × 11 cm) and cured at 60 °C for 2 hours, followed by 24 hours at 80 °C. The resulting monolithic polymer was purified with distilled water and tert-butanol and subsequently ground into powder for immobilization studies.

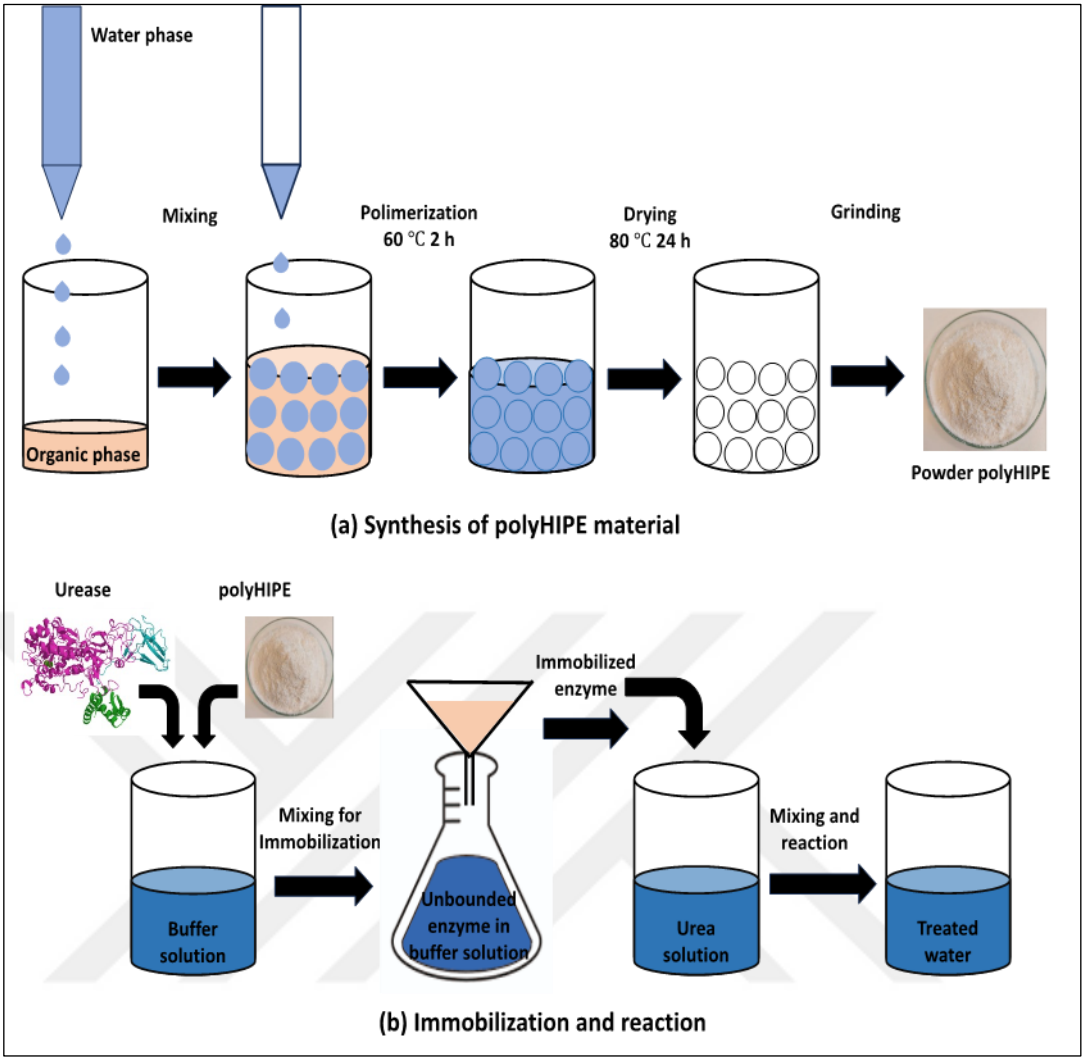

Figure 3.1: Schematic diagram of (a) synthesis of polyHIPE material with polymerization of aqueous phases into organic phase followed by drying and grinding (b) immobilization process of urease enzyme on synthesized polyHIPE support material then treated urea solution with immobilized urease enzyme.

3.2.1.3. Preparation of PGA Solution

PGA solution was prepared by polymerizing glutaraldehyde (GA, 25% w/v) at pH 10.5 for 30 minutes. The required volume of GA solution (25% w/v) was first determined according to the desired PGA percentage, diluted with water, and adjusted to pH 10.5 using 6 N NaOH. The mixture was then stirred at 400 rpm at room temperature for 30 minutes to allow polymerization. The resulting PGA solutions, containing glutaraldehyde concentrations ranging from 0% to 25%, were used as the aqueous phase in the synthesis of polyHIPE.

3.2.1.4. Synthesis of STR-DVB-PGA polyHIPE Support Material

PolyHIPE containing PGA was synthesized by polymerizing the continuous phase of a high-internal-phase emulsion (HIPE) consisting of 13% (v/v) organic phase and 87% (v/v) aqueous phase. The organic phase comprised styrene, divinylbenzene, and Span 80, while the aqueous phase contained potassium persulfate and polyglutaraldehyde. Polymerization was initiated by gradually adding the aqueous phase to the organic phase over 10 minutes under stirring at 450 rpm. Emulsification was maintained for 40 minutes using a top-mounted stirrer. The resulting emulsion was transferred to a cylindrical mold (2.7 cm × 11 cm) and cured at 60 °C for 2 hours, followed by 24 hours at 80 °C. The monolithic polymer was then purified with distilled water and tert-butanol, ground into powder, and used for immobilization studies.

3.2.2. Characterization of polyHIPE Material

The surface morphology and pore distribution of the synthesized polyHIPE materials were analyzed using a scanning electron microscope (SEM, Philips XL 30S FEG). The functional group composition was characterized by Fourier transform infrared spectroscopy (FTIR, Perkin Elmer FT-187 IR Spectrum 100) within the wavelength range of 4000–650 cm^{-1}.

3.2.3. Urease Immobilization

Immobilization was carried out by adding 500 mg of polyHIPE material to 10 mL of phosphate buffer (25 mM, pH 7.0) containing urease enzyme (1 mg/mL) and incubating at 25 °C for 24 hours. Following incubation, the polyHIPE material was washed with phosphate buffer to remove unbound enzyme. The supernatant and wash solutions were analyzed to quantify the unbound enzyme and determine the immobilization yield. Protein concentration was measured using the Bradford method (Bradford, 1976), with bovine serum albumin (BSA, Sigma–Aldrich) standard solutions (0–120 mg/L) employed to generate the calibration curve (Appendix A). The immobilized enzyme was stored in phosphate buffer (25 mM, pH 7.0) at 4 °C until use.

The amount of urease immobilized on the polyHIPE support and the immobilization efficiency were calculated using the following equations:

$$\text{Immobilization efficiency } = \frac{(E_0 - E)}{E} \times 100 \quad (3.1)$$

$$\text{Immobilized urease amount} = \frac{\text{mg enzyme}}{\text{g support}} = \frac{(E_0 - E)}{\text{g support}} \times 100 \quad (3.2)$$

where, E_0 and E refer to the initial amount of urease in the solution and the urease amount in the supernatant, respectively.

3.2.4. Characterization of Urea Containing Wastewaters

The experiments were initially carried out using synthetic wastewater containing urea to determine the optimal operating conditions, after which studies were conducted with human urine. For the synthetic wastewater experiments, solutions containing 20–200 mmol of urea were prepared. Human urine samples were collected from volunteers aged 20–30 years and stored at +4 °C until analysis. The characterization of urine samples included measurements of conductivity, pH, ammonium, urea, Total Kjeldahl Nitrogen (TKN), Chemical Oxygen Demand (COD), and phosphate. The results of the human urine characterization are presented in Table 3.3. below.

Table 3.3: Characterization of human urine samples.

Parameter	Unit	Value
Urea	mg/L	19350
Ammonia	mg/L	252
Chemical oxygen demand (COD)	mg/L	5980
pH	-	5.71
Phosphate	mg/L	1092
Conductivity	mS/cm	8.03

3.2.5. Urease Activity Assay

The specific activities of free and immobilized urease were determined using a modified method described by **[Srinivasa Rao et al., 1995].** Urease activity was evaluated based on its ability to hydrolyze urea into carbon dioxide and ammonia. For this purpose, 100 µL of free urease solution or 10 mg of immobilized urease were added to 5 mL of urea solution (pH 7.0). The mixtures were incubated at 25 °C with stirring for 5 minutes. Subsequently, 1 mL of the reaction mixture was treated with 1 mL of Nessler's reagent, and the volume was adjusted to 10 mL with distilled water.

The absorbance of the resulting brown-colored solution was measured against a blank at 480 nm using a UV spectrophotometer. A calibration curve was prepared using ammonium sulfate standard solutions at concentrations ranging from 0 to 1.2 mg/mL (Appendix B).

The relative activity of urease was defined as the number of micromoles of ammonia released per minute. The relative activity was calculated according to Equation (3.3):

$$\text{Relative activity (\%)} = \frac{\text{Activity}}{\text{Maximum activity}} \times 100 \qquad (3.3)$$

3.2.6. Optimization of the Immobilization Procedure

3.2.6.1. The Effect of polyHIPE Modification on Immobilization Efficiency

To evaluate the immobilization efficiency, two types of polyHIPE materials were tested: unmodified (STY–DVB) and polyglutaraldehyde-modified (STY–DVB–PGA). In addition, the effect of varying PGA content on the immobilization efficiency of the STY–DVB–PGA material was investigated.

3.2.6.2. The Effect of the amount of polyHIPE on Immobilization Efficiency

Immobilization experiments were performed using a fixed enzyme concentration of 1 mg/mL to investigate the effect of polyHIPE amount on immobilization efficiency. The reactions were carried out at pH 7 and 25 °C for 24 hours, using varying amounts of polyHIPE (50–500 mg). The results are reported as immobilization efficiency, relative activity, and the amount of immobilized enzyme expressed per unit mass of polyHIPE (mg urease/mg polyHIPE).

3.2.6.3. The Effect of Incubation Time on Immobilization Efficiency

The effect of incubation time on urease immobilization on the polyHIPE material was evaluated over periods ranging from 3 to 24 hours (3, 5, 8, 12, 15, 18, and 24 hours).

3.2.7. Investigation of the Enzyme Performance

A series of experiments was conducted to evaluate the performance of free and immobilized urease in both synthetic wastewater and human urine, with a focus on the effects of pH, temperature, and ionic strength.

The effect of pH on relative activity in synthetic urea-containing wastewater was assessed using buffer solutions across the pH range 4.0–9.0: acetate buffer (pH 4.0–5.5), phosphate buffer (pH 6.0–8.0), and Tris-HCl buffer (pH 8.5–10.0). Temperature effects were examined by conducting urease activity assays at 25–55 °C while maintaining pH 7.0. The influence of ionic strength was investigated using urea solutions containing NaCl at concentrations of 1, 2, and 3 g/L at pH 7.0 and 25 °C.

The performance of free and immobilized urease in human urine was further evaluated at pH values ranging from 4.0 to 9.0 (adjusted with NaOH and HCl) and at temperatures between 25 °C and 45 °C. Following the addition of free or immobilized enzyme to urine samples, the mixtures were incubated for 10 minutes, after which ammonia production was quantified, and relative activity was calculated under each condition.

3.2.8. Optimization of Relative Activity of Immobilized Enzyme based on BBD Experiment

To determine the optimal relative activity of the immobilized enzyme, both single-factor experiments and a three-factor Box–Behnken Design (BBD) at two levels were conducted. Experimental design and statistical analysis were carried out using Design Expert 12.0 software (Stat-Ease Inc., USA, licensed by ICAR-CMFRI). The factors evaluated were sodium chloride concentration (A: 0–3 g/L), pH (B: 4–9), and temperature (C: 25–55 °C). The experimental conditions are summarized in Appendix C. The relationship between the factors and the response was modeled using a second-order polynomial equation.

$$Y = \beta_0 + \beta_1 X_1 + \beta_2 X_2 + \beta_3 X_3 + \beta_{12} X_1 X_2 + \beta_{13} X_1 X_3 - \beta_{23} X_2 X_3 - \beta_{11} X_1^2 - \beta_{22} X_2^2 - \beta_{33} X_3^2 \quad (3.4)$$

the model used X_i as the independent coded factors, Y as the predicted response of relative activity of immobilized enzyme, β_0 as the intercept, and β_i, β_{ii}, and β_{ij} as the

linear coefficient, quadratic coefficient and interaction coefficients of the polynomial model, respectively.

3.2.9. Reusability and Shelf-life

The reusability of immobilized urease was assessed by incubating polyHIPE-immobilized enzyme in 100 mM urea solution (pH 7.0) at 25 °C for 10 minutes. After incubation, the polyHIPE material was separated, washed with phosphate buffer, and reused in fresh 100 mM urea solution. This cycle was repeated six times, and the relative activity of immobilized urease was measured after each cycle.The storage stability of free and immobilized urease was evaluated by monitoring relative activity during storage at 25 °C. Both forms of the enzyme were kept in phosphate buffer (25 mM, pH 7.0), and their initial activities were recorded daily for 10 days.

The reusability of immobilized urease in human urine was also investigated. PolyHIPE-immobilized urease was incubated with human urine (pH 7.0, 25 °C) for 10 minutes, then separated, washed with phosphate buffer, and reused in fresh urine. This process was repeated ten times, and relative activity was determined after each cycle. Storage stability under the same buffer conditions (25 mM phosphate buffer, pH 7.0, 25 °C) was assessed by daily activity measurements over a 10-day period.

3.2.10. Kinetics Studies

The kinetic properties of free and immobilized urease were evaluated using the Michaelis–Menten model and the Lineweaver–Burk method. In these assays, 100 µL of urease solution (1 mg/mL) or 40 mg of immobilized urease was used to catalyze the hydrolysis of urea at concentrations ranging from 10 to 100 mM. The resulting concentrations were converted to micromoles of NH_3, and the initial reaction rates (V_0) were calculated in IUB (International Union of Biochemistry) units, expressed as micromoles of NH_3 per milligram of enzyme per minute.

3.2.11. Design and Development of Enzyme Immobilized polyHIPE Reactor

Enzyme immobilization was performed using a polyHIPE reactor. The column employed in these experiments had a diameter of 10 mm, a height of 150 mm, and a volume of 12 mL (Figure 3.2). The column was packed with 1 g of polyHIPE support

material, which had been pre-immobilized by incubating in phosphate buffer containing urease (1 g/mL) for 15 h. This incubation period was previously optimized to ensure maximum immobilization efficiency. The efficiency of urease immobilization was assessed by determining the protein concentration in the effluent. After immobilization, the polyHIPE column was introduced into the reactor, and its structural integrity was carefully examined to confirm the absence of channels or air pockets.

Human urine was then introduced into the reactor at predetermined linear flow rates using a peristaltic pump, and the reactor was operated for at least 1 h at each flow condition. Ammonia nitrogen concentrations were measured at the reactor outlet, where no time-dependent variations were detected across the three flow rates. Urea and ammonia nitrogen concentrations were determined at both the inlet and outlet, and urea hydrolysis efficiencies were calculated for the column reactor operated at linear velocities of 0.5, 1, and 5 $m^3/m^2 \cdot h$.

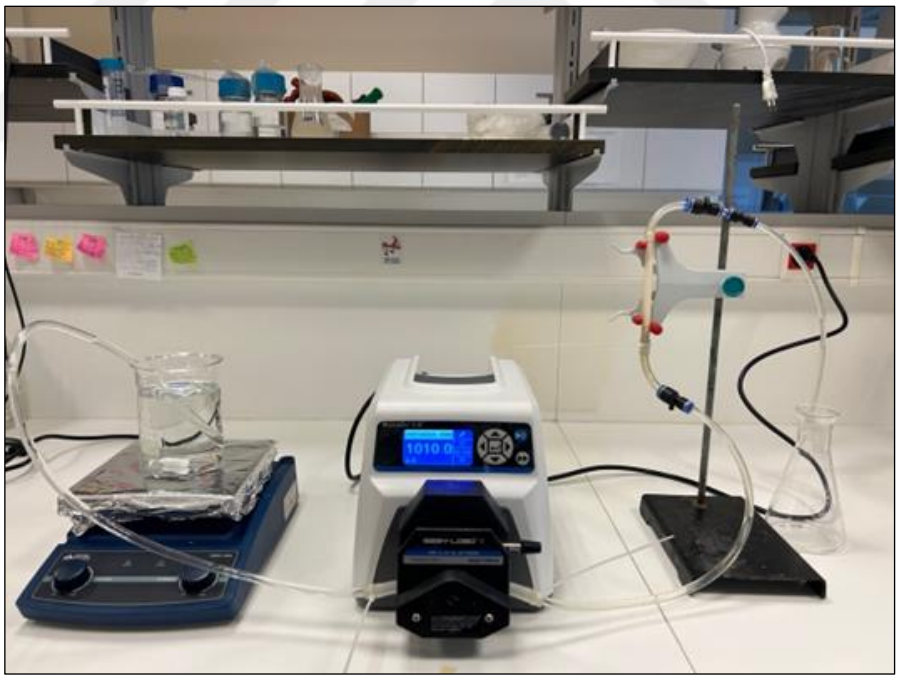

Figure 3.2: Enzyme immobilized polyHIPE reactor.

3.2.12. Hydrolysis of Urea to Ammonia and Production of Ammonium Sulfate by Enzymatic polyHIPE Reactor

In this section, wastewater containing urea was treated using urease immobilized on polyHIPE material. The process involved enzymatic hydrolysis of urea, subsequent

precipitation in sulfuric acid, and crystallization to produce ammonium sulfate. A schematic diagram of the ammonium sulfate recovery process from human urine using an immobilized urease-polyHIPE reactor is shown in Figure 3.3.

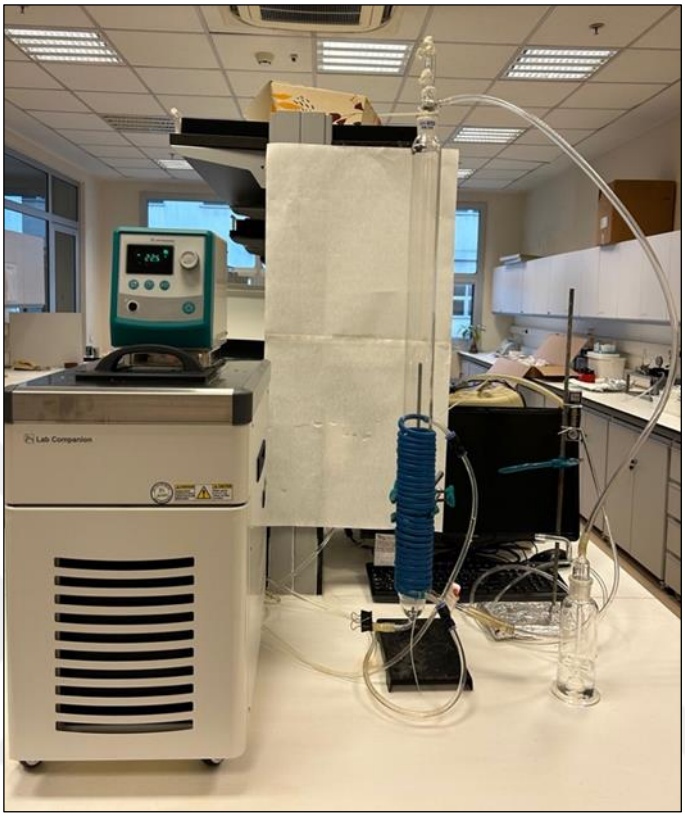

Figure 3.3: Ammonia stripping column.

Conventionally, ammonium sulfate is synthesized through the reaction of anhydrous ammonia with sulfuric acid:

$$2NH_3 + H_2SO_4 \longrightarrow (NH_4)_2SO_4 \quad (3.5)$$

In aqueous solutions, ammonia exists primarily as ammonium ions at pH 7. At higher pH values (10.5–11.5), ammonia shifts into the dissolved gas phase. Increasing the pH from 7 to 11.5 enhances the concentration of gaseous ammonia, which can then be removed by air stripping. According to **[Speight, 2017]**, this process is more efficient at slightly alkaline conditions (pH 8.5–9.0) and heating the solution to 60–65 °C further improves stripping efficiency.

In the present study, human urine was first hydrolyzed using immobilized urease to release ammonia. Ammonia recovery was then carried out via air stripping at varying pH values (9.0, 10.0, and 11.0) and temperatures (25, 35, 40, and 65 °C). A series of

experiments were performed to optimize stripping conditions. The setup consisted of a column (5 cm diameter, 70 cm length) fitted with a diffuser at the base, with temperature control provided by a water bath. For each batch run, 500 mL of human urine was introduced into the column, the water temperature was adjusted, and air (1 m^3/h) was passed through the column from the bottom to strip ammonia.

The stripped ammonia was recovered by crystallization as ammonium sulfate, using a 5% (v/v) aqueous sulfuric acid solution. Crystals were obtained by evaporating the saturated solution. The crystalline structure of ammonium sulfate was characterized by X-ray diffraction (XRD, Rigaku Rint 2200) at room temperature, employing Cu Kα radiation (40 kV, 40 mA) with a 2θ resolution of 2.0–25°.

3.2.13. Investigation the Effect of Ammonium Sulfate as Fertilizer on the Yield and Quality of Wheat

Wheat is a globally strategic crop and, in Türkiye, constitutes a primary source of both energy and protein in the human diet. According to 2008 data, wheat-based products account for approximately 40% of the daily energy intake in Türkiye **[Web 1].** An overview of national agricultural land use indicates that around 50% of cultivated areas are dedicated to cereals, of which nearly 70% are allocated to wheat production **[Web 1].**

Wheat (*Triticum aestivum L.)* is cultivated in Turkey for bread, pasta (Triticum durum), and biscuits (Triticum compactum). Among these, durum wheat is a tetraploid species (2n = 4x = 28, AABB) with distinctive quality characteristics and specialized applications compared to bread and biscuit wheat. Durum wheat is primarily grown for pasta production, which has led to its large-scale cultivation in Europe and North America. In addition, it is used in the production of bulgur, couscous, and a variety of breads, particularly in Türkiye, the Middle East, and North Africa **[Beres et al., 2020]**.

In this thesis, durum wheat was chosen as the plant material due to its broad utilization and high production demand. Specifically, the effect of ammonium sulfate—derived from human urine—on crop yield was investigated using the ‘Eminbey’ durum wheat variety. As a winter wheat, ‘Eminbey’ requires vernalization, i.e., exposure to a cold period, to initiate germination. Seeds of this variety were obtained from the Field Crops Research Institute in Ankara, Türkiye. Before germination, they underwent vernalization at 4 °C for six weeks, followed by sterilization according to the method

of **[Hurek et al., 1994].** Seedlings were incubated in darkness at 27 °C for two days on Murashige and Skoog (MS) medium lacking growth regulators.

The fertilizer treatment consisted of 0.5 g (equivalent to 5 kg/ha) of ammonium sulfate derived from urea-containing wastewater, supplemented with 0.5 g (5 kg/ha) of commercial phosphorus and potassium, applied to pots containing 2 kg of soil each. Additional applications of urine-derived ammonium sulfate were made during plant development: 7 g per pot at the tillering stage and 0.3 g per pot at the initial heading stage. In total, each pot received 1.5 g of pure nitrogen. Negative controls consisted of unfertilized pots, while positive controls contained the same nitrogen dosage supplied as commercial ammonium sulfate (Gübretaş).

Yield potential was evaluated based on several agronomic traits, including spike length, spikes per square meter, grain yield, thousand-grain weight, and grains per spike. Grain quality was assessed by measuring color parameters (brightness, redness, and yellowness) with a Gardner MiniScan XE Plus (Hunter Lab, Reston, USA), while grain size, moisture content (%), and hardness were determined using the Single Kernel Characterization System (SKCS 4100, Perten Instruments, Stockholm, Sweden). Data on yield and quality were analyzed using analysis of variance (ANOVA), and mean comparisons were performed with the least significant difference (LSD) test at $P \leq 0.05$, following a randomized block design, using the SPSS statistical software package. The gluten and starch contents of wheat grains cultivated in pots with either commercial fertilizer or human urine derived urea-based fertilizer were analyzed through outsourced service testing. Gluten content was determined according to the AACC method, while starch content was quantified using a commercial assay kit.

4. RESULTS AND DISCUSSION

4.1. Characterization Studies of polyHIPE Support Material

The polyHIPE materials were synthesized according to the formulations provided in Table 3.2 of the Materials and Methods section. Their surface morphology and pore distribution were characterized using SEM analysis, while FT-IR spectroscopy was employed to detect surface modifications and identify functional groups. The FT-IR spectra of the synthesized polyHIPEs are presented in Figures 4.1a–c. The Fourier-transform infrared (FT-IR) spectrum of the unmodified polyHIPE (polyHIPE0) showed peaks at 3340 cm^{-1} and 1635 cm^{-1}, corresponding to hydroxyl and carboxyl group vibrations, consistent with previous reports **[Z. Huang et al., 2018]**. After modification with PGA, the intensity of these signals decreased. In addition, new adsorption peaks were observed at 1721 cm^{-1}, 1400–1450 cm^{-1}, and 1026 cm^{-1}, which can be assigned to non-conjugated aldehyde groups, aliphatic C–H in-plane bonds, and aliphatic C–H out-of-plane bonds, respectively **[Dizge et al., 2008].**

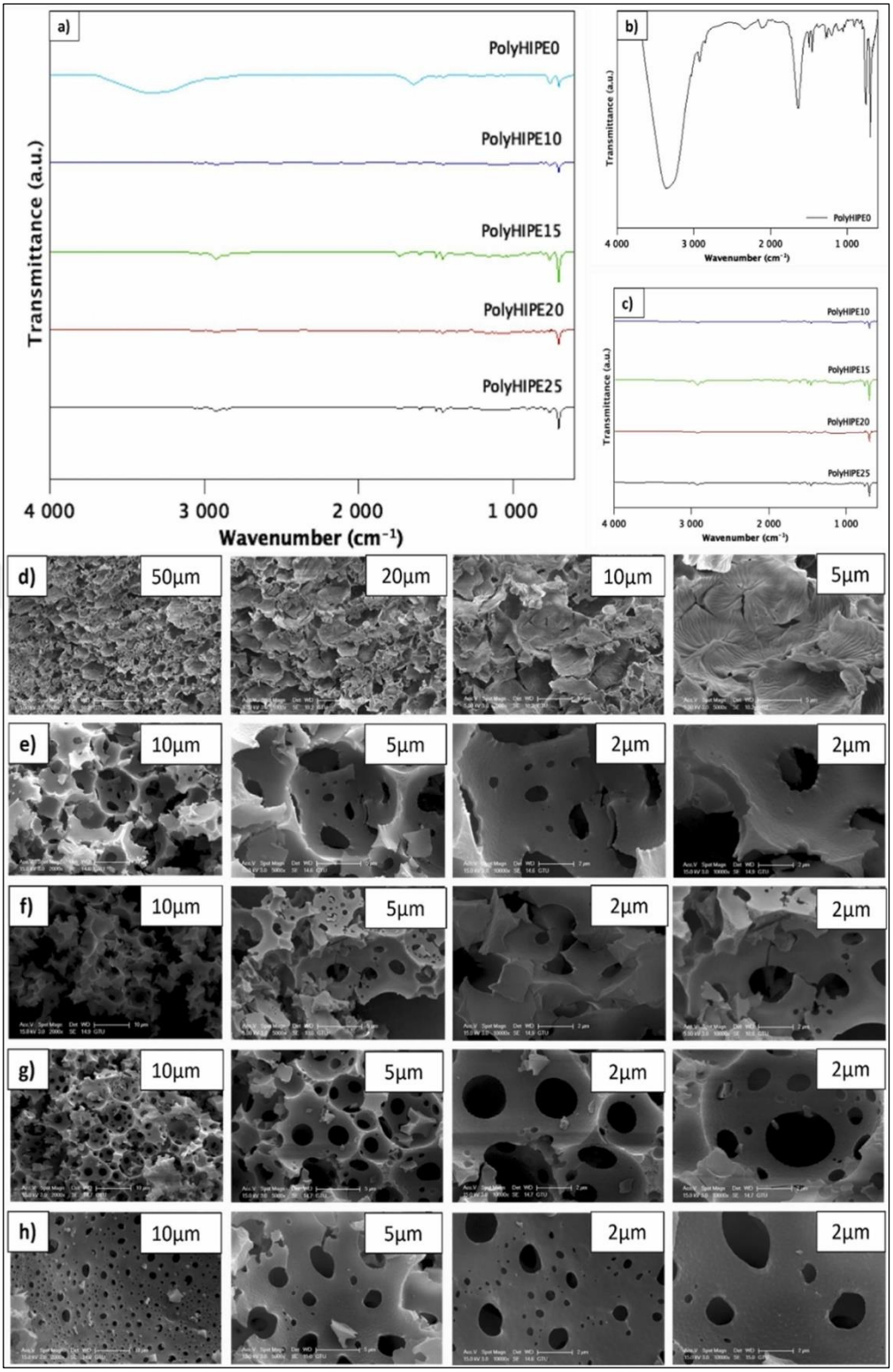

Figure 4.1: FT-IR analysis results of the (a) synthesized all polyHIPE materials, (b) polyHIPE0 (STR–DVB without GA) and (c) polyHIPE10 (STR–DVB containing for 10% GA), polyHIPE15 (STR–DVB containing for 15% GA), polyHIPE20 (STR–DVB containing for 20% GA), and polyHIPE25 (STR–DVB containing for 25% GA), SEM images of the synthesized polyHIPE materials (d) polyHIPE0, (e) polyHIPE10, (f) polyHIPE15, (g) polyHIPE20, and (h) polyHIPE25.

SEM micrographs of the five polyHIPE variants are shown in Figure 4.1d–h. All samples exhibited the characteristic features of polyHIPE materials, including voids and interconnected pore networks. Among them, polyHIPE20 and polyHIPE25 displayed particularly well-developed porous structures, which are key parameters for defining polyHIPE morphology. Adjusting the concentration of crosslinkers, such as glutaraldehyde, has been shown to influence the internal architecture and pore dimensions of these materials. Increasing the glutaraldehyde content in the HIPE system enhances the covalent binding capacity of the support material for enzymes, while simultaneously affecting pore size, surface area, and permeability **[Ruan et al., 2016].**

4.2. Optimization Studies on Support Materials for Immobilization Procedure

This study examined the influence of polyHIPE (STR–DVB) and PGA-modified polyHIPE (STR–DVB–PGA) on the immobilization efficiency of urease, using polyHIPE amounts ranging from 50 to 500 mg. In addition, the effect of incubation time (3–24 hours) on immobilization efficiency was also evaluated.

4.2.1. Investigation of the effect of polyHIPE Modifications on Immobilization Efficiency

Two different polyHIPE material unmodified (STR–DVB) and modified with polyglutaraldehyde (STY–DVB–PGA) tested to determine the highest immobilization efficiency. Additionally, the effect of the amount of PGA on immobilization efficiency of modified STY–DVB–PGA material also investigated.

The immobilization efficiencies of urease on the different polyHIPE materials are presented in Figure 4.2. The respective efficiencies for polyHIPE10, polyHIPE15, polyHIPE20, polyHIPE25, and polyHIPE0 were 81.1%, 86.7%, 95.1%, 80.8%, and 65.5%. When the PGA concentration was increased from 10% to 20%, the immobilization efficiency reached 95%. The highest efficiency was observed with polyHIPE20 (20% GA), and subsequent experiments were performed using this material.

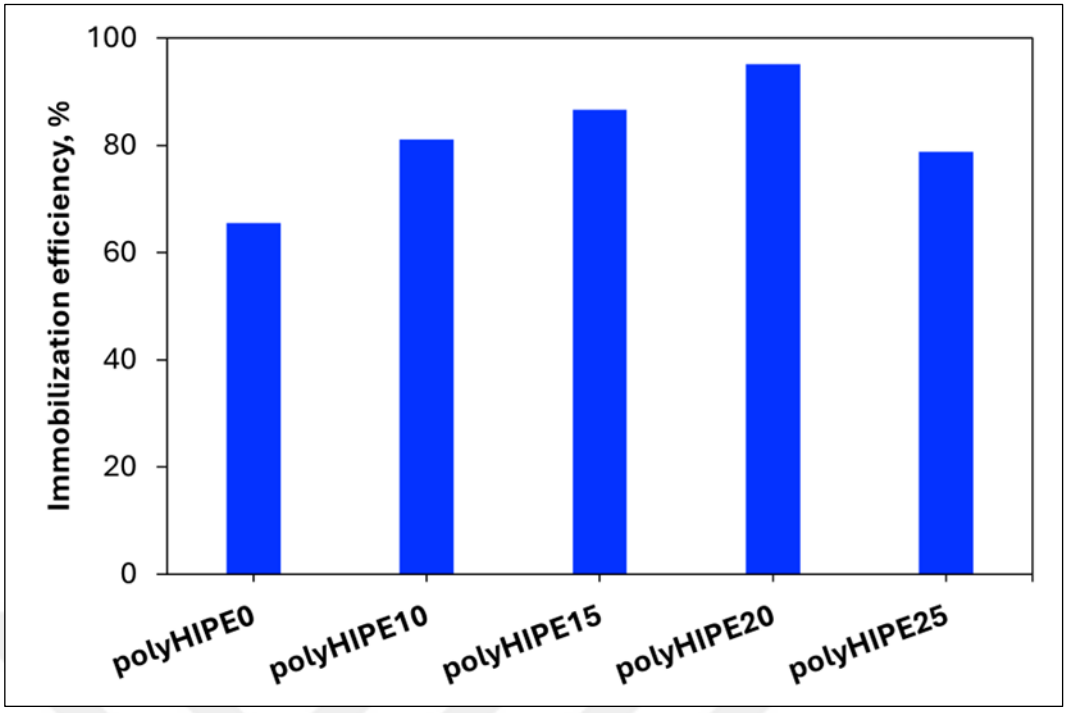

Figure 4.2: Urease immobilization efficiency of the synthesized polyHIPE materials (500 mg polyHIPE; 1 mg/mL urease amount; pH 7; 24-hour incubation time; 25˚C temperature).

Dizge et al., (2009) reported that the immobilization efficiency of lipase on PGA-containing polyHIPE was 76.0%, compared to 63.3% on polyHIPE without **[Dizge et al., 2009].** In monolithic polymeric systems such as polyHIPE, the incorporation of PGA into the emulsion promotes enzyme immobilization through both covalent and adsorption interactions, targeting protein functional groups such as amino, thiol, imidazole, and phenol groups. Increasing the PGA concentration in polyHIPE emulsions has been shown to enhance the permeability of the support material and improve enzyme activity. However, excessive PGA content may lead to the formation of a soft, non-elastic monolithic structure, ultimately reducing immobilization efficiency **[Ruan et al., 2016].**

4.2.2. Investigation of the effect of the amount of polyHIPE on Immobilization Efficiency

After the identification of polyHIPE20 as the optimal polyHIPE material, the impact of varying polyHIPE amounts on immobilization efficiency and immobilized enzyme activity was investigated (Figure 4.3a-c). Immobilization studies were conducted by adding varying quantities of polyHIPE20 to a constant enzyme concentration of 1 mg/mL at a pH of 7 and a temperature of 25°C for a duration of 24 hours. The outcomes

of these studies indicated that the immobilization efficiency exhibited a positive correlation with the amount of polyHIPE added, reaching a maximum of 95.1% with the addition of 500 mg of polyHIPE. However, the enzyme activity of the immobilized enzyme decreased with increasing polyHIPE amounts, reaching its lowest at 500 mg of polyHIPE. In contrast, while immobilization efficiencies remained comparable at 100, 150, and 200 mg of polyHIPE, enzyme activities exhibited an increase with elevated polyHIPE concentrations. This phenomenon indicates that the presence of inadequate binding sites on the support material at lower polyHIPE amounts resulted in enzymes binding to each other's active sites. Consequently, this led to increased enzyme activity, despite the presence of similar immobilization efficiencies.

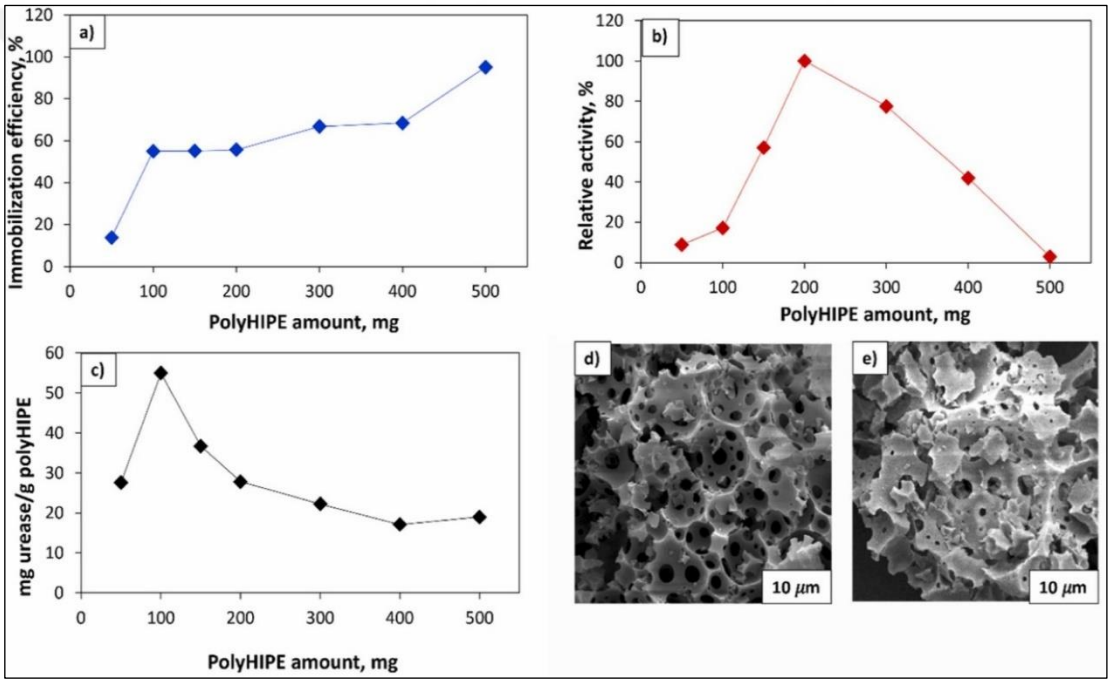

Figure 4.3: The effect of the amount of polyHIPE material on the immobilization efficiency (1 mg/mL enzyme concentration; incubation time 24 h; pH 7; 25°C temperature), (a) the immobilization efficiency with increasing polyHIPE amounts, (b) the enzyme activities with increasing polyHIPE amounts, (c) the amount of immobilized enzyme per unit polyHIPE with increasing polyHIPE amounts, SEM images of polyHIPE20 (d) before urease immobilization, (e) after urease immobilization.

SEM images of polyHIPE20 before and after urease immobilization illustrate its intricate microstructure. Prior to immobilization, polyHIPE20 exhibited interconnected microspheres with thin walls (Figure 4.3d). After immobilization, the porous architecture facilitated enzyme attachment, with both macro- and micro-pores contributing to an increased enzyme loading capacity (Figure 4.3e). These

observations align with previous reports highlighting the suitability of polyHIPE as a support for enzyme immobilization, owing to its high surface area and well-defined pore network **[Ruan et al., 2016].**

4.2.3. Investigation of the effect of Incubation Time on Immobilization Efficiency

The effect of incubation time on urease immobilization on polyHIPE material was investigated over periods ranging from 3 to 24 hours (3, 5, 8, 12, 15, 18, and 24 hours).

Incubation time significantly influenced both immobilization efficiency and the relative activity of the immobilized enzyme. As shown in Figure 4.4a, immobilization efficiency and enzyme activity gradually increased, reaching their maximum at 15 hours, after which they began to decline. A slight increase in both parameters was observed beyond 18 hours, could be due to the re-adsorption of desorbed enzymes, reflecting an adsorption–desorption mechanism. These results indicate that a 15-hour incubation period is optimal for urease immobilization on polyHIPE. Comparable findings were reported by Hormozi Jangi et al., (2020), who demonstrated that a 15-hour incubation yielded the highest immobilization efficiency and relative activity for urease on amino-functionalized magnetic nanoparticles **[Hormozi Jangi et al., 2020].**

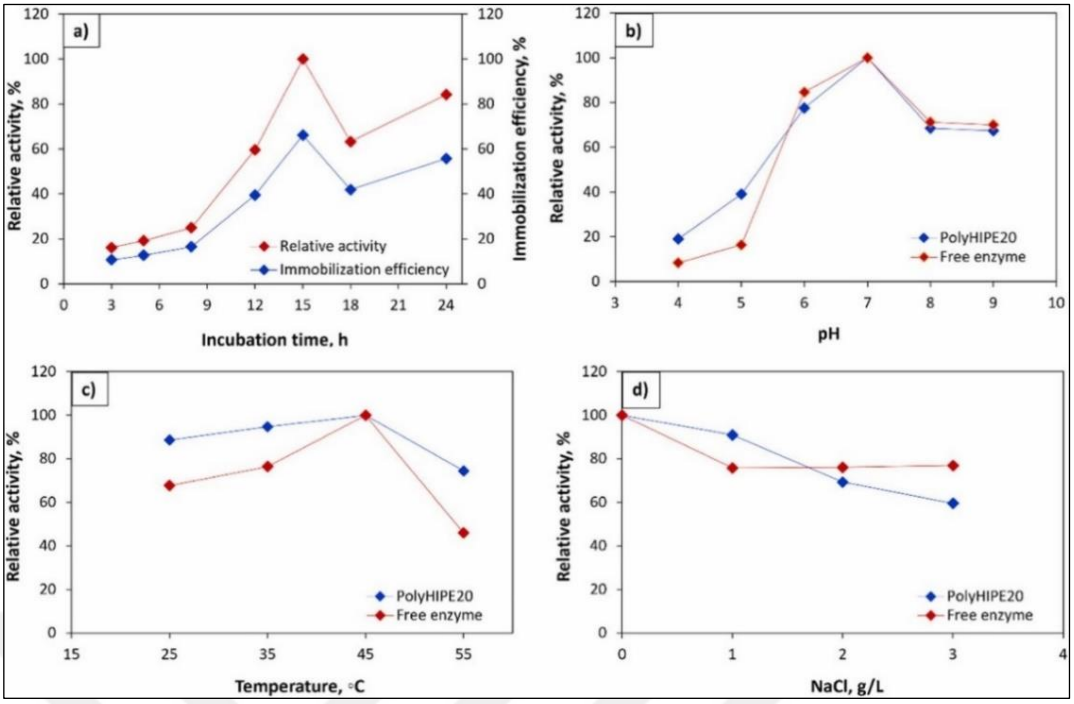

Figure 4.4: (a) The effect of incubation time on immobilization efficiency (1 mg/mL urease; pH 7; 25◦C, 200 mg polyHIPE), (b) the effect of pH (1 mg/mL urease; 25°C, 200 mg polyHIPE), (c) the effect of temperature (1 mg/mL urease; pH 7.0, 200 mg polyHIPE), (d) the effect of ionic strength (1 mg/mL urease; pH 7.0, 25°C, 200 mg polyHIPE), on both free and immobilized enzyme performance.

4.3. Investigation of both Free and Immobilized Enzyme's Performances in Synthetic Wastewater

4.3.1. The effect of pH on both Free and Immobilized Enzyme Performance

The effect of pH on the activities of both free and immobilized urease was evaluated across a pH range of 4.0–9.0, and the results are shown in Figure 4.4b. The relative activities of both enzyme forms increased with rising pH, reaching their maximum between pH 6.5 and 7.0.

These findings indicate that pH 7.0 represents the optimal condition for both free and immobilized urease. At higher, more alkaline pH values, enzyme activities declined significantly, could be due to ionic or structural alterations at the enzyme's active sites **[Swarnalatha et al., 2013].**Previous studies have similarly reported that urease exhibits optimal activity when immobilized at pH values between 6.5 and 8.0, with peak activity generally occurring around pH 7.0 **[Alatawi et al., 2018], [Al-Garawi et al., 2022], [Hormozi Jangi et al., 2020].**

4.3.2. The effect of Temperature on Immobilized and Free Enzyme Performance

Urease activity was evaluated over a temperature range of 25°C to 55°C, with both free and immobilized enzymes exhibiting optimal activity at 45°C (Figure 4.4c). The immobilized urease displayed a broader temperature tolerance compared to the free enzyme. At 25°C, 35°C, and 45°C, the immobilized enzyme consistently showed higher activity and was less sensitive to temperature fluctuations. This enhanced stability is attributed to the multi-point interactions between urease and the polyHIPE support, which limit conformational changes under increasing temperatures **[Daneshfar et al., 2015; Hormozi Jangi and Akhond, 2021; Yigitolu and Temoçin, 2010].** Additionally, the pronounced decline in free enzyme activity at temperatures above 45°C could be due to thermal denaturation and reduced structural stability of the free enzyme.

4.3.3. The Effect of Ionic Strength on Immobilized and Free Enzyme Performance

The effect of ionic strength on the performance of both immobilized and free enzymes was assessed using urea solutions containing different concentrations of NaCl (1, 2, and 3 g/L), with the results presented in Figure 4.4d. Both enzyme forms initially showed a decline in activity, after which their activity levels stabilized. Immobilized urease displayed only a slight reduction in activity at low salt concentrations, whereas free urease exhibited a marked decrease even at these lower levels.

Despite advances in biotechnology, the interactions between ionic liquids and proteins, as well as their effects on protein stability, remain not fully understood. Protein stability is influenced by factors such as enzyme state (free, covalently bound, or immobilized), solvent–protein interactions, and the chemical structure of the support material **[Bui-Le et al., 2020]**. Previous studies on the effects of various salts on enzyme stability have shown that these effects are complex and depend on factors such as pH, salt concentration, and the intrinsic properties of the enzyme **[Braham et al., 2021].** In the present study, the activity of the immobilized enzyme was better preserved compared to the free enzyme, particularly under low salt concentrations at pH 7.0.

4.4. Optimization of Relative Activity of Immobilized Enzyme based on BBD Experiment

A 15-run Box–Behnken Design (BBD) with three variables—NaCl concentration, pH, and temperature—was employed to evaluate and optimize the effect of environmental factors on the relative activity of the immobilized enzyme. To determine the most suitable conditions, the experiments were conducted in random order, and the variables were fitted to a second-degree polynomial model. The levels of the three factors were selected based on single-factor experiments, with the following ranges: NaCl concentration (0–3 g/L, A), pH (4–9, B), and temperature (25–55 °C, C). The corresponding experimental data and relative activity values are presented in Table 4.1.

Regression analysis was performed using Design Expert 12 software, and the second-degree polynomial equation describing the relative activity of the immobilized enzyme was obtained as follows (Equation 4.1):

$$\text{Relative activity} = 84 - 6.625A + 8B - 2.375C + 0AB + 0.25AC + 0BC - 0.12499A^2 - 13.375B^2 - 2.125C^2 \quad (4.1)$$

Table 4.1: ANOVA for response surface quadratic model of the relative activity of immobilized enzyme.

Source	Sum of Squares	df	Mean Square	F-value	p-value	
Model	1577.08	9	175.23	3504.63	< 0.0001	significant
A-NaCl	351.13	1	351.13	7022.50	< 0.0001	
B-pH	512.00	1	512.00	10240.00	< 0.0001	
C-Temperature	45.13	1	45.13	902.50	< 0.0001	
AB	0.0000	1	0.0000	0.0000	1.0000	
AC	0.2500	1	0.2500	5.00	0.0756	
BC	0.0000	1	0.0000	0.0000	1.0000	
A^2	0.0577	1	0.0577	1.15	0.3318	
B^2	660.52	1	660.52	13210.38	< 0.0001	
C^2	16.67	1	16.67	333.46	< 0.0001	
Residual	0.2500	5	0.0500			
Lack of Fit	0.2500	3	0.0833			
Pure Error	0.0000	2	0.0000			
Cor Total	1577.33	14				
Std. Dev.	0.2236	R^2		0.9998		
Mean	75.67	Adjusted R^2		0.9996		
C.V.%	0.2955	Predicted R^2		0.9975		
		Adeq Precision		192.3875		

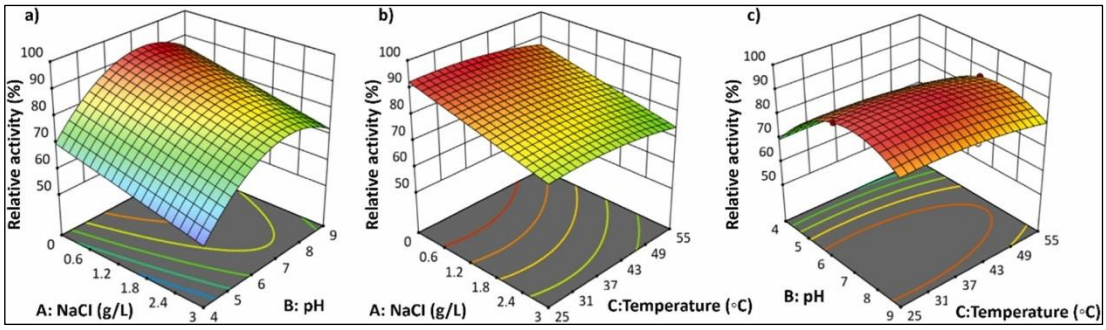

Figure 4.5: 3D surfaces plot for the relative activity of the immobilized urease: (a) the interaction between NaCI and pH; (b) the interaction between NaCI and temperature; (c) the interaction between pH and temperature.

Response Surface Methodology (RSM) plays a critical role in identifying optimal process parameters. The regression equation was analyzed to evaluate the correlations among the three variables, and the resulting polynomial model was used to generate response surface plots (Figure 4.5).

The effects of NaCl concentration and pH on the relative activity of immobilized urease are illustrated in Figure 4.5a. While both NaCl and pH had significant individual effects, their interaction was not significant. Increasing NaCl concentration led to a reduction in relative activity, whereas enzyme activity increased with rising pH up to approximately pH 8, beyond which a decline was observed.

The interaction between NaCl and temperature is presented in Figure 4.5b. Here, no significant interaction effect was detected, and relative activity exhibited only slight changes across the temperature range.

Figure 4.5c shows the combined effects of pH and temperature. Relative activity increased with rising pH and temperature; however, a decline was evident at higher values of both parameters.

Based on the polynomial equation model, the optimal conditions for relative activity were determined as follows: NaCl concentration of 0.007 g/L, pH 7.1, and temperature 40.8 °C. These findings were consistent with those obtained in the one-factor-at-a-time experimental results.

4.5. Reusability and Shelf-life of Immobilized Enzyme in Synthetic Wastewater

The reusability of the immobilized enzyme was assessed using a urea solution over six successive cycles at pH 7 and 25 °C (Figure 4.6a). Results showed that, while the activity of the free enzyme gradually declined, immobilized urease retained approximately 75% of its initial activity after the sixth cycle. Enzyme immobilization is known to preserve the three-dimensional conformation of protein macromolecules, particularly through covalent bonding, thereby protecting the enzyme from structural damage or excessive conformational changes during repeated use **[Alatawi et al., 2018].**

Comparable findings have been reported in the literature. Pithawala et al., (2010) observed that paraffin- and lac-immobilized urease retained only 40% of its initial activity after five cycles **[Pithawala et al., 2010].** Similarly, Kumar et al., (2009) found that alginate-immobilized urease maintained 54% of its initial activity after 14 days of use **[Kumar et al., 2009].** In contrast, Monier and El-Sokkary (2012) reported

that urease immobilized on cellulose cotton fibers retained 87.5% of its initial activity after six cycles **[Monier and El-Sokkary, 2012].**

The reduction in activity during repeated use of immobilized urease has been attributed to several factors, including enzyme desorption in adsorption and cross-linking methods, as well as enzyme denaturation in coating-based immobilization approaches **[Ispirli Doğaç et al., 2014].**

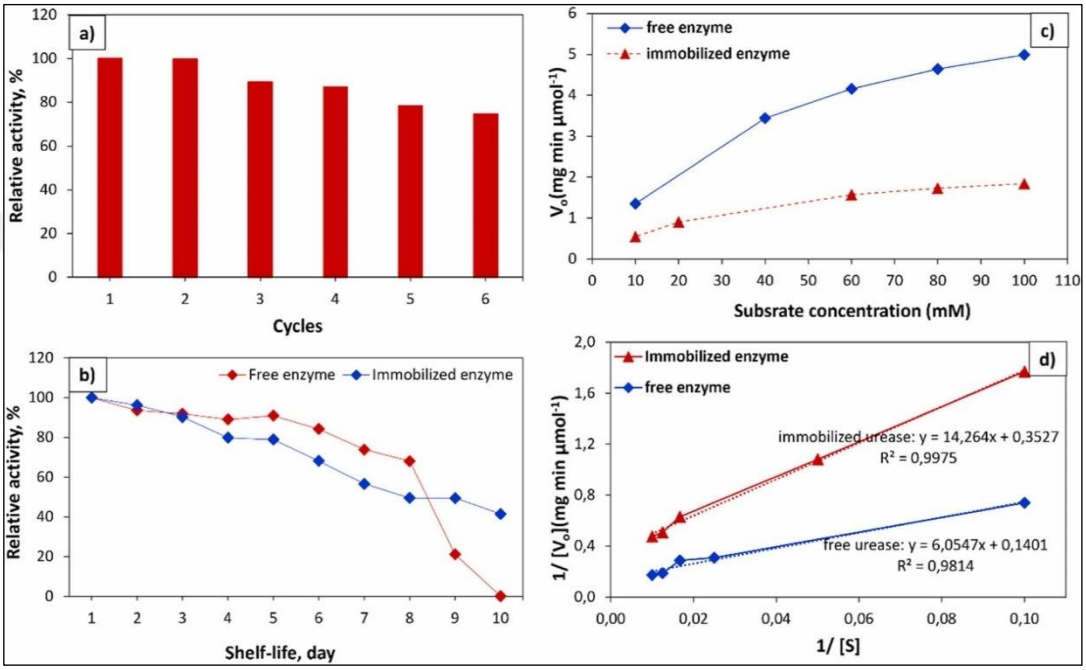

Figure 4.6: (a) Reusability studies of immobilized enzyme and (b) shelf-life of free and immobilized urease (100 mM urea solution, pH 7.0, 25°C) and Kinetic studies of free and immobilized urease (c) Michaelis Menten plots and (d) The Lineweaver–Burk plots (10-100 mM urea solution, pH 7.0, 25 °C).

The present study examined the thermal stability of free and immobilized ureases during storage at ambient temperature. Immobilization on the PolyHIPE20 support material significantly improved urease stability, with the immobilized enzyme retaining more than 40% of its initial activity after 10 days. In contrast, free urease was completely inactivated under the same conditions (Figure 4.6b).

Comparable findings have been reported in the literature. For instance, Daneshfar et al., (2015) showed that urease immobilized on an electrospun polyacrylonitrile mat retained 40% of its initial activity after 20 days of storage at 25 °C, whereas the free enzyme lost most of its activity **[Daneshfar et al., 2015].** The choice of support material—whether porous or non-porous—plays a critical role in determining the

functional properties of immobilized enzymes, particularly their shelf life and reusability stability **[Wang et al., 2019].**

As demonstrated in Figures 4.6a and 4.6b, porous monolithic supports such as polyHIPE20 offer considerable potential for improving both the reusability and storage stability of urease.

4.6. Kinetic Studies

The kinetic parameters of free and immobilized ureases were determined by evaluating their activity in relation to substrate concentration. Michaelis–Menten and Lineweaver–Burk plots are presented in Figures 4.6c and 4.6d, respectively, to calculate the kinetic constants (K_m and V_{max}). V_{max} values were obtained from the intercept ($1/V_{max}$) of the Lineweaver–Burk plots, while K_m values were derived from the slopes (K_m/V_{max}). The Lineweaver–Burk equation is expressed as follows (Equation 4.2) **[Monier and El-Sokkary, 2012]:**

$$1/V_0 = (K_m/(V_{max}[S])) + (1/V_{max}) \quad (4.2)$$

The kinetic parameters obtained using urea as the substrate are presented in Table 4.2 (free urease) and Table 4.3 (immobilized urease). Michaelis–Menten curves were generated by plotting V_0 against substrate concentration, while Lineweaver–Burk plots were obtained by plotting $1/V_0$ against 1/[urea]. Kinetic parameters for both enzyme forms were determined from the slopes and intercepts of the Lineweaver–Burk plots.

Table 4.2: Results for the determination of the kinetic parameters of free urease.

S (mM)	V (U/mg)	1/S (1/mM)	1/V	V_o(mg/min)
10	1,35	0,10	0,74	1,34
40	3,24	0,03	0,31	3,43
60	3,49	0,02	0,29	4,15
80	5,32	0,01	0,19	4,64
100	5,83	0,01	0,17	4,99

Table 4.3: Results for the determination of the kinetic parameters of immobilized urease.

[S]	V	1/[S]	1/[V]	V_o(mg/min)
10	0,57	0,10	1,77	0,55
20	0,92	0,05	1,08	0,90
60	1,59	0,02	0,63	1,57
80	1,97	0,01	0,51	1,73
100	2,11	0,01	0,47	1,84

At the optimum conditions the K_m and V_{max} values for free urease was obtained as 43.21 mM and 7.14 μmol mg^{-1} min^{-1}, the K_m and V_{max} values for immobilized urease was obtained as 35.75 mM and 2.5 μmol mg^{-1} min^{-1}, respectively. The V_{max} value gives information about how accelerate the enzyme catalyzes a reaction. A low V_{max} value is associated with a decrease in the enzyme's rate of converting substrate to product per minute when the enzyme reaches substrate saturation. In other immobilization and encapsulation studies with urease enzyme in the literature, it is reported that the V_{max} value of the enzyme decreases after immobilization applications **[Hormozi Jangi et al., 2020; Hormozi Jangi and Akhond, 2021;,Ispirli Doğaç et al., 2014].**Researchers stated that after the immobilization process, the substrate and enzyme interactions are inhibited due to the formation of different bond structures, as well as the modifications on the substrate diffusion surface may cause a decrease in the Vmax value **[Kutcherlapati et al., 2016; Ispirli Doğaç et al., 2014].**

The K_m value gives information about the affinity of the enzyme to the substrate. Low K_m value shows the enzyme's high affinity for the substrate at low substrate concentration. In the present study, the K_m value of the immobilized enzyme is lower than that of the free enzyme. This shows that the affinity of the immobilized enzyme to the substrate is higher than that of the free urease enzyme. It should be mentioned about that after immobilization the kinetic behaviors of enzyme could be affected by structural and environmental changes such as conformational changes, steric effects, mass transfer resistances, modification of local microenvironment etc. Moreover, the immobilization methods such as adsorption, cross-linking could be affected to change the kinetic behaviors of enzymes **[Ispirli Doğaç et al., 2014].**

A standard comparison was conducted to assess the effectiveness of the developed immobilization process in relation to various urease immobilization methods, encompassing both entrapment and covalent binding-based techniques documented in

the literature (refer to Table 4.4). According to the findings, polyHIPE20 demonstrates figures of merit that closely align with those of other immobilized urease methods previously reported in the literature.

Table 4.4: Evaluating the performance metrics of the developed PolyHIPE-urease in comparison to other reported immobilized ureases in the literature.

Immobilization support	Immobilization type	Opt. pH	Opt. T	Shelf-life	Reusability	V_{max}	K_m	References
Cellulosic cotton fibers	Covalent	6.5	35 °C	-	87.5% after 6 cycles	22.44 U mg^{-1}	9.54 mM	**[Monier and El-Sokkary, 2012]**
Free		7.0	30 °C	-	-	31.25 U mg^{-1}	8.75 mM	
TiO_2 beads and TiO_2-chitosan beads	Adsorption/crosslinking (A); coated with chitosan-urease mixture (B)	7.0	30 °C (A) 40 °C (B)	-	50% after 11 cycles (A) 50% after 16 cycles (B)	0.899 U (A) 0.402 U (B)	0.321 mM (A); 0.121 mM (B)	**[Ispirli Doğaç et al., 2014]**
Free		7.5	35 °C	-	-	1.22U	0.071 mM	
Electrospun polyacrylonitrile mat	Covalent	6.5	50 °C	40% after 20 days at 25 °C	70% after 15 cycles	10.1 µmol NH_3 min^{-1} mg^{-1}	57.6 mM	**[Daneshfar et al., 2015]**
Free	-	7.0	37°C	Lost all activity after 20 days at 25 °C	-	17.54 µmol NH_3 min^{-1} mg^{-1}	40.35 mM	
Amino functionalization of carboxymethyl cellulose	Covalent	8.0	45°C	75% after 7 days at 25 °C	88% after 10 cycles	2 ± 0.2 µmol NH_3/min·mg	14 ± 0.7 mM	**[Alatawi et al., 2018]**
Free		7.0	35°C	Lost its activity	-	5 ± 0.2 µmol NH_3/min·mg	11 ± 0.5 mM	

Table 4.4: Continued

Metal–organic frameworks	Biomimetic mineralization	7.0	50 °C	54.07% after 12 days at 25 °C	58.86% after 5 cycles	-	-	**[Liang et al., 2020]**
Free	-	7.0	50 °C	16.55% after 12 days at 25 °C	-	-	-	
NEQC-340	Covalent	8.0	60.0 °C	97.7% after 40 days at 37 °C	88.5% after 17 cycles	3.93 μmol mg^{-1} min^{-1}	8.0 mM	**[Hormozi Jangi et al., 2020]**
Free	-	7.0	37.0 °C	40% after 10 days at 37 °C	-	5.31 μmol mg^{-1} min^{-1}	26.0 mM	
NEQC-340@Urease	Encapsulation	7.0	45.0 °C	81% after 15 days at 25 °C	55 % after 10 cycles	4.41 μmol mg^{-1} min^{-1}	33.28 mM	**[Hormozi Jangi and Akhond, 2021]**
Free	-	7.0	37.0 °C	40 % after 10 days at 25 °C	-	5.26 μmol mg^{-1} min^{-1}	22.65 mM	
Electrospun nanofibers	Covalent	7.0	45.0 °C	-	30% after 10 cycles	139 $\mu mol.min^{-1}.mg^{-1}$,	4.57 μM	**[Amani et al., 2022]**
Free	-	7.5	35.0 °C	-	-	213 $\mu mol.min^{-1}.mg^{-1}$,	0.68 μM	
Fe_3O_4 nanoparticles		7.0	40 °C	49% after 12 weeks at 4 °C	59% after 20 cycles	3.1 μmol/ml·min	54.6 mM	**[Almaghrabi and Almulaiky, 2023)**
Free	-	7.0	35 °C	13% after 12 weeks at 4 °C	-	4.4 μmol/ml·min	49.5 mM	
PolyHIPE	Covalent	7.0	45 °C	Higher than 40% after 10 days at 25 °C	75% after 6 cycles	2.5 μmol mg^{-1} min^{-1}	35.75 mM	**This study**
Free	-	7.5	45 °C	Lost all of its activity after 10 days at 25 °C	-	7.14 μmol mg^{-1} min^{-1}	43.21 mM	

4.7. Investigation of both Free and Immobilized Enzyme's Performances in Human Urine

The results comparing the relative activity of free and immobilized urease enzymes according to experiments performed with human urine at different pH and temperature conditions are presented in Figure 4.7. Both free and immobilized urease lost their initial activity in alkaline and acidic pH values. From Figure 7.7a, the maximum relative activity of both free and immobilized enzymes was obtained at pH 7. Similar results were obtained in a study conducted on covalently immobilized urease on poly (AAm-AGE) cryogel. The researcher reported that the maximum activity of both free and immobilized urease in human serum was obtained at a pH of 7 **[Yavaşer Boncooğlu, 2024].** Enzyme activity depends on pH due to the carboxyl and amino functional groups. At low pH, both functional groups are positively charged. As pH increases, the carboxyl group is the first to release protons, controlled by the dissociation equilibrium constant. The enzyme exhibits maximum activity at an average pH of 7-8. However, as pH increases further, the amino groups also become negatively charged, leading to decreased enzyme activity. The lower activity of immobilized urease enzyme in an alkaline environment compared to the free enzyme is attributed to ionic binding. After immobilization, the enzyme's functional groups undergo chemical changes. The support material becomes activated and positively charged, binding to the enzyme's negatively charged carboxyl group and trapping it within the support material **[Yang et al., 2019].**

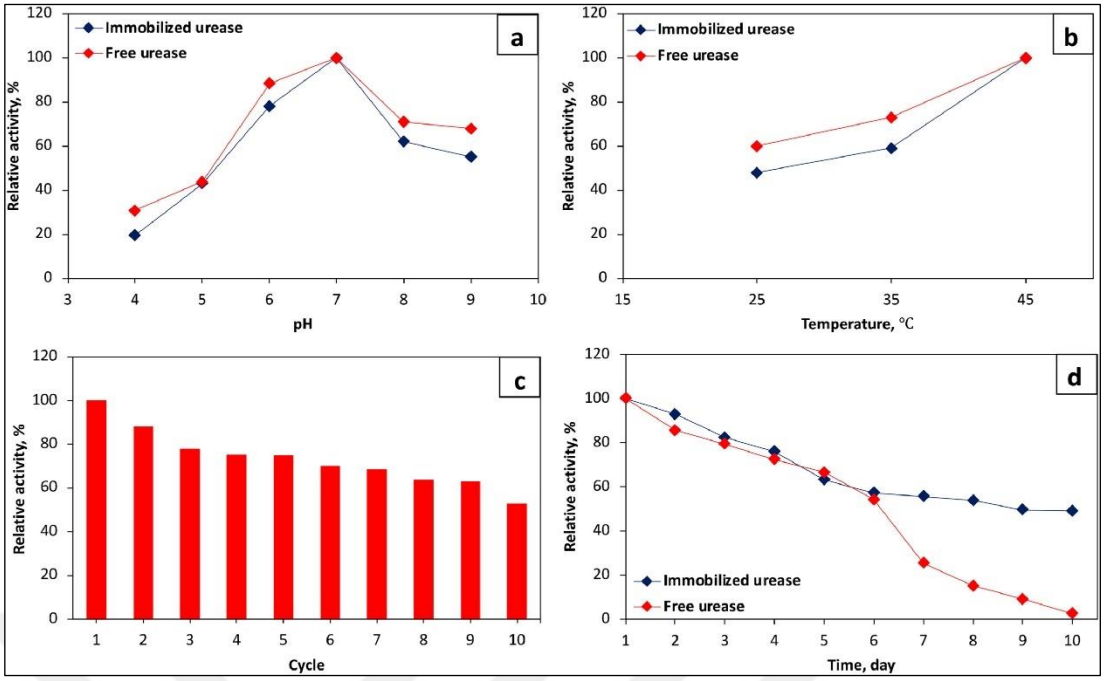

Figure 4.7: The effect of (a) pH (1 mg/mL urease; 25 °C, 200 mg of polyHIPE), (b) temperature (1 mg/mL urease; pH 7.0, 200 mg of polyHIPE) on enzyme performance for both immobilized and free enzyme in human urine, (c) the reusability of immobilized enzyme, and (d) storage time of both free and immobilized enzyme (human urine, pH 7.0, 25 °C).

Figure 4.7b demonstrates the relative activity results of both free and immobilized enzymes in human urine at temperatures ranging from 25 to 45°C. According to the results in Figure 4.7b, the maximum relative activity for both free and immobilized enzymes was obtained at 45°C. Similar results for the temperature profile of the immobilized urease enzyme have been reported in the literature **[Diasi et al., 2024; Hormozi Jangi and Akhond, 2021].**

4.8. Investigation of Reusability and Storage Time of Immobilized Ureases in Human Urine

It is crucial to maintain enzymes in a stable and active state throughout operational processes. Ensuring the storage stability and reusability of enzymes is paramount for the cost-effective treatment of human urine and the recovery of valuable products. The reusability of immobilized urease enzyme was evaluated performing experiments with real human urine at pH 7, 25 °C for 10 cycles. As illustrated in Figure 4.7c, the immobilized enzyme demonstrated a retention of approximately 53 % of its initial activity following 10 cycles of operation. The ionic interactions between the enzyme and the support material at various points contribute to stability against environmental

factors and potential inhibitors **[Kara et al., 2006].** The literature presents a range of results concerning the reusability of immobilized urease, with outcomes varying depending on the type of support material and reaction medium used. For instance, Liang et al., (2020) found that immobilized urease in metal-organic frameworks through biomimetic mineralization retained 58.86 % of its initial activity after 5 cycles **[Liang et al., 2020].** Diasi et al., (2024) reported that covalently immobilized urease enzyme on chitosan-coated magnetic iron oxide nanoparticles lost its activity in human urine after 6 repeated uses **[Diasi et al., 2024].** In contrast, Kutlu et al. (2020) observed that urease immobilized in electrospun PVA/chitosan nanofibers retained 85 % of its initial activity in artificial blood serum after 10 operational cycles **[Kutlu et al., 2020].** The decrease in initial activity of immobilized ureases during various operational cycles could be attributed to the absorption/desorption mechanism of the enzyme as well as denaturation due to the immobilization methods **[Ispirli Doğaç et al., 2014].**

As shown in Figure 4.7d, the immobilized enzyme retained approximately 50 % of its initial activity after 10 days of storage at room temperature, whereas the free enzyme almost lost of all its activity. Similarly, Liang et al. (2020) reported that free and immobilized urease@ZIF-8 retained 16.55 % and 54.07 % of their initial activities, respectively, over a 12-day incubation period at room temperature **[Liang et al., 2020].** The improved shelf life of immobilized enzymes offers cost advantages in storage, transport, and operational processes **[Liang et al., 2020].** Based on the reusability and shelf-life results in the present study, it appears that immobilizing the urease enzyme into the polyHIPE material could be a promising alternative support material for processing human urine, enhancing the reusability and storage stability of the urease enzyme.

4.9. Design and Development of Enzyme Immobilized polyHIPE Reactor

The results obtained with the enzyme-immobilized polyHIPE reactor are presented in Figure 4.8, showing urea hydrolysis efficiency and effluent ammonia nitrogen concentration as a function of the linear feed rate. When the immobilized enzyme reactor was operated at linear feed rates of 0.5 and 1 $m^3/m^2 \cdot h$, the urea hydrolysis effieciency were 96.6% and 95.8%, respectively. However, when the linear feed rate was increased to 5 $m^3/m^2 \cdot h$, the urea hydrolysis efficiency decreased to 47.5%. Studies

on immobilized enzyme-packed column reactors are limited in the literature, with most of the present work focusing on batch systems. In a study investigating urea removal from wine using an immobilized urease packed reactor, a reactor with a diameter of 7 mm and a length of 10 mm was used, and the optimum feed rate was determined to be approximately 2 $m^3/m^2 \cdot h$, similar to our findings **[Fidaleo and Tavilli, 2021]**.

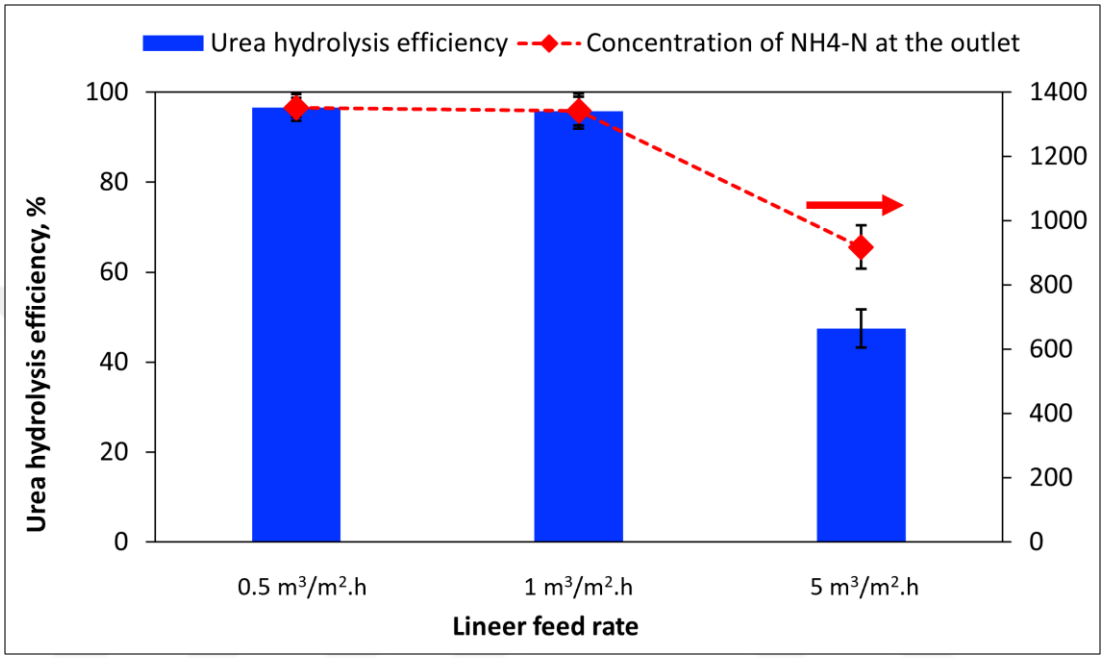

Figure 4.8: Immobilized enzyme reactor studies (human urine at pH 7 and 25 °C for a duration of 1 hour).

As seen from the results, the linear feed rate—one of the most critical operational parameters in packed reactors—plays a significant role in urea conversion. At higher feed rates, the urea hydrolysis efficiency decreased due to insufficient contact time. Therefore, the choice of flow rate should be made based on the desired maximum urea hydrolysis efficiency. Considering the present results, urea hydrolysis efficiencies above 95% were achieved even at a linear feed rate of 1 $m^3/m^2 \cdot h$.

4.10. The Recovery of Ammonium Sulfate via Ammonia Stripping

Chemical precipitation, ammonium stripping, and electrochemically driven extraction are employed to recover high-value compounds like urea, struvite, ammonium sulfate, and ammonium chloride from human urine for biotechnological applications **[He et al., 2024].** Ammonium stripping is particularly advantageous in batch-scale operations

due to its low cost, simplicity, and ability to maintain constant pH and temperature. Additionally, it requires no backwashing or regeneration, does not produce toxic compounds that could harm biological systems, and allows for a controlled operational process. In the present study, following the enzymatic hydrolysis of urea to ammonia in human urine, ammonia was recovered as ammonium sulfate using the ammonium stripping method. In the present study, the primary focus was not on developing a novel ammonia stripping reactor or achieving the highest possible stripping efficiencies. Instead, a conventional reactor setup was employed solely for the purpose of producing ammonium sulfate from enzymatically hydrolyzed human urine. Operating the ammonia stripping process with innovative reactor designs may significantly increase the ammonia removal efficiency **[Değermenci and Yildiz, 2021].**The series experiments were conducted to optimize the operational parameters for stripping ammonia from human urine, which is converted from urea through enzymatic hydrolysis. The ammonia was subsequently stripped from the urine and captured in a 5% (v/v) sulfuric acid solution. The saturated sulfuric acid solution was evaporated to obtain ammonium sulfate crystals, which were then dried and characterized using XRD analysis.

Figure 4.9a and Figure 4.9e demonstrates that ammonia stripping studies at 25 °C exhibited low efficiency, even at pH 11. However, increasing the temperature notably increased the amount of ammonia stripped, even at lower pH values. Especially, stripping efficiencies exceeding 80 % were achieved at pH 10 and 11 in studies conducted at 40 °C and 65 °C (Figure 4.9c–e). At 65 °C, efficiencies of approximately 80 % were achieved even at pH 9, with almost complete stripping observed at pH 10 (Figure 4.9d, e).

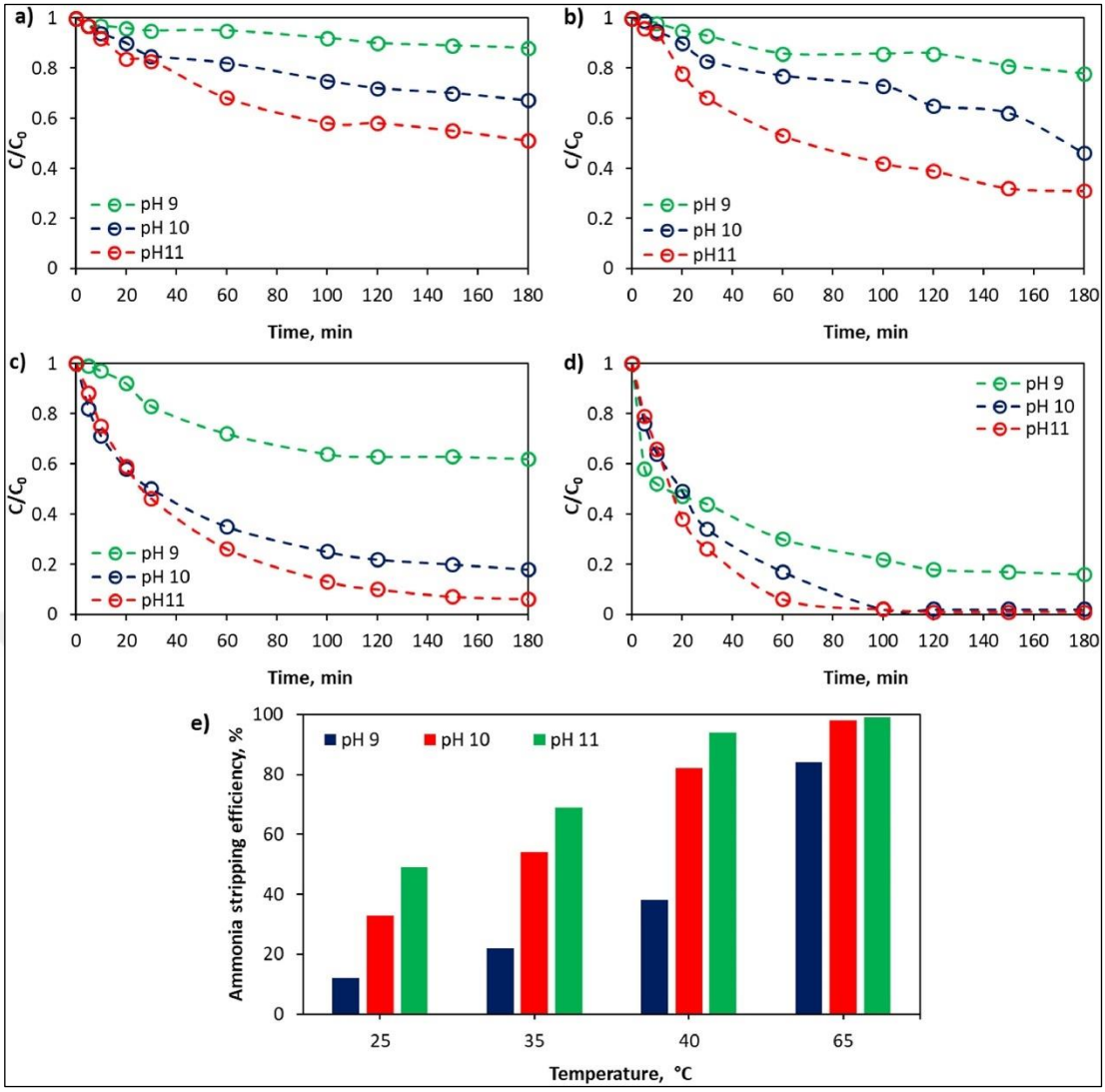

Figure 4.9: The results of the ammonia stripping studies conducted at different pH levels (9, 10, and 11) are presented for the following temperatures: (a) 25 °C, (b) 35 °C, (c) 40 °C, and (d) 65 °C (e) summarizes the stripping efficiencies across all tested temperatures and pH levels.

After enzymatic hydrolysis of urea to ammonia, ammonium sulfate was produced by capturing and crystallizing ammonia in sulfuric acid through air stripping. XRD analyses were performed on both the obtained human urine-derived ammonium sulfate and a commercial sample for comparison, as shown in Figure 4.10. The XRD patterns clearly indicate identical crystalline structures for both samples, confirming them as ammonium sulfate. Figure 4.10 demonstrates diffraction peaks (2θ: 16.98, 20.23, 20.47, 22.84, 29.28, 29.80) characteristic of ammonium sulfate. These observed sulfate peaks correspond well with those documented in the literature **[Hamdan et al., 2016; D. Li et al., 2018; Liu et al., 2011; Tizzoni et al., 2015].**

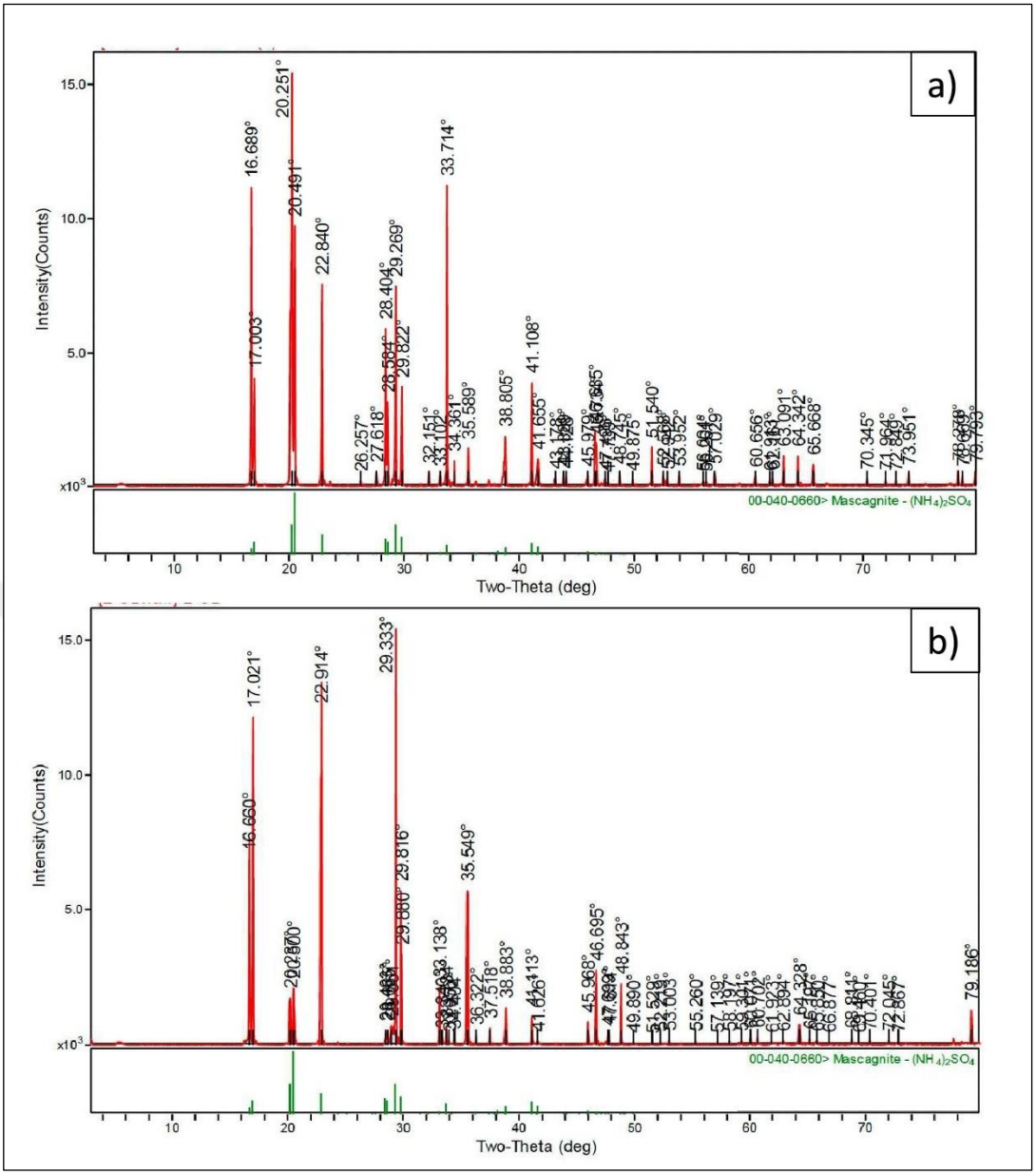

Figure 4.10: The XRD analysis results of (a) commercial ammonium sulfate and (b) ammonium sulfate produced from human urine via enzymatic hydrolysis.

4.11. Application of the Urea derived Ammonium Sulfate as Fertilizer in Pot Trials

Approximately 70 seeds of the Eminbey wheat variety were surface sterilized by immersion in 70% ethanol for 5 minutes, with intermittent rinsing between treatments. The seeds were then agitated in 5% Domestos (a commercial bleach solution) for 25 minutes. Following this, the seeds were rinsed thoroughly with sterile distilled water until all foam residues were eliminated. Since the Eminbey wheat variety is classified as winter wheat, vernalization was required. Sterilized seeds were placed in sterile

Petri dishes lined with sterile filter paper, which was slightly moistened. The seeds were then vernalized at +4°C for 5 days (Figure 4.11).

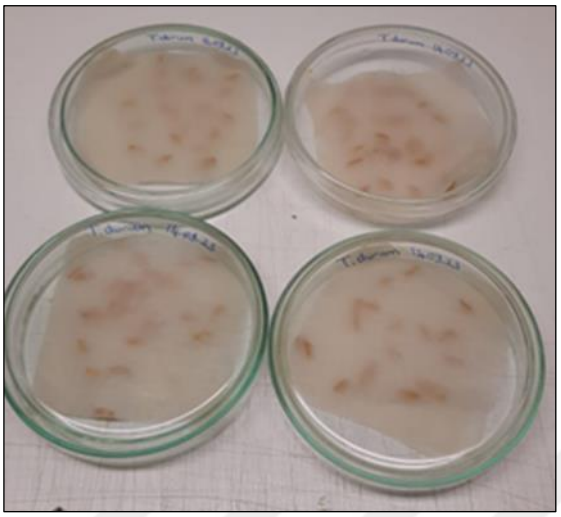

Figure 4.11: Vernalization of sterilized wheat seeds.

Germinated wheat seeds were mixed with a homogeneous soil:sand mixture (1:1) collected from the Gebze Technical University campus. The soil was analyzed at the Kocaeli Provincial Directorate of Agriculture. The prepared mixture soils for the greenhouse were sterilized at 121°C for 20 minutes. The sterilized soils were then evenly divided into pots measuring 30 cm in both length and depth. The results of the soil analysis are presented in Table 4.5.

Table 4.5: Soil analysis report.

Analysis Name	Limit Values*	Result	Unit
Texture	–	37.4	–
pH	6.50–7.50 (Neutral)	7.9	–
Salt	0.00–0.15 (Non-saline)	0.01	%
Lime	15.0–25.0% (High in lime)	19.81	%
Organic Matter	3.0–4.0% (Good)	2.33	%
P_2O_5 (Phosphorus)	>9 kg/ha (High)	8.88	kg/ha
K_2O (Potassium)	>30 kg/ha (High)	24.61	kg/ha

Pot experiments were conducted in the greenhouse of the Department of Molecular Biology and Genetics at Gebze Technical University under a 16/8-hour light/dark photoperiod and at a temperature of 18°C. Vernalized wheat seeds were germinated in sterilized soil for 5 days (Figure 4.12). Two seeds were sown in slightly moistened soil

per pot (Figure 4.13). Each experimental group consisted of 30 pots, with 10 replications per group.

Figure 4.12: Wheat seeds germinated after the vernalizationstage.

Figure 4.13: Transplantation stage of germinated wheat seeds into pots.

A total of 60 seeds were sown per pot, including 2 vernalized wheat seeds. Plants were maintained under greenhouse conditions at 15–20°C until emergence and at 20–25°C and 70% humidity after emergence. Soil moisture in the pots was monitored daily, and irrigation was conducted every other day. The general appearance of the sown trials after 7 days is shown in Figure 4.14.

Figure 4.14: General view of the experimental groups after 7 days.

Durum wheat is the second most widely cultivated wheat globally, after bread wheat, and is used in various applications such as pasta production, baking, and other food products. A variety of mineral, organic, or inorganic fertilizers are employed in wheat farming. To achieve wheat with high yield and nutritional value, fertilization and irrigation practices must be conducted in a controlled and conscientious manner. One of the critical factors influencing wheat yield and quality parameters is the nitrogen and phosphate content in the fertilizers used. Currently, urea, ammonium sulfate, ammonium hydroxide, and others serve as primary nitrogen sources in fertilizers. While the impact of urea-based nitrogen fertilizers on wheat yield and quality parameters is well-documented, research into the potential of ammonium sulfate as a fertilizer is ongoing **[Assefa et al., 2023].**

In this study, the potential of ammonium sulfate obtained from human urine as fertilizer was evaluated in the terms of yield parameters on durum wheat. Based on the results from Figure 4.15 and Figure 4.16, the plant length in each experimental group were as follows: negative control (N) as 54.2 cm, positive control (A) as 54.8 cm, and ammonium sulfate obtained from human urine (B) as 55.2 cm. There were no statistically significant differences observed among them. According to the results in Figure 10 and Figure 11, the experimental group with the longest spike length (6.2 cm) was the one treated with ammonium sulfate derived from human urine (B), followed by the group treated with commercial ammonium sulfate (A) (5.8 cm), and then the negative control group (N) (5.6 cm). However, there were no statistically significant differences observed among these groups.

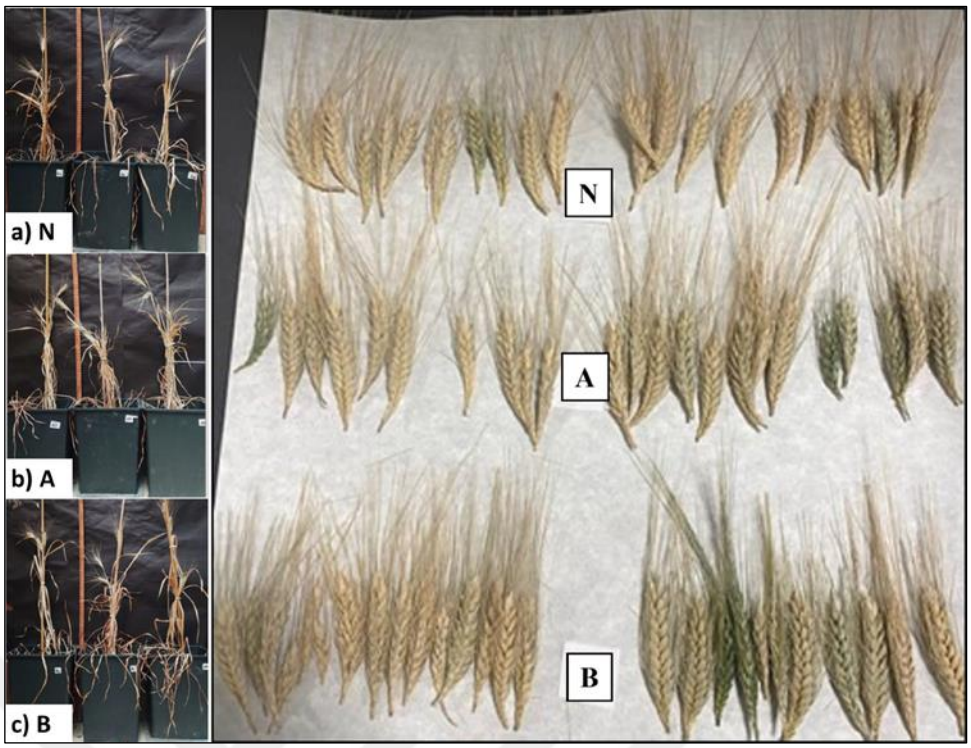

Figure 4.15: The length of plants in: (a) the negative control group, (b) the group treated with ammonium sulfate, (c) the group treated with ammonium sulfate obtained from human urine, the length of spake in: the negative control group (N), the group treated with commercial ammonium sulfate (A), the group treated with ammonium sulfate from human urine (B).

Among the experimental groups, the highest number of spikelets was observed in the group treated with ammonium sulfate (A) (17.1), followed by the group treated with ammonium sulfate obtained from human urine (B) (16.8), and the negative control group (N) (16.3), respectively. There were no statistically significant differences observed among these groups in terms of the number of spikelets (Figure 4.16).

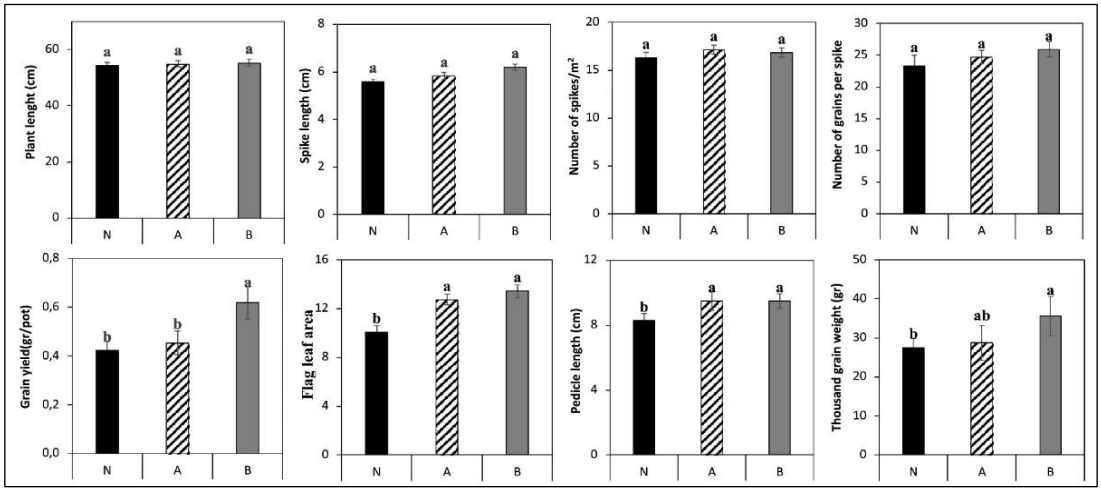

Figure 4.16: The effects of ammonium sulfate derived from human urine on plant growth parameters, including plant height, spike length, number of spikes per square meter, grains per spike, grain yield, flag leaf area, pedicle length, thousand-grain weight, and hectoliter weight. Values represent means ± standard error (n = 3). [a-b] Bars within each experimental group not sharing a common lowercase letter are significantly different ($p < 0.05$). (N: negative control, A: commercial ammonium sulfate, B: ammonium sulfate from human urine).

The experimental group with the highest number of grains per spike was the one treated with ammonium sulfate obtained from human urine (B) (25.9), followed by the group treated with commercial ammonium sulfate (A) (24.7), and the negative control group (N) (23.3). There were no statistically significant differences observed among these groups in terms of the number of grains per spike (Figure 4.16). Regarding grain yield per pot among each experimental group, the highest yield was recorded in the ammonium sulfate group (B) (0.62 g) derived from human urine. There were no statistically significant differences observed between the group treated with regular ammonium sulfate (A) and the negative control group (N) (Figure 4.16). In relation to the flag leaf area of each experimental group, the group with the largest area was the one treated with ammonium sulfate obtained from human urine (B) (13.4 cm^2), followed by the group treated with ammonium sulfate (A) (12.7 cm^2), and then the negative control group (N) (10.1 cm^2). A statistically significant difference was observed among the negative control groups (Figure 4.16). There was no statistically significant difference in pedicel length between the ammonium sulfate group (B) (9.5 cm) and (A) (9.5 cm). However, a statistically significant difference was observed between these groups and the negative control group (N) (8.3 cm) (Figure 4.16). Among the experimental groups, the highest thousand grain weight was recorded in the ammonium sulfate group derived from human urine (B) (35.9 g), followed by the

group treated with commercial ammonium sulfate (A) (28.8 g), and then the negative control group (N) (27.5 g). A statistically significant difference was observed between the ammonium sulfate group derived from human urine (B) and the negative control group (N) (Figure 4.16).

Additionally, the hectoliter weights of each experimental group are investigated (Table 4.6). According to the results, the hectoliter weights were as follows: ammonium sulfate group derived from human urine (B) measured at 94.32 kg/hl, negative control (N) measured at 63.17 kg/hl, and ammonium sulfate group (A) measured at 55.42 kg/hl.

Table 4.6: Hectoliter weights.

Experiment groups	**Hectoliter weight (kg/hl)**
Negative control (N)	63.17
Positive control (Ammonium sulphate) (A)	55.42
Ammonium sulphate obtained from human urine(B)	94.32

The L* (brightness), a*(redness), and b* (yellowness) values of wheat in both grain and crushed forms across each experimental group are detailed in Table 4.7. In grain form, L* (brightness) values varied among the groups, with the highest observed in the positive control group, ammonium sulfate (A) (52.2), and the lowest in the group obtained from human urine (B) (50.7), although there was no statistically significant difference between the negative control group (N). The groups did not significantly differ in terms of a* (redness) values. Regarding b* (yellowness) values, the negative control group recorded the highest value (24.93), while there were no statistically significant differences between the other groups.

Table 4.7: The values of L* (brightness), a* (redness), and b* (yellowness) for wheat in both grain and cracked forms are presented across all experimental groups. Values are means (n = 3). [a-c] Each characteristic not sharing a common lower case letter are different for each experimental group ($p<0.05$).

Experiment groups (Grain)	**L***	**a***	**b***
Negative control (N)	51.7a	9.07a	24.93a
Commercial ammonium sulphate (A)	52.2a	9.02a	24.68a
Ammonium sulphate obtained from human urine(B)	50.7b	9.06a	24.92a
Experiment groups (Crushed)	**L***	**a***	**b***
Negative control (N)	79.54b	3.92a	18.13b
Commercial ammonium sulphate (A)	77.72c	3.92a	20.26a
Ammonium sulphate obtained from human urine(B)	80.39a	3.11b	14.71c

In crushed form, the highest L* value among the experimental groups was found in the ammonium sulfate group obtained from human urine (B) (80.39), whereas the lowest was observed in the ammonium sulfate group (A) (77.72). The a* value was highest in both the negative control (N) and the ammonium sulfate group (A) (3.92), and lowest in the group obtained from human urine (B) (3.11). The b* value was highest in the ammonium sulfate group (A) (20.26) and lowest in the group obtained from human urine (B) (14.71).

The grain size, moisture content, and hardness index values of the wheat in each experimental group are presented in Table 4.8 and Figure 4.17. In terms of grain size, the highest value was in the ammonium sulfate group obtained from human urine (2.48), while the lowest was in the ammonium sulfate group (2.32). No statistically significant difference was found between them. For moisture content, the highest value was in the ammonium sulfate group obtained from human urine (B) (16.84%), and the lowest was in the negative control group (14.24%). Regarding hardness values, the highest was in the ammonium sulfate group obtained from human urine (B) (83.35), and the lowest was in the ammonium sulfate group (A) (75.56).

Gluten content was found to be 30% across all three groups, with no significant differences observed. Similarly, the carbohydrate content ranged between 68% and 70% across the trials, showing no significant variation.

Table 4.8: The grain size, moisture (%),and hardness values of the wheat in different experimental groups are presented.

Experiment groups	Grain size	Moisture (%)	Hardness
Negative control (N)	2.33±0.32a	14.24±0.43c	80.26±16.93a
Commercial ammonium sulphate (A)	2.32±0.37a	15.56±0.55b	75.56±20.58a
Ammonium sulphate obtained from human urine (B)	2.48±0.41a	16.84±0.56a	83.35±17.08a

Values are means ± standard error (n = 3). [a-c] Each characteristic not sharing a common lower-case letter are different for each experimental group ($p<0.05$).

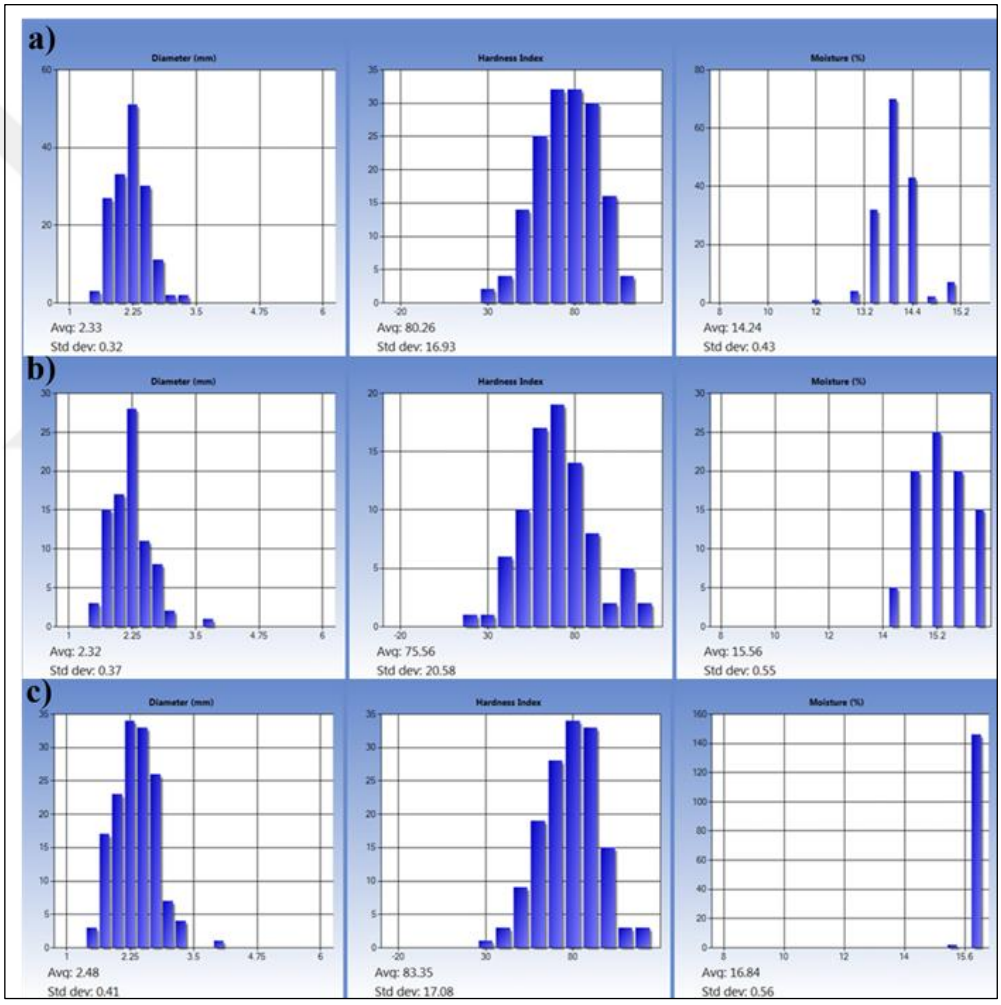

Figure 4.17: Distribution of grain size, hardness index, and moisture content in wheat: (a) Negative control group (N); (b) Commercial ammonium sulfate group (A); (c) Ammonium sulfate derived from human urine group (B).

When the yield parameters measured in the present study were evaluated, it was found that ammonium sulfate obtained from human urine had no negative effect when used

as a fertilizer for durum wheat. Although there was no statistically significant difference in many criteria compared to commercial ammonium sulfate, the highest hectoliter weight, which is important for yield, was obtained in trials using ammonium sulfate derived from human urine. It may be attributed to the positive effects of the more than 200 volatile organic compounds, including alcohols, ketones, hydrocarbons, and sulfur- and nitrogen-containing compounds **[Smith et al., 2008],** in human urine on soil health and microbial activity, which support plant growth. It was reported that C compounds in organic fertilizers enhance soil health and microbial activity, supporting nutrient release, root development, and plant growth while addressing nutrient deficiencies in previous studies **[Lazcano et al., 2021].** These findings suggest that ammonium sulfate from human urine could be a viable alternative fertilizer without adverse effects on durum wheat yield.

Synthetic fertilizers, particularly nitrogen-based types, are produced through energy-intensive processes such as the Haber-Bosch method, which contributes significantly to global CO_2 emissions. The Haber-Bosch process for producing synthetic nitrogen fertilizers consumes substantial amounts of fossil energy, primarily natural gas, and emits approximately 465 million tons of CO_2 annually **[Mauerer et al., 2023].** In contrast, recycling human urine as a fertilizer utilizes an abundant waste stream, reducing reliance on energy-intensive industrial processes and associated emissions. Quantitative data, such as life cycle assessments, can highlight the reduction in greenhouse gas emissions and energy savings, providing a clearer picture of the sustainability benefits of this method.

5. CONCLUSION

According to first aim of this thesis study, we investigated the immobilization of urease enzyme on various polyHIPE materials, covering characterization, immobilization efficiency, and enzyme activity. SEM analysis revealed typical polyHIPE features in all materials, with interconnected pore structures. FT-IR analysis showed changes in functional groups upon modification, with the highest changes observed in polyHIPE20 containing 20% PGA. PolyHIPE20 with 20% PGA exhibited the highest immobilization efficiency at 95%. A 15-hour incubation period was found optimal for urease immobilization. Both free and immobilized urease displayed optimal activity at pH 7 and 45°C in synthetic wastewater. Immobilized urease demonstrated enhanced thermal stability and performed well under varying ionic strength conditions. It maintained activity through multiple cycles and showed good shelf-life stability. Kinetic analysis indicated a lower K_m value for the immobilized enzyme, suggesting higher substrate affinity, but a lower V_{max} value, indicating reduced substrate conversion rate at saturation. Overall, this study provides valuable insights into factors influencing urease immobilization efficiency and performance, relevant for enzyme-based applications like biosensors and bioreactors.

In treating urea-rich wastewater through enzymatic hydrolysis, a significant challenge lies in the loss of enzyme reusability and stability over time during operational cycles. However, the present study reveals that immobilizing urease enzyme through covalent bonding to polyHIPE solid support material can overcome this issue by maintaining the enzyme's shelf life and reusability during operational cycles.

After we demonstrated immobilized urease enzyme’s performances in synthetic wastewater, this present study was investigated also the enzymatic hydrolysis of human urine into ammonium sulfate using immobilized urease on polyHIPE support material and examines the potential application of the recovered ammonium sulfate as a fertilizer for durum wheat cultivation. The effects of factors such as shelf life, reusability, pH, and temperature stability were investigated for both free and immobilized urease. The optimal pH and temperature for both free and immobilized urease enzymes were found to be 7 and 45◦C, respectively. Also, immobilized enzymes retained 53% of its initial activity after 10 reuse cycles and maintained 50%

of its activity after being stored for 10 days at room temperature. The polyHIPE support material improves the urease enzyme's stability, thereby extending its shelf life and reusability during the enzymatic hydrolysis of human urine. At 65°C, ammonia stripping efficiencies reached approximately 80% at pH 9, while nearly complete ammonia removal was achieved at pH 10. XRD analysis indicated that the crystal structure of the recovered ammonium sulfate is similar to that of commercial ammonium sulfate. The potential of using recovered ammonium sulfate as a fertilizer in durum wheat cultivation was evaluated based on high yield and nutritional value. Although no statistically significant differences were observed in many of the yield parameters compared to commercial ammonium sulfate, the group treated with human urine-derived ammonium sulfate showed the highest hectoliter weight, a key indicator of grain quality. These findings suggest that ammonium sulfate from human urine could be a viable alternative fertilizer without adverse effects on durum wheat yield.

This study reveals the potential of source-separated urine as a sustainable nutrient source through effective ammonia stripping and highlights the applicability of polyHIPE materials in the process. To advance this technology, future research should focus on scaling up both the urine collection infrastructure and the polyHIPE synthesis process, addressing challenges related to material production efficiency and cost. Real-world applicability requires further exploration of temperature and pH ranges to ensure optimal process performance under practical conditions. Public perception remains a critical challenge; therefore, public engagement campaigns and strict safety protocols are essential to promote acceptance and safe agricultural use of urine-derived fertilizers. Ensuring safety and quality through regulatory guidelines, pilot projects, and case studies will help build trust and facilitate the adoption of these fertilizers in agriculture. These efforts, combined with pilot-scale studies, will help overcome existing limitations and pave the way for integrating this innovative approach into mainstream sustainable agricultural practices. Additionally, life cycle assessment is recommended for future research to characterize the potential environmental impacts of using ammonium sulfate from human urine as a fertilizer on wheat growth.

REFERENCES

Abraham R., Goldfarb D S., (2025). Perspectives on Water Utilization in Hemodialysis: Nephrologists' Responsibilities. In *Blood Purification*, S. Karger AG.

Aggarwal S., Ikram S., (2025). Aluminum Oxide Nanoparticles-Impregnated Aminated Silica Surfaces for Covalent Immobilization of Urease via Glutaraldehyde Activation: Stability and Kinetic Studies. *ChemistrySelect*, 10(15).

Akay G., (2023). Hydrogen, Ammonia and Symbiotic/Smart Fertilizer Production Using Renewable Feedstock and CO2 Utilization through Catalytic Processes and Nonthermal Plasma with Novel Catalysts and In Situ Reactive Separation: A Roadmap for Sustainable and Innovation-Based Technology. In *Catalysts* (Vol. 13, Issue 9).

Akbari S., Kroon M., Parihar V S., Koivisto J T., Hannula M., Kellomäki M., Hyttinen J., (2024). Synthesis and Characterization of PolyHIPE-Gellan Gum Material with Tunable Macroporosity for Tissue Engineering Applications. *Macromolecules*, 57(13), 6295–6308.

Alatawi F S., Monier M.,Elsayed N H., (2018). Amino functionalization of carboxymethyl cellulose for efficient immobilization of urease. *International Journal of Biological Macromolecules*, 114.

Al-Garawi Z S., Taha A A., Abd A N., Tahir N T., (2022). Immobilization of Urease onto Nanochitosan Enhanced the Enzyme Efficiency: Biophysical Studies and in Vitro Clinical Application on Nephropathy Diabetic Iraqi Patients. *Journal of Nanotechnology*, 2022.

Almaghrabi O., Almulaiky Y Q., (2023). A biocatalytic system obtained via immobilization of urease onto magnetic metal/alginate nanocomposite: Improving reusability and enhancing stability. *Biocatalysis and Biotransformation*, 41(6).

Al-Tayawi A N., Gulyás N S., Gergely G., Fazekas Á F., Szegedi B., Hodúr C., Lennert J R., Kertész S., (2023). Enhancing ultrafiltration performance for dairy wastewater treatment using a 3D printed turbulence promoter. *Environmental Science and Pollution Research*, 30(50).

Amani A., Kalajahi S T., Yazdian F., Mirzababaei S., Rashedi H., Faramarzi M A., Vahidi M., (2022). Immobilization of urease enzyme on chitosan/polyvinyl alcohol electrospun nanofibers. *Biotechnology Progress*, 38(5).

Anas M., Liao F., Verma K K., Sarwar M A., Mahmood A., Chen Z L., Li Q., Zeng X P., Liu Y., Li Y R., (2020). Fate of nitrogen in agriculture and environment: agronomic, eco-physiological and molecular approaches to improve nitrogen use efficiency. In *Biological Research* (Vol. 53, Issue 1), BioMed Central Ltd.

Andler S M., Goddard J M., (2018). Stabilization of Lipase in Polymerized High Internal Phase Emulsions. *Journal of Agricultural and Food Chemistry*, 66(14).

Asiain-Mira R., Zamora P., Monsalvo V., Torrente-Murciano L., (2024). Effect of functional groups on the adsorption of urea on activated carbon. *Carbon*, 228.

Assefa A., Derebe B., Gebrie N., Shibabaw A., Getahun W., Beshir O., Worku A., (2023). Grain yield and quality responses of durum wheat (Triticum turgium L. var. durum) to nitrogen and phosphorus rate in Yilmana Densa, Northwestern Ethiopia. *Heliyon*, 9(7).

Ben Hmida M., Mechichi T., Piccoli G B., Ksibi M., (2023). Water implications in dialysis therapy, threats and opportunities to reduce water consumption: a call for the planet. In *Kidney International,* (Vol. 104, Issue 1).

Beres B. L., Rahmani E., Clarke J. M., Grassini P., Pozniak C J., Geddes C M., Porker K D., May W E., Ransom J K., (2020). A Systematic Review of Durum Wheat: Enhancing Production Systems by Exploring Genotype, Environment, and Management (G × E × M) Synergies. In *Frontiers in Plant Science,* (Vol. 11).

Bertilsson G O B., Kirchmann H., (2021). Sustainable N fertilizer production based on a loop: Straw - biogas – 'Haber-Bosch' process. *Agricultural Systems*, 190.

Bradford M M., (1976). A rapid and sensitive method for the quantitation of microgram quantities of protein utilizing the principle of protein-dye binding. *Analytical Biochemistry*, 72(1–2).

Braham S A., Siar E H., Arana-Peña S., Carballares D., Morellon-Sterling R., Bavandi, H., de Andrades D., Kornecki J F., Fernandez-Lafuente R., (2021). Effect of concentrated salts solutions on the stability of immobilized enzymes: Influence of inactivation conditions and immobilization protocol. *Molecules*, 26(4).

Bui-Le L., Clarke C J., Bröhl A., Brogan A P S., Arpino J A J., Polizzi K M., Hallett, J P., (2020). Revealing the complexity of ionic liquid–protein interactions through a multi-technique investigation. *Communications Chemistry*, 3(1).

Califano V., Costantini A., (2021). Enzyme immobilization and biocatalysis. In *Catalysts*, (Vol. 11, Issue 7).

Choi J., Chung J., (2019). Evaluation of urea removal by persulfate with UV irradiation in an ultrapure water production system. *Water Research*, 158.

Choi S J., Crane L., Kang S., Boyer T H., Perreault F., (2024). Removal of urea in ultrapure water system by urease-coated reverse osmosis membrane. *Water Research X*, 22.

Courtney C., Randall D G., (2023). Concentrating stabilized human urine using eutectic freeze crystallization for liquid fertilizer production. *Water Research*, 233.

Dai C., Han S., Ma C., McClements D J., Xu D., Chen S., Liu X., Liu F., (2024). High internal phase emulsions stabilized by pea protein isolate-EGCG-Fe3+ complexes: Encapsulation of β-carotene. *Food Hydrocolloids*, 150, 109607.

Daneshfar A., Matsuura T., Emadzadeh D., Pahlevani Z., Ismail A F., (2015). Urease-carrying electrospun polyacrylonitrile mat for urea hydrolysis. *Reactive and Functional Polymers*, *87*, 37–45.

Değermenci N., Yildiz E., (2021). Ammonia stripping using a continuous flow jet loop reactor: mass transfer of ammonia and effect on stripping performance of influent ammonia concentration, hydraulic retention time, temperature, and air flow rate. *Environmental Science and Pollution Research*, 28(24), 31462–31469.

Demirhan C D., Tso W W., Powell J B., Pistikopoulos E N., (2019). Sustainable ammonia production through process synthesis and global optimization. *AIChE Journal*, 65(7).

Dhavalikar P., Shenoi J., Salhadar K., Chwatko,M., Rodriguez-Rivera G., Cheshir J., Foudazi R., Cosgriff-Hernandez E., (2021). Engineering toolbox for systematic design of polyhipe architecture. *Polymers*, 13(9).

Diasi M., Singh R., Mahapatra A Das., Renuka L., Patel H., Ganatra H., Datta B., (2024). Ammonium release in synthetic and human urine by a urease immobilized nanoconstruct. *RSC Advances*, 14(10).

Dizge N., Keskinler B., Tanriseven A., (2008). Covalent attachment of microbial lipase onto microporous styrene–divinylbenzene copolymer by means of polyglutaraldehyde. *Colloids and Surfaces B: Biointerfaces*, *66*(1), 34–38.

Dizge N., Keskinler B., Tanriseven A., (2009). Biodiesel production from canola oil by using lipase immobilized onto hydrophobic microporous styrene-divinylbenzene copolymer. *Biochemical Engineering Journal*, *44*(2–3).

Fidaleo M., Tavilli E., (2021). Urea removal in rosé and red wines by immobilised acid urease in a packed bed reactor. *Food and Bioproducts Processing*, *126*, 42–50.

Gao X., Zhang S., Wang P., Jaroniec M., Zheng Y., Qiao S Z., (2024). Urea catalytic oxidation for energy and environmental applications. In *Chemical Society Reviews* (Vol. 53, Issue 3).

Ge W., Lin L., Wang S Q., Wang Y., Ma X., An Q., Zhao L., (2023). Electrocatalytic urea oxidation: advances in mechanistic insights, nanocatalyst design, and applications. In *Journal of Materials Chemistry A* (Vol. 11, Issue 28).

Habib S., Weinman S T., (2022). Modification of polyamide reverse osmosis membranes for the separation of urea. *Journal of Membrane Science*, *655*.

Hafez E., Ragab A., Kobata T., (2014). Water-Use Efficiency and Ammonium-N Source Applied of Wheat under Irrigated and Desiccated Conditions. *International Journal of Plant & Soil Science*, *3*(10).

Hamdan N M., Alawadhi H., Jisrawi N., (2016). Particulate matter pollution in the United Arab Emirates: Elemental analysis and phase identification of fine particulate pollutants. *Proceedings of the World Congress on New Technologies*.

He J., Zhou J., Yang K., Luo L., Wang P., Wang Z., Ma J., (2024). Pulsed electric field drives chemical-free membrane stripping for high ammonia recovery from urine. *Water Research*, *251*, 121129.

Hormozi Jangi S R., Akhond M., (2021). High throughput urease immobilization onto a new metal-organic framework called nanosized electroactive quasi-coral-340 (NEQC-340) for water treatment and safe blood cleaning. *Process Biochemistry*, *105*, 79–90.

Hormozi Jangi S R., Akhond M., Dehghani Z., (2020). High throughput covalent immobilization process for improvement of shelf-life, operational cycles, relative activity in organic media and enzymatic kinetics of urease and its application for urea removal from water samples. *Process Biochemistry*, *90*, 102–112.

Huang Y., Zhang H., Yang X., Chen Q., Zheng W., Shen J W., Guo Y., (2024). A review: current urea sorbents for the development of a wearable artificial kidney. In *Journal of Materials Science,* (Vol. 59, Issue 26, pp. 11669–11686). Springer.

Huang Z., Yao P., Zhu Q., Wang L., Zhu Y., (2018). The polystyrene-divinylbenzene stationary phase hybridized with oxidized nanodiamonds for liquid chromatography. *Talanta*, *185*.

Hurek T., Reinhold-Hurek B., Van Montagu M., Kellenberger E., (1994). Root colonization and systemic spreading of Azoarcus sp. strain BH72 in grasses. *Journal of Bacteriology*, *176*(7).

Ispirli Doğaç Y., Deveci I., Teke M., Mercimek B., (2014). TiO2 beads and TiO2-chitosan beads for urease immobilization. *Materials Science and Engineering C*, *42*, 429–435.

Jackson C E., Doyle I., Khan H., Williams S F., Aldemir Dikici B., Barajas Ledesma E., Bryant H E., English W R., Green N H., Claeyssens F., (2023). Gelatin-containing porous polycaprolactone PolyHIPEs as substrates for 3D breast cancer cell culture and vascular infiltration. *Frontiers in Bioengineering and Biotechnology*, 11.

Kara F., Demirel G., Tümtürk H., (2006). Immobilization of urease by using chitosan-alginate and poly(acrylamide-co-acrylic acid)/κ-carrageenan supports. *Bioprocess and Biosystems Engineering*, *29*(3), 207–211.

Kovačič J M., Ciringer T., Ambrožič-Dolinšek J., Kovačič S., (2022). Use of Emulsion-Templated, Highly Porous Polyelectrolytes for In Vitro Germination of Chickpea Embryos: a New Substrate for Soilless Cultivation. *Biomacromolecules*, *23*(8).

Kumar S., Dwevedi A., Kayastha A M., (2009). Immobilization of soybean (Glycine max) urease on alginate and chitosan beads showing improved stability: Analytical applications. *Journal of Molecular Catalysis B: Enzymatic*, *58*(1–4).

Kutcherlapati S N R., Yeole N., Jana T., (2016). Urease immobilized polymer hydrogel: Long-term stability and enhancement of enzymatic activity. *Journal of Colloid and Interface Science*, *463*, 164–172.

Kutlu N., İspirli Doğaç Y., Deveci İ.,Teke M., (2020). Urease immobilized electrospun PVA/chitosan nanofibers with improved stability and reusability characteristics: an application for removal of urea from artificial blood serum. *Preparative Biochemistry and Biotechnology*, *50*(5).

Lazcano C., Zhu-Barker X., Decock C., (2021). Effects of organic fertilizers on the soil microorganisms responsible for n2o emissions: A review. In *Microorganisms,* (Vol. 9, Issue 5).

Li D., Fan R., Guo X., Yang S., Zhang Z., (2018). Phase Equilibria in the Aqueous Ternary System (NH4)2SO4 + Na2SO4 + H2O at T = (303.15 and 313.15) K and p = 0.1 MPa. *Journal of Chemical and Engineering Data*, *63*(3).

Li Y., Zhang L., Liu W., Zhou Z., (2023). Simultaneous removal of urea nitrogen and inorganic nitrogen from high-salinity wastewater by Halomonas sp. H36. *Environmental Science and Pollution Research*, *30*(2).

Liang X., Li Q., Shi Z., Bai S., Li Q., (2020). Immobilization of urease in metal–organic frameworks via biomimetic mineralization and its application in urea degradation. *Chinese Journal of Chemical Engineering*, *28*(8), 2173–2180.

Liu X., Yang Y., Wu B., Lv C., Wei H., Gao P., Zhang H., Dai Q., Chen Y., (2025). Effects of Nitrogen Application on Crop Production and Nitrogen Use in Rice–Wheat Rotation. *Agronomy*, *15*(5).

Liu X., Zhong Q., Wang J., Ji X., Jia Y., Xu Y., Li L., (2011). Study on ammonium sulfate crystallization in the ammonium desulphurization process in a coal-based power plant in the petrochemical industry. *Energy Sources, Part A: Recovery, Utilization and Environmental Effects*, *33*(22).

Luther A. K., Desloover J., Fennell D E., Rabaey K., (2015). Electrochemically driven extraction and recovery of ammonia from human urine. *Water Research*, *87*, 367–377.

Maghraby Y R., El-Shabasy R M., Ibrahim A H., Azzazy H M E S., (2023). Enzyme Immobilization Technologies and Industrial Applications. In *ACS Omega,* (Vol. 8, Issue 6).

Mahalik K., Sahu J N., Patwardhan A V., Meikap B C., (2010). Kinetic studies on hydrolysis of urea in a semi-batch reactor at atmospheric pressure for safe use of ammonia in a power plant for flue gas conditioning. *Journal of Hazardous Materials*, *175*(1–3).

Malakian A., Zhou M., Zowada R T., Foudazi R., (2019). Synthesis and in situ functionalization of microfiltration membranes via high internal phase emulsion templating. *Polymer International*, *68*(7).

Mauerer M., Rocksch T., Dannehl D., Schuch I., Mewis I., Förster N., Ulrichs C., Schmidt U., (2023). Replacing Mineral Fertilizer with Nitrified Human Urine in Hydroponic Lettuce (Lactuca sativa L.) Production. *Sustainability (Switzerland)*, *15*(13).

McKenzie T J., Ayres N., (2023). Synthesis and Applications of Elastomeric Polymerized High Internal Phase Emulsions (PolyHIPEs). In *ACS Omega,* (Vol. 8, Issue 23).

Monier M., El-Sokkary A., M A., (2012). Modification and characterization of cellulosic cotton fibers for efficient immobilization of urease. *International Journal of Biological Macromolecules*, *51*(1–2), 18–24.

Mukimin A., Ningsih K., Muhammad F., Ghozali A A., Rochman F F., (2025). A novel electrochemical advanced oxidation technology using a low-cost graphite plate anode for batik-printing wastewater treatment. *Journal of Environmental Chemical Engineering*, *13*(5).

Murshid S., Antonysamy A J.,Dhakshinamoorthy G P., Jayaseelan A., Pugazhendhi A., (2023). A review on biofilm-based reactors for wastewater treatment: Recent advancements in biofilm carriers, kinetics, reactors, economics, and future perspectives. In *Science of the Total Environment,* (Vol. 892).

Osorio-Tejada J., Tran N N., Hessel V., (2022). Techno-environmental assessment of small-scale Haber-Bosch and plasma-assisted ammonia supply chains. *Science of the Total Environment*, *826*.

Owen R., Sherborne C., Evans R., Reilly G C., Claeyssens F., (2020). Combined porogen leaching and emulsion templating to produce bone tissue engineering scaffolds. *International Journal of Bioprinting*, *6*(2).

Öngören Ç S., (2013), "Farkli Azot Gübre Formlarinin Buğday (Triticum Aestivum L.) Çeşitlerinde Verim Ve Kalite Üzerine Etkisinin Belirlenmesi",Yüksek lisans Tezi, Adnan Menderes Üniversitesi.

Pandorf M., Hochmuth G., Boyer T H., (2019). Human Urine as a Fertilizer in the Cultivation of Snap Beans (Phaseolus vulgaris) and Turnips (Brassica rapa). *Journal of Agricultural and Food Chemistry*, *67*(1).

Pashneh-Tala S., Field J., Fornesa B., Molins Colomer M., Jackson C E., Balcells M., Martorell J., Claeyssens F., (2023). Versatile, elastomeric and degradable polyHIPEs of poly(glycerol sebacate)-methacrylate and their application in vascular graft tissue-engineering. *Materials Today Advances*, *20*, 100432.

Pithawala K., Mishra N., Bahadur A., (2010). Immobilization of urease in alginate, paraffin and lac. *Journal of the Serbian Chemical Society*, *75*(2), 175–183.

Powlson D S., Dawson C J., (2022). Use of ammonium sulphate as a sulphur fertilizer: Implications for ammonia volatilization. *Soil Use and Management*, *38*(1).

Pradhan S K., Nerg A M., Sjöblom A., Holopainen J K., Heinonen-Tanski H., (2007). Use of human urine fertilizer in cultivation of cabbage (Brassica oleracea) - Impacts on chemical, microbial, and flavor quality. *Journal of Agricultural and Food Chemistry*, *55*(21).

Pulko I., Kolar M., Krajnc P., (2007). Atrazine removal by covalent bonding to piperazine functionalized PolyHIPEs. *Science of the Total Environment*, *386*(1–3).

Ruan G., Wu Z., Huang Y., Wei M., Su R., Du F., (2016). An easily regenerable enzyme reactor prepared from polymerized high internal phase emulsions. *Biochemical and Biophysical Research Communications*, *473*(1).

Saito T., Takano Y., (2022). QM/MM Molecular Dynamics Simulations Revealed Catalytic Mechanism of Urease. *Journal of Physical Chemistry B*, *126*(10).

Satyam S., Patra S., (2024). Innovations and challenges in adsorption-based wastewater remediation: A comprehensive review. *Heliyon*, *10*(9).

Shaban A., Basiouny M E., AboSiada O A., (2024). Comparative study of the removal of urea by electrocoagulation and electrocoagulation combined with chemical coagulation in aqueous effluents. *Scientific Reports*, *14*(1).

Simha P., Zabaniotou A., Ganesapillai M., (2018). Continuous urea–nitrogen recycling from human urine: A step towards creating a human excreta based bio–economy. *Journal of Cleaner Production*, *172*, 4152–4161.

Smith S., Burden H., Persad R., Whittington K., De Lacy Costello B., Ratcliffe N M., Probert C S., (2008). A comparative study of the analysis of human urine headspace using gas chromatography-mass spectrometry. *Journal of Breath Research*, *2*(3).

Speight J G., (2017). Environmental inorganic chemistry for engineers. In *Environmental Inorganic Chemistry for Engineers*.

Srinivasa Rao M., Chellapandian M., Krishnan M R V., (1995). Immobilization of urease on gelatin - poly (HEMA) copolymer preparation and characterization. *Bioprocess Engineering*, 13(4).

Swarnalatha V., Esther R A., Dhamodharan R., (2013). Immobilization of α-amylase on gum acacia stabilized magnetite nanoparticles, an easily recoverable and reusable support. *Journal of Molecular Catalysis B: Enzymatic*, 96.

Thumbarathy D., (2018), “a Preparation of functional polyHIPE polymers for agro-process and bio-process applications”, PhD Thesis, Newcastle University.

Tizzoni A C., Corsaro N., D’Ottavi C., Licoccia S., Sau S., Tarquini P., (2015). Oxygen production by intermediate metal sulphates in sulphur based thermochemical water splitting cycles. *International Journal of Hydrogen Energy*, 40(11).

Urbańczyk E., Sowa M., Simka W., (2016). Urea removal from aqueous solutions—a review. In *Journal of Applied Electrochemistry* (Vol. 46, Issue 10, pp. 1011–1029). Springer Netherlands.

van Gelder M K., Jong J A W., Folkertsma L., Guo Y., Blüchel C., Verhaar M C., Odijk M., Van Nostrum C F., Hennink W E., Gerritsen K G F., (2020). Urea removal strategies for dialysate regeneration in a wearable artificial kidney. In *Biomaterials* (Vol. 234).

Vedovello P., Sanches L V., da Silva Teodoro G., Majaron V F., Bortoletto-Santos R., Ribeiro C., Putti F F., (2024). An Overview of Polymeric Hydrogel Applications for Sustainable Agriculture. In *Agriculture (Switzerland)* (Vol. 14, Issue 6). Multidisciplinary Digital Publishing Institute (MDPI).

Volpin F., Jiang J., El Saliby I., Preire M., Lim S., Hasan Johir M. A., Cho J., Han D S., Phuntsho S., Shon H K., (2020). Sanitation and dewatering of human urine via membrane bioreactor and membrane distillation and its reuse for fertigation. *Journal of Cleaner Production*, 270.

Wahab W A A., (2025). Review of research progress in immobilization and chemical modification of microbial enzymes and their application. In *Microbial Cell Factories,* (Vol. 24, Issue 1). BioMed Central Ltd.

Wang H., Zheng X., Fang L., Lu S., (2023). Urea Electrooxidation in Alkaline Environment: Fundamentals and Applications. *ChemElectroChem*, 10(13).

Wang M., Wang M., Zhu Y., Zhang S., Chen J., (2019). Enzyme immobilized millimeter-sized polyHIPE beads with easy separability and recyclability. *Reaction Chemistry and Engineering*, 4(6), 1136–1144.

Wang Q., Huang N., Wang W., Wu Y., Xue S., Xu H., Chen Z., Wu Y., Wu Q., Hu H., (2023). Urea removal for ultrapure water production by VUV/UV/chlorine under acidic aqueous conditions: Facile elimination and efficient denitrification. *Journal of Cleaner Production*, 401.

Weerakoon D., Bansal B., Padhye L P., Rachmani A., James Wright L., Silyn Roberts G., Baroutian S., (2023). A critical review on current urea removal technologies from water: An approach for pollution prevention and resource recovery. *Separation and Purification Technology*, 314, 123652.

Web 1, (2008), http://faostat.fao.org (Access date:18/09/2023).

Wu Y., Huang J., Guo Z., Yang Q., Xia C., Zheng Z., (2025). Preparation of Polymerized High Internal Phase Emulsion Membranes with High Open-Cellular Extent and High Toughness via RAFT Polymerization. *Polymers*, 17(4).

Yang D., Fan J., Cao F., Deng Z., Pojman J. A., Ji, L., (2019). Immobilization adjusted clock reaction in the urea-urease-H + reaction system. *RSC Advances*, 9(7), 3514–3519.

Yavaşer Boncooğlu R., (2024). Urease immobilized poly(AAm-AGE) cryogel for depletion of urea from human serum. *Process Biochemistry*, 136, 273–281.

Yigitolu M., Temoçin Z., (2010). Immobilization of Candida rugosa lipase on glutaraldehyde-activated polyester fiber and its application for hydrolysis of some vegetable oils. *Journal of Molecular Catalysis B: Enzymatic*, 66(1–2), 130–135.

Zaher A., Shehata N., (2021). Recent advances and challenges in management of urea wastewater:A mini review. *IOP Conference Series: Materials Science and Engineering*, 1046(1).

Zhang J., Wang Z., He C., Liu X., Zhao W., Sun S., Zhao C., (2019). Safe and Effective Removal of Urea by Urease-Immobilized, Carboxyl-Functionalized PES Beads with Good Reusability and Storage Stability. *ACS Omega*, 4(2), 2853–2862.

Zhang K., Duan Y., Graham N., Yu W., (2023). Efficient electrochemical generation of active chlorine to mediate urea and ammonia oxidation in a hierarchically porous-Ru/RuO2-based flow reactor. *Journal of Hazardous Materials*, 444.

Zhang T., Sanguramath R A., Israel S., Silverstein M S., (2019). Emulsion Templating: Porous Polymers and beyond. In *Macromolecules,* (Vol. 52, Issue 15).

Zhang X., Yang Y., Ngo H H., Guo W., Wen H., Wang X., Zhang J., Long T., (2021). A critical review on challenges and trend of ultrapure water production process. In *Science of the Total Environment,* (Vol. 785).

Zowada R., Foudazi R., (2023). Macroporous hydrogels for soil water retention in arid and semi-arid regions. *RSC Applied Polymers*, 1(2).

Zuo Z., Chen Y., Xing Y., Li S., Yang S., Jiang G., Liu T., Zheng M., Huang X., Liu Y., (2023). The advantage of a two-stage nitrification method for fertilizer recovery from human urine. *Water Research*, 235.

Zverina L., Pinelo M., Woodley J. M., Daugaard A E., (2021). Monolithic flow reactor for enzymatic oxidations. *Journal of Chemical Technology and Biotechnology*, 96(9), 2488–2495.

BIOGRAPHY

Büşra ŞAHİN received her bachelor's degree from the Department of Biology at Istanbul University, Türkiye in 2016. She pursued her master's degree at the Biotechnology Institute of Gebze Technical University and graduated in 2021. She has been pursuing her doctoral studies at the Biotechnology Institute of Gebze Technical University since the fall of 2021.

PUBLICATIONS AND PRESENTATIONS FROM THE THESIS

Sahin B., Ozbey-Unal B., Dizge N., Keskinler B., Balcik C., (2024).Optimization of immobilized urease enzyme on porous polymer for enhancing the stability, reusability and enzymatic kinetics using response surface methodology. *Colloids and Surfaces B: Biointerfaces*, 240, 113986.

Sahin B., Ozbey-Unal B., Arslan N., Çiftçi Y Ö., Keskinler B., Balcik C., (2025). Pee-cycling: Boosting fertilizer potential of human urine using urease-immobilized polymeric high internal phase emulsion. *Resources, Conservation and Recycling*, 215, 108168.

APPENDICES

APPENDIX-A:BSA STANDARD CURVE FOR THE DETERMINATION OF AMOUNT OF PROTEIN BY BRADFORD METHOD.

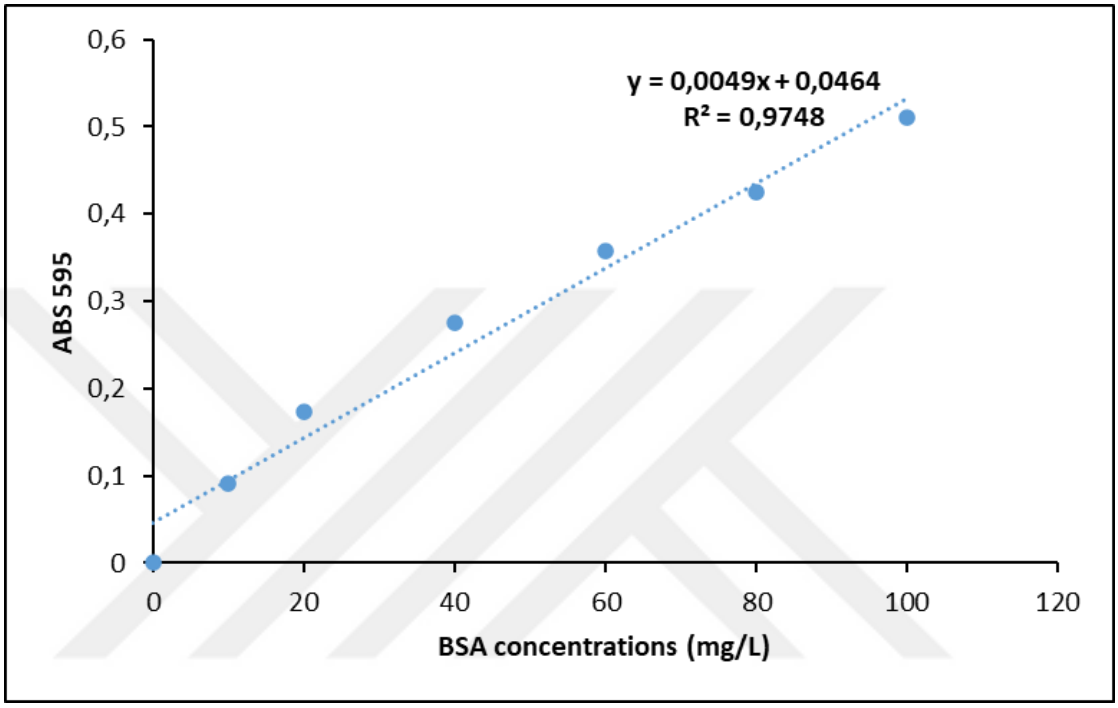

APPENDIX-B: AMMONIUM SULPHATE STANDARD CURVE FOR THE DETERMINATION OF AMMONIA BY [Srinivasa Rao et al., 1995].

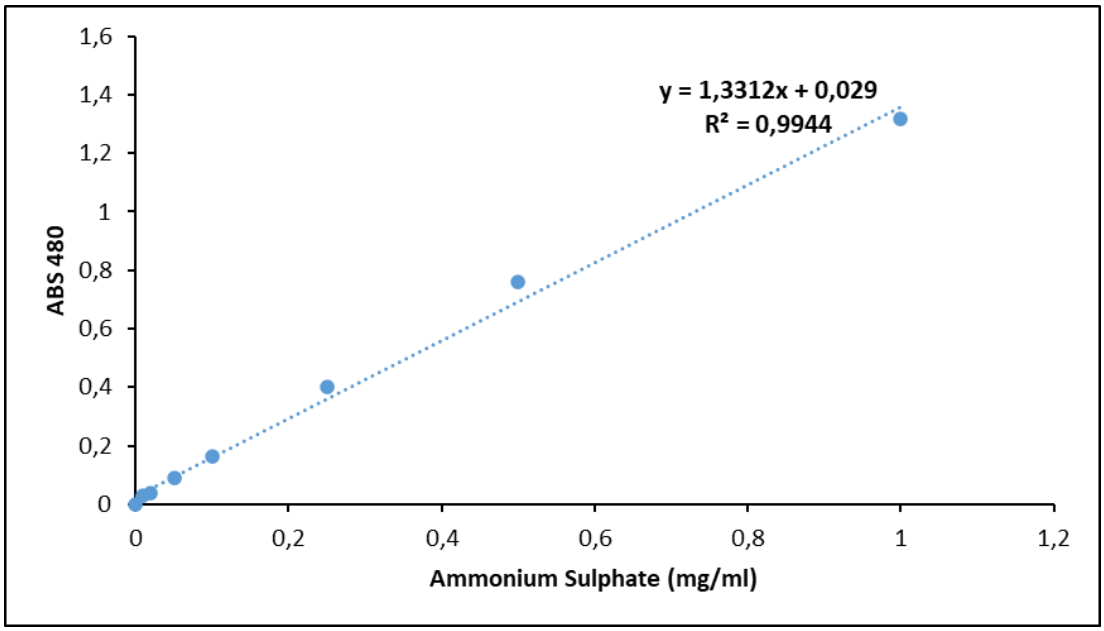

APPENDIX-C: BOX-BEHNKEN DESIGN ON THE RELATIVE ACTIVITY.

	Factor 1	Factor 2	Factor 3	Responses
Run	**A: NaCI, g/L**	**B: pH**	**C: Temperature, °C**	**Relative activity, %**
1	1.5	4	55	58
2	3	4	40	56
3	0	4	40	69
4	1.5	4	25	63
5	3	6.5	25	77
6	3	9	40	72
7	1.5	6.5	40	84
8	1.5	9	55	74
9	1.5	6.5	40	84
10	0	9	40	85
11	1.5	6.5	40	84
12	0	6.5	55	86
13	0	6.5	25	91
14	1.5	9	25	79
15	3	6.5	55	73